SSC-174

Investigation of Residual Stresses

In Steel Weldments

by

KOICHI MASUBUCHI and **D. C. MARTIN**

SHIP STRUCTURE COMMITTEE

SHIP STRUCTURE COMMITTEE

MEMBER AGENCIES:

BUREAU OF SHIPS, DEPT. OF NAVY
MILITARY SEA TRANSPORTATION SERVICE, DEPT. OF NAVY
UNITED STATES COAST GUARD, TREASURY DEPT.
MARITIME ADMINISTRATION, DEPT. OF COMMERCE
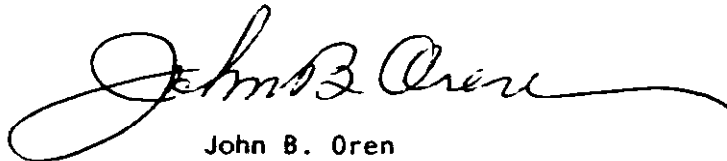AMERICAN BUREAU OF SHIPPING

September 1966

Dear Sir:

Novel methods of measuring residual stresses in mild steel are constantly being proposed to obviate their effects in the brittle fracture problem. The Ship Structure Committee undertakes, whenever possible, the most favorable approaches. One such proposal suggested the use of a hydrogen-induced-cracking technique. The attached report represents the results and description of such a study undertaken at Battelle Memorial Institute.

In sponsoring their research project, the Ship Structure Committee received guidance and review from the National Academy of Sciences through its Ship Hull Research Committee, and a project advisory committee (SR-167, "Residual Stresses in Steel Weldments"). The Academy undertakes this research advisory service to the Ship Structure Committee through a contract arrangement.

Comments on this report would be welcome and should be adressed to the Secretary, Ship Structure Committee.

Sincerely yours,

John B. Oren
Rear Admiral, U. S. Coast Guard
Chairman, Ship Structure Committee

SSC-174

Final Report

on

Project SR-167

"Investigation of Residual Stresses
in Steel Weldments"

to the

Ship Structure Committee

INVESTIGATION OF RESIDUAL STRESSES
IN STEEL WELDMENTS

by

Koichi Masubuchi and D. C. Martin

Battelle Memorial Institute
Columbus, Ohio

under

Department of the Navy
Bureau of Ships Contract NObs 92521

Washington, D. C.
National Academy of Sciences - National Research Council
September 1966

ABSTRACT

The objective of this research was to determine whether a hydrogen-induced-cracking technique could be used to study residual stresses in weldments, especially complex weldments.

Experimental hydrogen-induced-cracking tests were made on 45 weldments in mild steel, HY-80 steel, a commercial high-strength structural steel, and SAE 4340 steel. Extensive cracks were found in weldments made in SAE 4340 steel (oil quenched and tempered at 500 F) after hydrogen charging for relatively short times. Systematic crack patterns that could be related to residual stress distributions were obtained on various complex weldments. When steels of lower strengths were used, longer charging time was required to produce cracks, and crack patterns were less pronounced. The hydrogen-induced-cracking technique does not seem to work on mild-steel weldments.

It has been found that hydrogen-induced cracking is stress sensitive rather than plastic-strain sensitive. This has been proved by hydrogen-induced-cracking tests on mechanically stress-relieved specimens and press-fit specimens in which residual stresses were produced by purely elastic deformation.

Other experimental investigations conducted in this research include:

(1) Stress-corrosion-cracking tests on weldments

(2) Metallographic examinations of hydrogen-induced and stress-corrosion cracks

(3) Measurements of residual stresses by stress-relaxation technique using strain gages.

It was found that distributions of residual stresses in mild-steel and SAE 4340 steel weldments were quite similar despite the considerable differences in the yield strengths of the two base plates and the weld metals. This was proved in butt joints up to 38 inches long and complex welded structures.

Analytical investigations of crack patterns have been made. Mathematical equations have been developed to express relationships among the residual-stress distribution, properties of the material, and the crack pattern. The analytical investigations were used for interpreting crack patterns obtained experimentally.

CONTENTS

INTRODUCTION

Various techniques involving the use of electrical and mechanical strain gages have been developed for measuring residual stresses in weldments.[1-4]* However, in complex weldments, the measurement of residual stresses is extremely time consuming and costly. The photoelastic-coating technique[5] has been used to determine stress distributions in complex structures. However, the high temperature encountered during welding would damage such a coating if placed on a weldment before welding.

Considerable research has been carried out on the hydrogen-induced delayed fracture of high-strength steels.[6,7] It has been found that in hydrogen-embrittled steels:

(1) Fracture occurs at stresses far below the yield stress of the material

(2) Cracks induced by hydrogen are always at 90 degrees to the principal stress.

These findings indicated that hydrogen-induced cracking might provide a good method for studying residual stresses.

Research has been conducted, since December, 1958, at Battelle Memorial Institute under Contracts Nos. NObs-77028, NObs-84738, and NObs-92521 to determine whether a hydrogen-induced-cracking technique could be used to study residual stresses in weldments, especially complex weldments. With the hydrogen-induced-cracking technique, a weldment is made with steel which is ductile enough so that cracks are not formed during welding. After welding, the weldment is charged with hydrogen electrolytically to embrittle the material to such an extent that cracks are formed by residual stresses. The distribution of residual stress is estimated from the crack pattern. In addition to experimental investigations, analytical investigations were made to determine relations between the residual-stress distribution and the crack pattern.

This report summarizes all the work conducted under Contracts Nos. NObs-77028, NObs-84738, and NObs-92521.

The following Battelle reports were prepared under the contracts:

---

* References are listed at the end of this report.

Report No.	Contract Number	Type	Date	Period Covered
1	NObs-77028	Quarterly Progress	January 31, 1959	12-15-58 to 1-31-59
2		Ditto	April 30, 1959	2-15-59 to 4-30-59
3		"	July 31, 1959	4-30-59 to 7-31-59
4		Summary	November 30, 1959	12-15-58 to 11-30-59
5		Quarterly Progress	February 29, 1960	11-30-59 to 2-29-60
6		Ditto	May 31, 1960	3-01-60 to 5-31-60
7		"	August 31, 1960	6-01-60 to 8-31-60
8		Summary	December 31, 1960	12-15-58 to 12-31-60
9	NObs-84738	Summary	December 31, 1961	5-15-61 to 12-31-61
10		Summary	August 31, 1962	5-15-62 to 7-31-62
11		Progress	August 1, 1963	2-01-63 to 8-01-63
12		Summary	December 31, 1963	1-01-63 to 12-31-63

In addition to the above reports, the following paper covering the work conducted under Contract No. NObs-77028 was prepared:

Masubuchi, K. and Martin, D. C., "Investigation of Residual Stresses by Use of Hydrogen Cracking", The Welding Journal, 40 (12), Research Supplement, 553-s to 563-s (1961).

EXPERIMENTAL INVESTIGATIONS

Phases of Investigation and Objectives

Experimental investigations were carried out in five phases:

Phase 1: Hydrogen-induced-cracking tests on weldments

Phase 2: Hydrogen-induced-cracking tests on press-fit specimens

Phase 3: Stress-corrosion-cracking tests on weldments

Phase 4: Metallographic examinations of cracks

Phase 5: Measurement of residual stresses by stress-relaxation technique:

Previous research has shown that the type of material has considerable effect on the hydrogen-induced delayed fracture characteristics. Simcoe, et al.[7] conducted fracture tests on cathodically charged specimens made with SAE 4340 steel heat treated to various strength levels. It was found that as the strength of the material increased, fracture occurred at lower stress in a shorter time. Investigations were conducted on simple weldments made with several types of steel to determine whether residual stress would cause cracking during hydrogen charging. Investigations also were carried out on complex weldments.

Residual stresses in weldments are caused by plastic deformations which take place during the welding thermal cycle. Hydrogen-induced-cracking tests were conducted on specimens which had stresses of known distributions caused by purely elastic deformation in an attempt to ascertain whether cracks are caused by elastic stresses and to obtain a better interpretation of the crack pattern. Tapered pins were pressed into ring specimens to produce stresses of various magnitudes which were measured with strain gages.

The use of a stress-corrosion-cracking technique is another way of obtaining cracks in a welded joint. McKinsey[8] obtained a system of transverse cracks in a butt joint placed in a boiling concentrated nitrate solution. Rädeker[9] reported on a study of the use of the stress-corrosion-cracking technique as a method to prove the existence of residual stresses in a welded joint. Several types of welded joints were tested, and crack patterns were observed that appeared to be related to the residual stresses. Limited studies of the stress-corrosion-cracking technique were conducted to learn whether the crack patterns produced by stress corrosion are similar to those obtained by hydrogen charging.

Limited metallographic investigations were made of sections cut through cracks to characterize the modes of hydrogen-induced and stress-corrosion cracking.

Measurement of residual stresses by stress-relaxation techniques using strain gages were made on eight weldments made from mild steel and heat-treated SAE 4340 steel.

TABLE 1. CHEMICAL COMPOSITIONS OF BASE PLATES.

	Mild Steel[a]	HY-80 Steel[b]	Commercial High-Strength Structural Steel[c]	SAE 4340 Steel[d]
Carbon	0.24/0.37	0.17	0.10 /0.20	0.36 /0.43
Manganese	0.76/0.82	0.25	0.60 /1.00	0.69 /0.71
Silicon	0.19/0.20	0.22	0.15 /0.35	0.24 /0.33
Sulfur		0.018	0.050 max	0.015/0.017
Phosphorus		0.012	0.040 max	0.006/0.017
Nickel		2.53	0.70 /1.00	1.68 /1.88
Chromium		1.40	0.40 /0.80	0.78 /0.83
Molybdenum		0.36	0.40 /0.60	0.24 /0.35
Vanadium			0.03 /0.10	0.24
Copper			0.15 /0.50	
Boron			0.002/0.006	

(a) Ranges of chemical compositions obtained on two steel plates from which Specimens GM1 and 3CM were prepared.

(b) Values obtained on a 2-inch-thick plate from which Specimen GH1 was prepared.

(c) Ranges of chemical compositions in which this type of steel was made.

,(d) Ranges of chemical compositions obtained on four steel plates from which most of SAE 4340 steel weldments were prepared.

Base Plates and Fabrication of Welded Specimens

Base Plates

The following four types of steel were used:

(1) Mild steel, ABS Class B and ASTM A212-B (approximate tensile strength: 75,000 psi)

(2) Quenched-and-tempered low-alloy high-strength steel, HY-80 (approximate tensile strength: 100,000 psi)

(3) A commercial high-strength structural steel which is currently supplied under Grade F, ASTM A514-64 (approximate tensile strength: 120,000 psi)[10]*

---

* At the time when this steel was used in this research, this steel was not covered by ASTM A514-64.

(4) Ultrahigh-strength steel, SAE 4340 (approximate tensile strength: 150,000 psi in the as-rolled condition).

Specimens were prepared from steel plates 1/2 inch to 2-1/2 inches thick. Table 1 shows the chemical compositions of the steels.

In most cases, the commercial high-strength structural steel and SAE 4340 steel were heat treated prior to welding. Two different heat treatments were used for the commercial high-strength structural steel as follows:

Soft condition: water quenched from 1650 F and tempered at 1150 F for 1 hour (approximate tensile strength: 120,000 psi)

Hard condition: water quenched from 1650 F and tempered at 350 F for 1 hour (approximate tensile strength: 150,000 psi).

The "soft condition" is the heat-treatment condition recommended for increasing notch toughness of this steel.

Most of SAE 4340 steel plate was oil quenched from 1550 F and tempered at 500 F for 1 hour. Mechanical properties of SAE 4340 steel after this treatment were:

Yield stress (at 0.2 percent offset) = 224,000 psi

Ultimate tensile strength = 260,700 psi

Elongation in 2-inch gage length = 14.0 percent.

Some weldments were made in SAE 4340 steel which had been given the following treatments:[11]

(1) As-rolled (approximate tensile strength: 150,000 psi)

(2) Oil quenched from 1550 F and tempered at 1000 F for 1 hour (approximate tensile strength: 175,000 psi)

(3) Oil quenched from 1550 F and tempered at 750 F for 1 hour (approximate tensile strength: 220,000 psi)

(4) Oil quenched from 1550 F and tempered at 600 F for 1 hour (approximate tensile strength: 240,000 psi).

Thus, welded specimens were made in steels with a variety of tensile strengths.

Fabrication of Welded Specimens

Sixty-three welded specimens were prepared, including 14 specimens made from mild steel, 5 from HY-80 steel, 7 from the commercial high-strength structural steel, and 37 from SAE 4340 steel. Various types of weldments were prepared to produce a variety of residual-stress distributions. Table 2 summarizes how these specimens were prepared (plate thickness, treatment prior to welding, types of

TABLE 2.   WELDED SPECIMENS.

Specimen Code Number	Plate Thickness, inch	Treatment Prior to Welding	Type of Specimen	Welding Process	Tests Conducted		
					Hydrogen Cracking	Stress Corrosion	Strain Measurement
1. MILD STEEL							
FM5	1/2	Stress relieved		Submerged arc		O	
FM6(a)	1/2	Stress relieved			O		
FM7	1/2		Simple butt joint 12" x 16"			O	
FM8(a)	1/2				O		
OM1	5/8(b)	Stress relieved		E6010			O
TM1	5/8		Simple butt joint, 24" x 38"				O
TM2	5/8				O		
C1	3/4		Simple butt joint, 12" x 16"			O	
GM1	2		Simple butt joint, 16" x 20"		O		
PB-1	3/4		Slit-groove weld, 12" x 16"	E7016 and E6010(d)	O		
PB-2	3/4	Stress relieved			O		
C2	3/4		Circular-groove weld	E6010		O	
C3	3/4					O	
3CM	7/16	Stress relieved	Complex structure, Type D				O
2. HY-80 STEEL							
FH1	1/2		Simple butt joint, 12" x 16"	E10016		O	
FH2(a)	1/2				O		
GH1	2		Simple butt joint, 16" x 20"	E11018	O		
PH-1	1/2		Slit-groove weld, 12" x 16"	E10016	O		
PH-2	1-1/2	Stress relieved			O		
3. COMMERCIAL HIGH-STRENGTH STRUCTURAL STEEL							
AT-B3	3/4	Soft Condition	Simple butt joint, 12" x 16"	E10016	O		
FT1	1/2			E10016 and E12015(e)	O	O	
FT2	1/2				O		
FT3(a)	1/2				O		
AT-B2	3/4	Hard Condition			O		
AT-B1	3/4		Butt joint with repair weld, 12" x 16"	E10016	O		
AT-F1	3/4		Fillet weld, heavy continuous		O		
4. SAE 4340 STEEL							
4-1. Butt Joints and Groove Welds							
P4-1	3/4	As rolled	Slit-groove weld, 12" x 16"	MIG (4340 wire)	O		
R5	5/8(b)	Tempered at 1000 F	Simple butt joint, 12" x 16"	E15016	O		

Notes: (a) Welds were radiographed before hydrogen charging tests.

     (b) Ground to 1/2 inch thick after welding.

     (c) Bead-on-plate specimens were mechanically stress relieved by loading the specimens in a testing machine.

     (d) E7016 electrodes were used for the first pass.

     (e) E10016 electrodes were used for the first pass.

TABLE 2. (Continued)

Specimen Code Number	Plate Thickness, inch	Treatment Prior to Welding	Type of Specimen	Welding Process	Hydrogen Cracking	Stress Corrosion	Strain Measurement
4-1. Butt Joints and Groove Welds (Continued)						
R4	5/8(b)	Tempered at 750 F		E15016	O		
P4-3	3/4	Tempered at 600 F			O		
F41	1/2		Simple butt joint, 12" x 16"	MIG (6130 wire)		O	
F43	1/2					O	
F45(a)	1/2				O		
F47	1/2				O		
F48	1/2					O	
F49(a)	1/2				O		
R1	5/8(b)						O
O41	5/8(b)				O		
O42	5/8(b)			E15016	O		
R2	5/8(b)				O		
R3	5/8(b)				O		
T41	5/8	Tempered at 500 F	Simple butt joint, 24" x 38"				O
T42	5/8		Simple butt joint 26" x 38"		O		
T43N	5/8		Simple butt joint, 21" x 38"	Narrow-Gap	O		
S1	3/4		Simple butt joint, 12" x 16"				O
S2	3/4		Simple butt joint, 18" x 32"				O
B21-1	1/2		Butt joint with repair weld, 12" x 16"	E15016	O		
B23	1/2		Cross-butt joint		O		
B32	1/2		Circular-groove weld		O		
4-2. Fillet Welds and Complex Structures						
A4-F1	5/8		Fillet weld, heavy continuous		O		
A4-F2	5/8		Fillet weld, light continuous		O		
A4-F3	5/8		Fillet weld, heavy intermittent		O		
A4-F4	5/8	Tempered at 500 F	Fillet weld, light intermittent		O		
B11	1/2		Complex structure, Type A	E15016	O		
B12	1/2		Complex structure, Type B		O		
B13	1/2		Complex structure, Type C		O		
3C41	7/16		Complex structure, Type D				O
3C42	7/16				O		
4-3. Bead-on-Plate Specimens for Studying Effects of Mechanical Stress Relieving						
D8	1/4(c)		As welded(c)		O		
D3	1/4(c)	Tempered at 500 F	Loaded to 20 percent of yielding(c)	E15016	O		
D4	1/4(c)		Loaded to 40 percent of yielding(c)		O		
D5	1/4(c)	Tempered at 500 F	Loaded to 60 percent of yielding(c)	E15016	O		
D6	1/4(c)		Loaded to 80 percent of yielding(c)		O		

specimen, and welding process) and how they were used.* Forty-five specimens were used for the hydrogen-induced-cracking tests, 10 for the stress-corrosion-cracking tests, and 8 for the measurement of residual stresses by stress-relaxation techniques.

Types of Welded Specimens. Eight types of welded specimens were prepared:

    (1) Simple butt joints, as shown in Figure 1

    (2) Butt joints with repair welds

    (3) Slit-groove welds, as shown in Figure 2(a)

    (4) Cross butt joint, as shown in Figure 2(b)

    (5) Circular-groove welds, as shown in Figure 2(c)

    (6) Fillet welds, as shown in Figure 3

    (7) Complex welded structures, as shown in Figure 4

    (8) Bead-on-plate specimens.

The simple butt joint, shown in Figure 1(a), can be considered as the typical welded joint. Thirty-seven simple butt joints of various sizes were prepared. Most specimens were 1/2 by 12 by 16 inches when welded. Large welds in heavy plates up to 2-1/2 inch thick, 26 inches wide, and 38 inches long, also were prepared in an attempt to produce maximum residual-welding stresses. Figure 1(b) shows the single-vee bevel used for 1/2-inch-thick joint. For heavy plates, double-vee bevels were used, as shown in Figure 1(c). Figure 1(d) shows the joint preparation for the Narrow-Gap welding of a 5/8-inch-thick plate.

To study the effect of repair welds on the distribution of residual stresses, repair welds were made on two butt joints, 12 by 16 inches in size. On Specimen B21-1 made in SAE 4340 steel, the weld metal in a 6-inch-long portion in the center of the 16-inch-long weld was removed and a short transverse groove, about 2 inches long, also was made at one end of the 6-inch-long portion; then these longitudinal and transverse grooves were welded.** A similar repair weld was made in Specimen AT-B1 made from the commercial high-strength structural steel.

Five slit-groove welds, as shown in Figure 2(a), were prepared. A 6-inch-long straight groove was made in a plate 12 by 16 inches and the groove was welded. In the slit-groove weld, a sudden change of residual-stress distribution occurs at the end of the weld.

Figure 2(b) shows a cross-butt joint (Specimen B23). Figure 2(c) shows Specimen B32, an SAE 4340 steel specimen which had a circular groove 3 inches in diameter. A similar circular-groove weld was made in mild steel (Specimen C3).
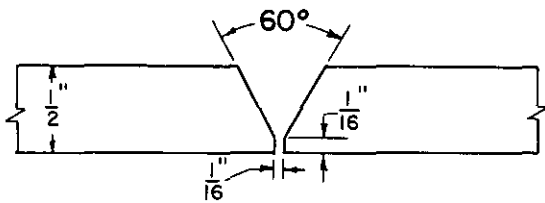
---

* Table 2 also shows BMI reports, prepared under Contracts Nos. NObs-77028 and NObs-84738, which contain detailed information on the specimens.

** See Figure 10.
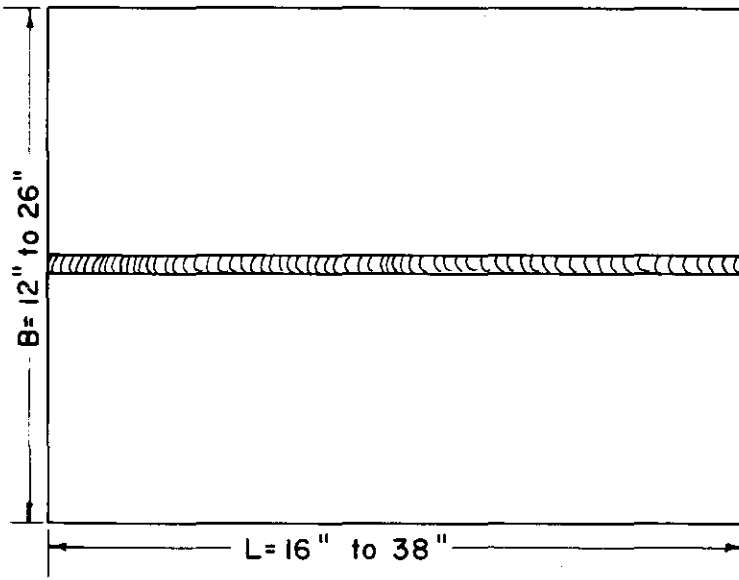
a. General View

b. Joint Preparation for 1/2-Inch-Thick Plate (Shielded Metal-Arc, Submerged Arc, and MIG Processes), Specimens FM5, FM6, FM7, FM8, FH1, FH2, FT1, FT2, FT3, F41, F43, F45, F47, F48, and F49
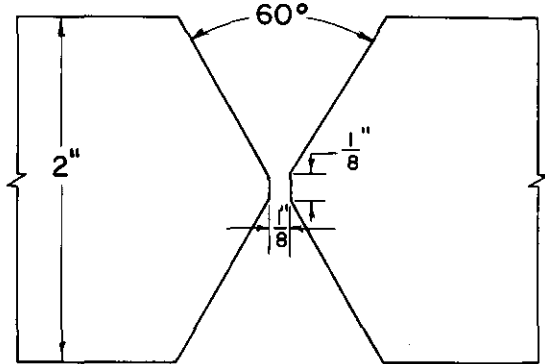
c. Joint Preparation for 2-Inch-Thick Plate (Shielded Metal-Arc Process), Specimens GM1, GH1, and GH2
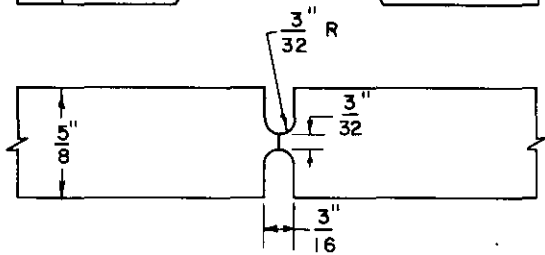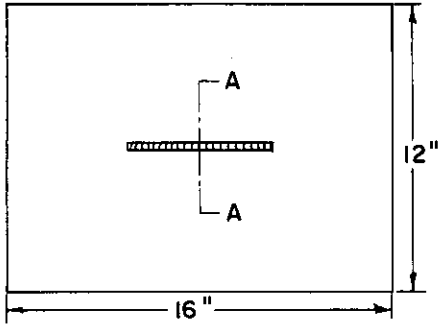
d. Joint Preparation for the Narrow-Gap Process (5/8-Inch-Thick Plate), Specimen T43N

Fig. 1.   Simple Butt Joints.

Figure 3 shows fillet welds made in SAE 4340 steel. The following specimens were prepared:

(1) Heavy, continuous welding (Specimen A4-F1)

a. Slit-Groove Weld

Section A-A
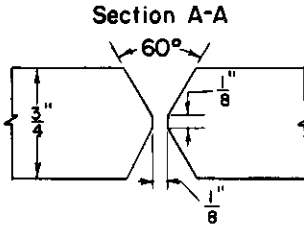
Joint preparation for 3/4-inch-
thick plate, Specimens PB-I,
PB-2, C2, P4-I
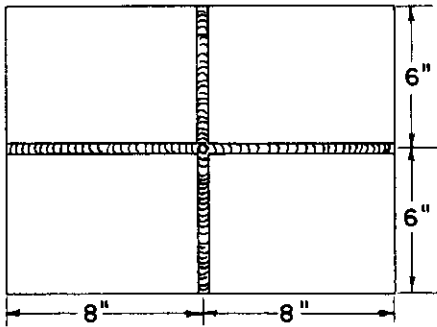
b. Cross-Butt Joint, Specimen B23
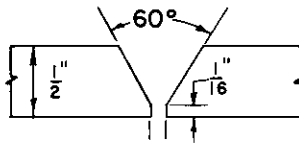
Joint preparation

Fig. 2. *Slit -
groove weld,
cross - butt
joint, and
circular -
groove weld.*

Section B-B

Joint preparation
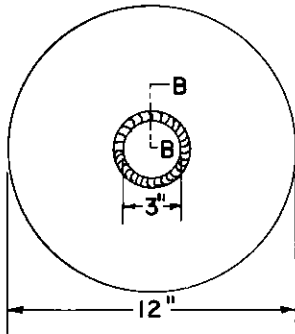
c. Circular-Groove (3 inches in diameter) Weld, Specimen B32

    (2) Light, continuous welding (Specimen A4-F2)

    (3) Heavy, intermittent welding (Specimen A4-F3)

    (4) Light, intermittent welding (Specimen A4-F4).

The heavy welds were made in six passes, while one pass was used to make the light
weld. Figure 3(b) shows the intermittent weld; 2-inch-long welds with a 4-inch
pitch. A fillet weld also was prepared with the commercial high-strength structural
steel plate 3/4 inch thick, Specimen AT-F1. The specimen was welded with the
heavy, continuous technique.

a. General view,
continuous weld

b. Intermittent weld
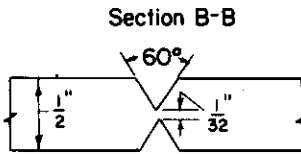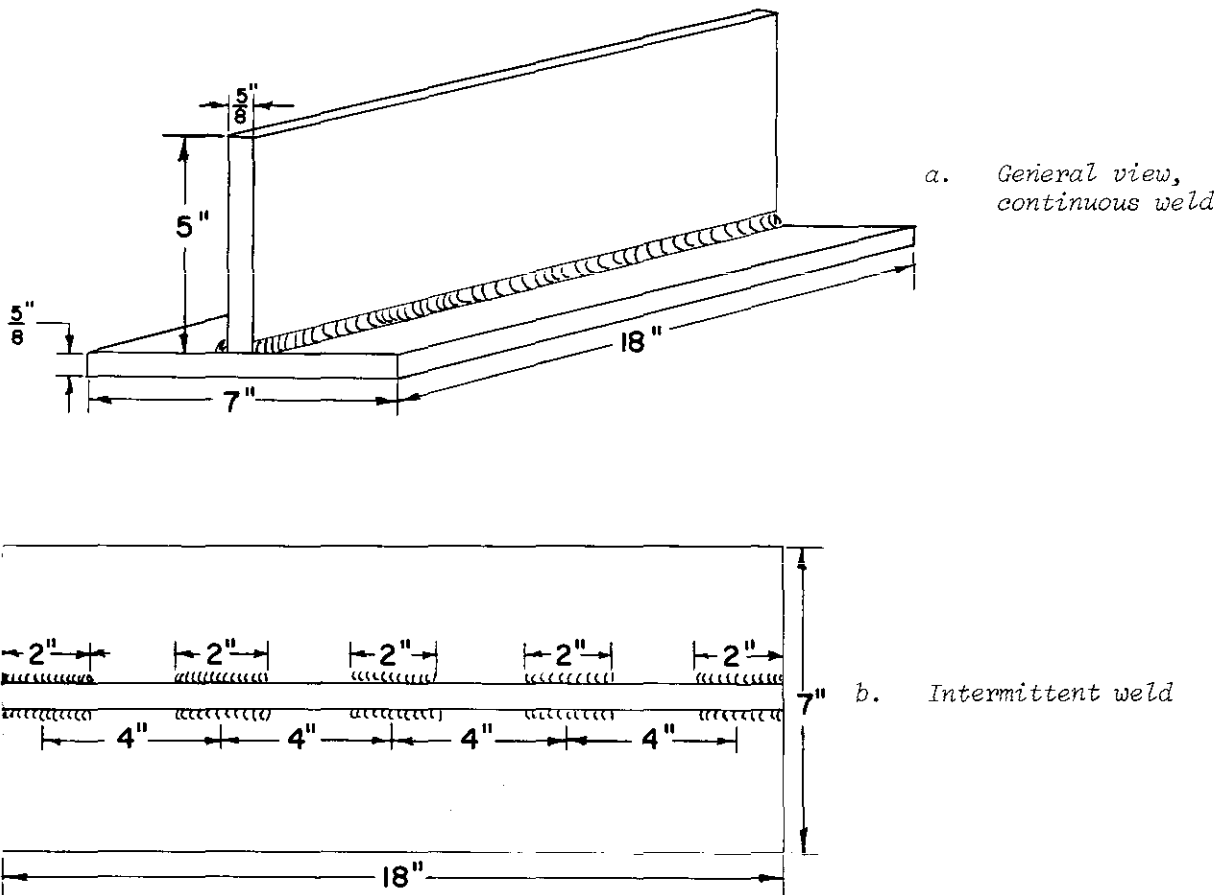
Fig. 3. Fillet welds, SAE 4340 steel specimens A4-F1, A4-F2, A4-F3, and A4-F4.
Commercial high-strength heat-treated structural-steel specimens were
prepared with 3/4-inch-thick plates.

To study residual stresses in complex welded structures, four types of
complex structures were prepared:

Type A: structure with directly intersecting longitudinal and
          transverse frames, as shown in Figure 4(a):   Specimen B11

Type B: structure with a through longitudinal frame and transverse
          frames with 2-inch-radius cut-outs, as shown in Figure
          4(b):   Specimen B12

Type C: structure with longitudinal and transverse frames both
          having 2-inch-radius cut-outs: Specimen B13

Type D: structure with a longitudinal frame, as shown in Figure
          4(c):   Specimens 3CM, 3C41, and 3C42.

Types A, B, and C structures were made with a longitudinal through frame
and two transverse frames welded to a bottom plate. One end of the longitudinal
frame continued to a free edge of the bottom plate, while the other end stopped
short of the opposite free edge of the bottom plate, making an abrupt structural
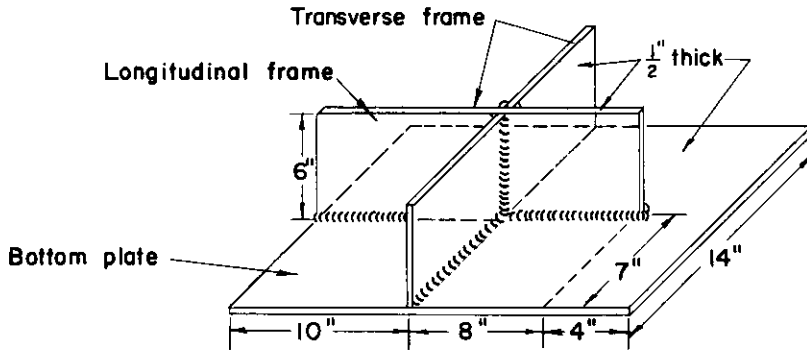
a. Type A, Structure With Directly Intersecting Longitudinal and
Transverse Frames, Specimen B II
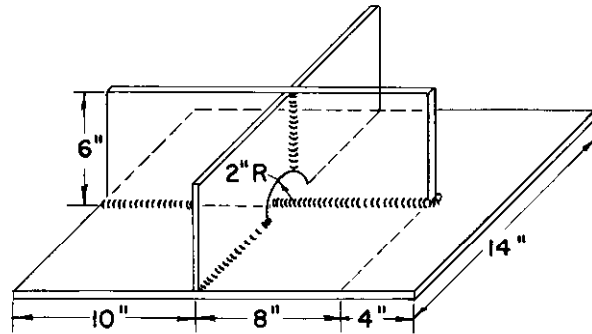
b. Type B, Structure With a Through Longitudinal Frame and Transverse
Frames With 2-Inch-Radius Cutouts, Specimen B 12
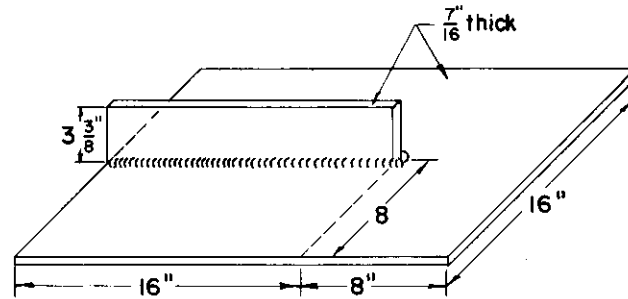
c. Type D, Structure With a Longitudinal Frame, Specimens 3CM,
3C41 and 3C42

*Fig. 4.   Complex welded structures.   Type C is a structure with longitudinal
and transverse frames both having 2-inch-radius cutouts, Specimen B13.*

discontinuity. These specimens were made from heat-treated SAE 4340 steel plates
1/2 inch thick, and they were used for the hydrogen-induced-cracking tests.

Type D had a longitudinal frame and a bottom plate. These specimens
were prepared from mild steel and SAE 4340 steel plates 7/16 inch thick, and they
were used as follows:

(1)   Specimen 3CM, made in mild steel, and Specimen 3C41, made in
SAE 4340 steel, were used for measuring residual stresses by
stress-relaxation techniques

(2) Specimen 3C42, made in SAE 4340 steel, was used for the hydrogen-induced-cracking test.

Bead-on-plate specimens were prepared from 1/2-inch-thick SAE 4340 steel plates oil quenched and tempered at 500 F. The specimens were 3-1/2 by 16 inches, and a 9-inch-long section in the center of the specimen was reduced to 1/4-inch thickness by grinding before welding. After weld beads were laid on both surfaces of the reduced section, the specimens were loaded in a testing machine to different stress levels. The objective of this phase of research was to determine whether hydrogen-induced cracking is caused by residual stresses or by plastic strains. Since high-tensile longitudinal residual stresses exist in regions near the weld, additional plastic deformation occurs in the regions when a tensile load in the longitudinal direction is applied to the welded specimen. However, the magnitude of residual stress decreases because of this additional plastic strain. This phenomenon is known as "mechanical stress relieving". If hydrogen-induced cracking is sensitive to plastic strain, more cracking should occur in mechanically stress-relieved specimens than in as-welded specimens. If hydrogen cracking is sensitive to stress, there should be less cracking in mechanically stress-relieved specimens.

Welding Procedures. Most specimens were welded with covered electrodes. The electrodes used for each type of steel were as follows:

Mild steel: E6010 (E7016 electrodes also were used on some specimens)

HY-80 steel: E10016 and E11018

Commercial high-strength structural steel: E10016 and E12015

SAE 4340 steel: E15016.

Several different diameters of electrodes, ranging from 1/8 inch to 3/16 inch were used. Each specimen was welded with suitable-size electrodes under the optimum conditions for the joint design and thickness. For example, typical welding conditions for E15016 electrodes were about 120 amperes for 1/8-inch-diameter electrodes, about 150 amperes for 5/32-inch-diameter electrodes, and about 170 amperes for 3/16-inch-diameter electrodes.

Several specimens were welded with submerged-arc, inert-gas metal-arc (MIG), and the Narrow-Gap welding process. The Narrow-Gap process is a new automatic gas-shielded metal-arc welding process developed at Battelle for the Bureau of Ships (Contract No. NObs-86424).[12] Very narrow welds--say a 1/4-inch-wide square-butt weld for a 2-inch-thick plate--can be made by this new process.

Two mild-steel specimens (FM5 and FM6) were welded with the submerged-arc process as follows:

Electrode: mild steel, 5/32 inch in diameter

Welding conditions: welding current, 550 amperes; arc voltage, 30 volts; travel speed, 17 ipm for backing passes and 25 ipm for the finishing pass; contact-to-work distance, 3/4 inch.

Four SAE 4340 steel specimens were welded with the inert-gas metal-arc process. Specimens F41, F43, and F45 were welded as follows:

Electrode: SAE 6130, 1/16 inch in diameter

Shielding gas: argon containing 2 percent oxygen

Welding conditions: welding current, 320-360 amperes; arc voltage, 30 volts; travel speed, 17 ipm; contact-to-work piece, 3/4 inch; shield-gas flow, 50 cfh.

Specimen P4-1 was welded with the MIG process using SAE 4340 steel wire 1/16 inch in diameter. Specimen T43N was welded with the Narrow-Gap process as follows:

Electrode: H-11, 0.035 inch in diameter

Shielding gas: 80 percent argon and 20 percent CO_2

Welding conditions: welding current, 190-200 amperes; arc voltage, 26 volts; travel speed, 18 ipm; wire-feed rate, 450 ipm; contact-to-work distance, 1/2 inch; shield-gas flow, 50 cfh.

The joint shown in Figure 1(d) was welded in four passes.

Preheat was not used on mild steel, HY-80 steel, and the commercial high-strength structural steel specimens. Most SAE 4340 steel specimens were welded with 400 F preheat and interpass temperature. A preheat and interpass temperature of 350 F was used on the bead-on-plate specimens used in the experiment on mechanical stress relieving since they had small heat capacity.

Inspection After Welding. All welded specimens were inspected to ensure that the specimens did not contain cracks before further testing.* Some specimens were radiographically inspected.

Mechanical Stress Relieving. The bead-on-plate specimens were mechanically stress relieved by loading in a testing machine to various stress levels as follows:

	Applied Stress, psi	Ratio of Applied Stress to Tensile Yield Stress
Specimen D3	45,200	0.20
Specimen D4	90,000	0.40
Specimen D5	134,000	0.60
Specimen D6	180,000	0.805

Specimen D8 was hydrogen charged in the as-welded condition.

---

* Specimens which had cracks were discarded or rewelded.

TABLE 3. SUMMARY OF PROCEDURES AND RESULTS OF HYDROGEN-INDUCED-CRACKING TESTS ON WELDED SPECIMENS.

| Specimen Code Number | Description of Specimen | Hydrogen-Charging Test Conditions | | | | Results |
		Current, amperes	First Checking Time After Cracking, hours	Total Charging Time, hours	Special Treatments[a]	
			1. MILD STEEL			
FM6	Simple butt joint, submerged arc	300		47	R	No crack
FM8	Simple butt joint	300		126-1/2	R	No crack
TM2	Large butt joint	130		219	C,S	Very small cracks in HAZ
GM1	2" thick large butt joint	350		379		Very small cracks in HAZ
PB-1	Slit-groove weld	300		20	E	No crack
PB-2	Slit-groove weld	300		18-1/2	E	No crack
			2. HY-80 STEEL			
FH2	Simple butt joint	300		140-1/2	R	No crack
JH1	2" thick large butt joint	350	73-1/4	216	X	Transverse cracks (Figure 6)
PH-1	Slit-groove weld	300		20	E	No crack
PH-2	1-1/2" thick slit-groove weld	300		22	E	Small cracks in HAZ
			3. COMMERCIAL HIGH-STRENGTH STRUCTURAL STEEL			
AT-B3	Soft condition, butt joint	300		4-1/2	E	No crack
FT2	Hard condition, butt joint			7-3/4	X	Cracks were observed after 24 hours without further hydrogen charging after 7-3/4 hours
FT3	Hard condition, butt joint	300	16-1/2	24	R,X	One crack extended greatly in the last 7-1/2 hours of charging
AT-B2				15	E	No crack
AT-B1	Hard condition, butt joint with repair			5	E	No crack
AT-F1	Hard condition, fillet weld			18	E	Long longitudinal crack on back surface of bottom plate

Notes: (a) Special treatments: R = radiographed before hydrogen charging
E = electropolished before hydrogen charging
O = observation of cracks during hydrogen-charging test
C = cooling the specimen to embrittle the material
B = baking in a furnace immediately after hydrogen-charging test
X = radiographic inspection of hydrogen-induced cracks
S = sectioning specimen for inspecting cracks.

(b) All SAE 4340 steel specimens except Specimens P4-1, R5, R4, and P4-3 were oil quenched and tempered at 500 F.

TABLE 3. (Continued)

4. SAE 4340 STEEL

4-1. Butt Joints and Groove Welds[b]

P4-1	As rolled, slit groove, MIG	300		14	E	No crack
R5	Tempered at 1000 F, butt joint	} 150	2	6-3/4	O	Transverse cracks, average length 1-1/4" (Figure 7)
R4	Tempered at 750 F, butt joint		About 1	6	O	Transverse cracks, average length 1-1/4"
P4-3	Tempered at 600 F, butt joint	300		1	E	Transverse cracks, average length 3-1/2"
F45	Simple butt joint, MIG		4	7	R,X	Transverse cracks, average length 2-1/2"
F47	} Simple butt joints		2-3/4	2-3/4	X	Transverse cracks, average length 2"
F49			4-1/2	4-1/2	X	Transverse cracks, average length 2-1/2"
O41			3/4	3	O	Transverse cracks, average length 2"
O42	} Simple butt joint	} 150	4/5	2-1/4	O	Transverse cracks, average length 2-1/2", and longitudinal crack along HAZ (Figure 8)
R2			5/6	2	O,B	Transverse cracks, average length 3", and longitudinal crack along HAZ (Figure 9)
R3			1-1/6	1-1/3	O,B	One transverse crack, 1-1/2" long and short transverse cracks
T42	Large butt joint	130		1	B	Transverse cracks, average length 4"
T43N	Large butt joint, Narrow-Gap process	130		1/4		Short transverse cracks about 1-1/2" long
B21-1	Butt joint with repair welds	250		5	E	Cracked (Figure 10)
B23	Cross-butt joint	270		3	E	Cracked (Figure 11)
B32	Circular-groove weld	150		4-1/2	E	Cracked (Figure 12)

4-2. Fillet Welds and Complex Structures

A4-F1	Heavy, continuous fillet weld	} 300	16	E	Cracked (Figure 13)
A4-F2	Light, continuous fillet weld		6	E	Cracked (Figure 14)
A4-F3	Heavy, intermittent fillet weld	} 300	6-1/2	E	Cracked (Figure 15)
A4-F4	Light, intermittent fillet weld		15	E	Cracked (Figure 16)
B11	Type A	} 350	3	E	Cracked (Figure 17)
B12	Type B		2-1/2	E	Cracked
B13	Type C		2-1/2	E	Cracked (Figure 18)
3C42	Type D		1-1/2	B,X	Cracked

4-3. Bead-on-Plate Specimens for Studying Effects of Mechanical Stress Relieving

D8	As welded			E	Cracked (Figure 19a)
D3	20 percent yield			E	Cracked
D4	40 percent yield	} 75	} 6	E	Cracked (Figure 19b)
D5	60 percent yield			E	Cracked
D6	80 percent yield			E	No crack (Figure 19c)

Hydrogen-Induced-Cracking Tests on Weldments

Experimental hydrogen-induced-cracking tests were made on 45 weldments including 6 mild-steel weldments, 4 HY-80 steel weldments, 6 commercial high-strength structural-steel weldments, and 29 SAE 4340 steel weldments. Table 3 summarizes procedures and results of hydrogen-induced-cracking tests on welded specimens.

Experimental Methods

Cleaning Specimen Surfaces. Except in case of large butt-welded joints, specimen surfaces were ground either before or after welding to get smooth, clean surfaces. During the early stage of this research, specimen surfaces were further electropolished to remove thin layers (about 1.5 mil thick) affected by grinding and to eliminate possible effects of residual stresses caused by the grinding operation. Those specimens that were electropolished are identified in Table 3 by Notions E. Electropolishing operations were omitted in later tests, since it was found that the electropolishing had little effect on the hydrogen-induced crack pattern.

Hydrogen-Induced-Cracking Test Procedure. The specimens were charged with hydrogen by immersing them in an electrolyte with the specimens as the cathode of a cell. The electrolyte was 4 percent H_2SO_4 to which was added 5 drops per liter of poison. The poison was 2 grams of phosphorus dissolved in 40 milliliters of carbon disulfide. The anode was a set of lead strips.

Figure 5 shows the hydrogen-charging test set-up used on Specimens R5, R4, 041, 042, R2, and R3.[*] The electrolyte, approximately 200 liters in volume, was kept in a barrel. The specimens were placed in a container which had transparent walls so that the initiation and propagation of cracks could be observed. The electrolyte was circulated by a pump between the barrel and the container. A d-c welding generator was used as the power source. Hydrogen gas generated during the test was removed from the container through a duct. Other welded specimens were placed in the barrel or a specially made large tank, instead of the container, during the hydrogen-induced-cracking test.

The current density ranged between 0.35 to 0.8 amperes per square inch of exposed specimen surface. In the test of fillet welds and complex welded structures, efforts were made to concentrate the electric current in the weld area; lead anodes were placed near the corner of the fillet welds and edges of frames of the complex structures were covered with a plastic tape. The total charging time ranged from 15 minutes for an SAE 4340 steel specimen (T43N) to 379 hours for a mild-steel specimen (GM1). When hydrogen charging was conducted for longer than 48 hours, poison was added to the electrolyte at a rate of approximately 1.5 drops per liter of the electrolyte for every 48 hours' charging.

Most specimens were at room temperature before and after hydrogen charging. Specimen TM2, a mild-steel butt joint 5/8 by 24 by 38 inches in size, was cooled to -30 F after hydrogen-charging tests in an attempt to embrittle the material and to promote cracking.

---

[*] Two press-fit specimens (K4, LT1) also were hydrogen charged in the container.
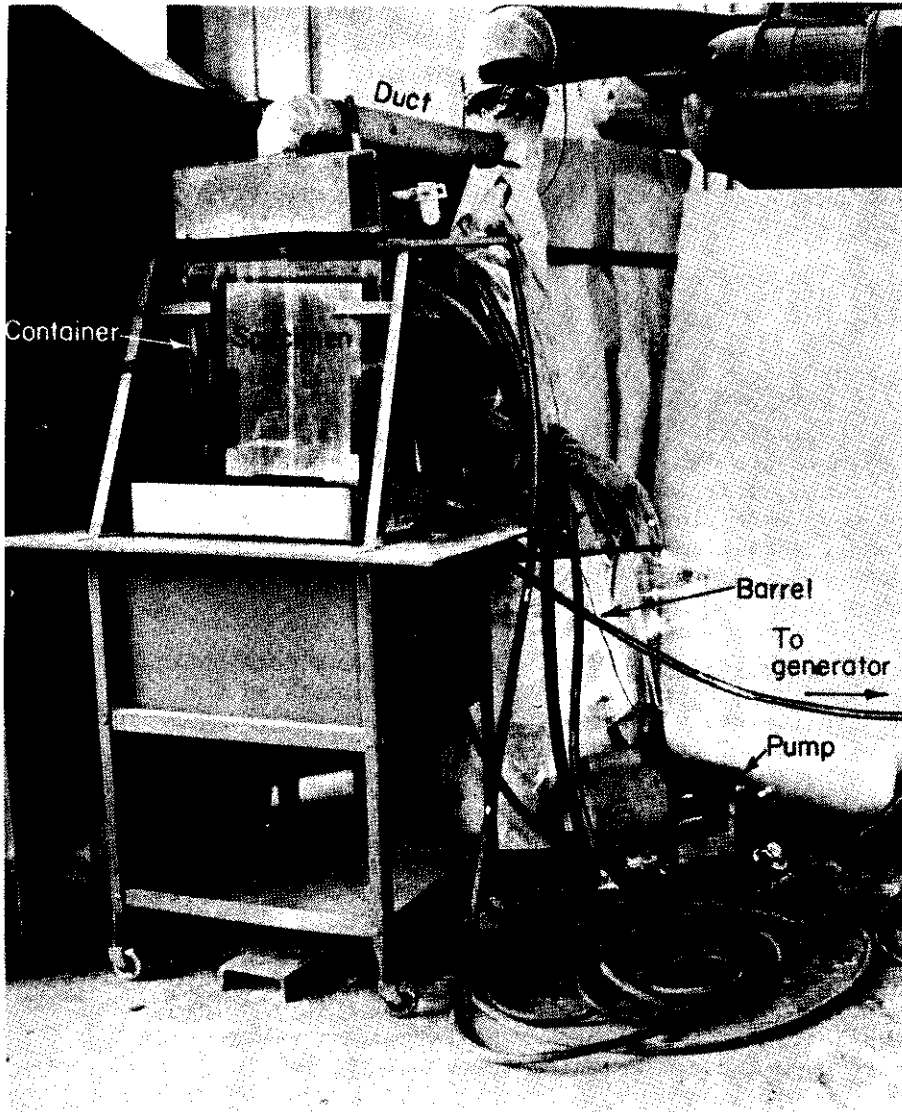
Fig. 5. *Set-up for hydrogen-induced cracking tests on some welded specimens and press-fit specimens. The specimens were hydrogen charged in a container with transparent walls. The electrolyte was circulated by a pump between the container and the barrel. Other specimens were hydrogen charged in the barrel or a specially made large tank.*

Inspection for Cracking. On those specimens that were hydrogen charged in the container with transparent walls, the specimen surfaces were inspected for cracking during the hydrogen-charging test. The d-c generator was turned off, at short intervals, to eliminate hydrogen bubbles in the electrolyte so that inspection of the specimen surface was better. When a specimen was hydrogen charged in the barrel the hydrogen charging was interrupted occasionally and the specimen was removed from the electrolyte to inspect for cracking.

After the hydrogen-induced-cracking test, all specimens were inspected for cracking by use of liquid penetrants. Some specimens were radiographically inspected for hydrogen-induced cracks; these specimens are identified in Table 3 by Notations X. On Specimen TM2, sections were cut from the plate and examined for cracking.

Fig. 6. *Radiograph of simple-butt joint (Specimen GHT) made from HY-80 steel 2 inches thick after hydrogen-induced-cracking test for 216 hours. The weld runs vertically through the center of the picture.*

Weld

Baking Specimens After Hydrogen Charging.

During this Research, it was found that hydrogen-induced cracks often extended without further hydrogen charging and the extended cracks caused misinterpretation of the residual-stress pattern. An investigation was made of the effectiveness of taking the specimens after the hydrogen charging to remove hydrogen and to prevent the delayed fracture. Immediately after hydrogen-charging operations were completed, two specimens (R2 and R3) were placed in a furnace at 400 F for 2 hours on Specimen R2 and for 1 hour on Specimen R3. Specimens T42 and 3C42 also were baked at 400 F for 2 hours.

Experimental Results, Part 1 Effects of Types of Steel, Heat Treatment, and Plate Thickness on Hydrogen-Induced-Cracking Test Results

Results of hydrogen-induced-cracking tests on welded specimens are summarized in Table 3. The specimens were prepared from four types of steels with various strength levels as follows:

	Approximate Tensile Strength, psi	Number of Specimens Tested
Mild steel (as rolled)	75,000	6
HY-80 steel (quenched and tempered)	100,000	4
Commercial high-strength structural steel (treated to the "soft condition")	120,000	1
Commercial high-strength structural steel (treated to the "hard condition")	150,000	5
SAE 4340 steel (as rolled)	150,000	1
SAE 4340 steel (oil quenched and tempered at 1000 F)	175,000	1
SAE 4340 steel (oil quenched and tempered at 750 F)	220,000	1
SAE 4340 steel (oil quenched and tempered at 600 F)	240,000	1
SAE 4340 steel (oil quenched and tempered at 500 F)	260,000	25

Mild Steel. Six mild-steel specimens 1/2 to 2 inches thick were charged with hydrogen up to 379 hours. In order to promote cracking, the following variations were investigated:

(1) Large welds were made in heavy plate to obtain maximum residual stresses

(2) Long time hydrogen charging

(3) Cooling specimens after hydrogen charging to embrittle the material.

For example, Specimen TM2 (a simple butt joint 5/8 by 24 by 38 inches in size) was hydrogen charged for 1 hour, removed from the electrolyte and cooled to -300 F for 1 hour. The test was repeated with the charging time increased to 2 hours. Charging was resumed and continued for an additional 216 hours and then the specimen was cooled to -30 F for 4 hours. No cracks were visible on the surface after these operations. Sections were cut from the plate and examined for cracking; very small cracks were found in the heat-affected zone. Very small cracks also were found in the heat-affected zone of Specimen GM1 (a simple butt joint 2 by 16 by 20 inches in size) hydrogen charged for 379 hours. No cracks were found in 4 other specimens hydrogen charged up to 126-1/2 hours.

HY-80 Steel. Four HY-80 steel specimens 1/2 to 2 inches thick were charged with hydrogen up to 216 hours. Figure 6 shows a print of a radiograph of a 2-inch-thick butt joint (Specimen GH1) after hydrogen charging for 216 hours. Transverse cracks were obtained in the weld metal. Some cracks appeared to be quite deep, but the cracks did not appear to penetrate into the base plate. Small cracks were observed in the heat-affected zone of a 1-1/2-inch-thick weld (Specimen PH-2), but no cracks were found in Specimens FH2 and PH-1.

Commercial High-Strength Structural Steel. A hydrogen-induced-cracking test was conducted on one weldment made in the commercial high-strength structural steel heat treated to the "soft condition". No cracks were observed after hydrogen charging for 4-1/2 hours.
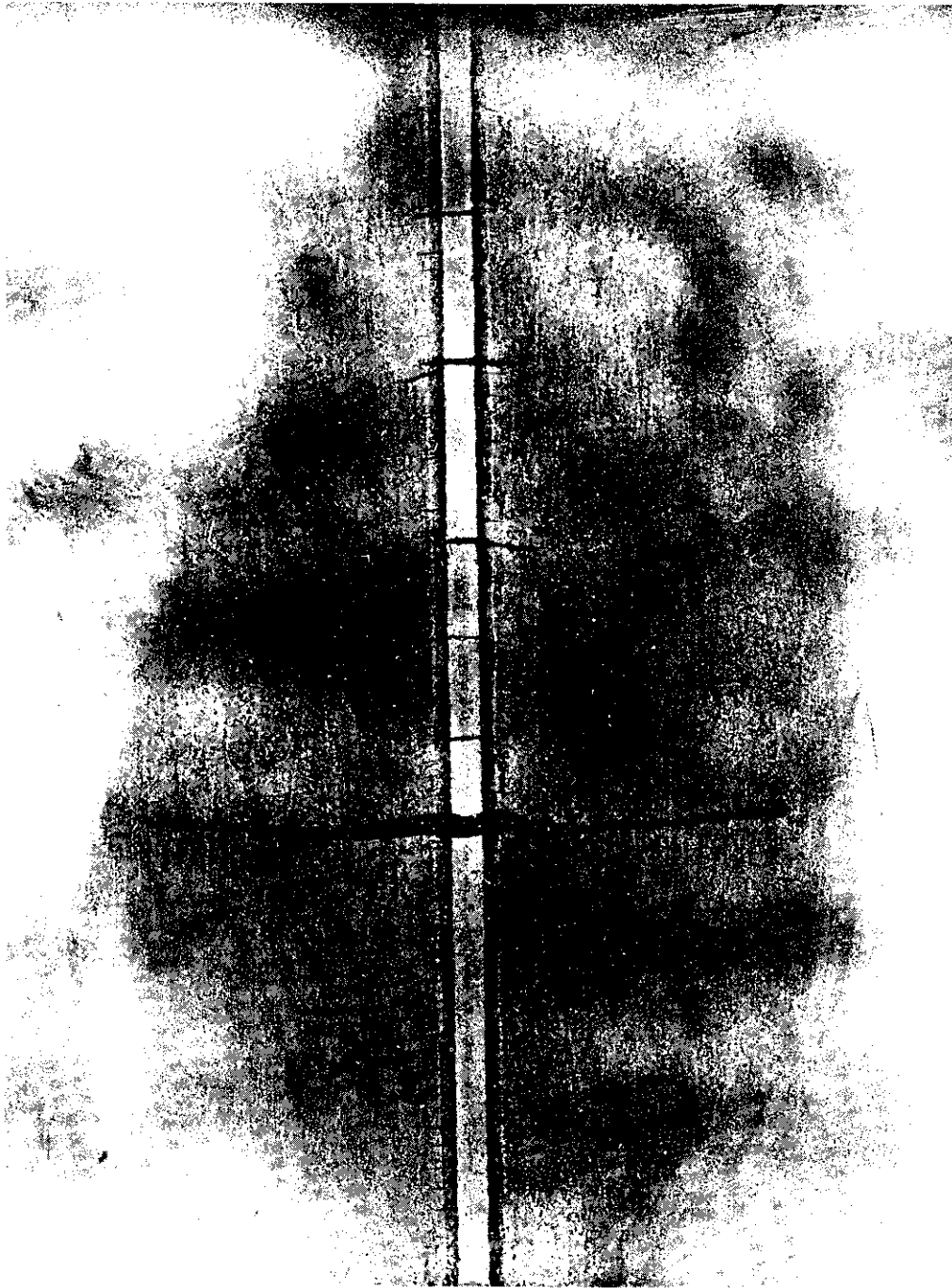
Fig. 7.   Crack patterns in a simple-butt joint made from SAE 4340 steel oil quenched and tempered at 1000 F (Specimen F5) after hydrogen-induced-cracking test for 7-3/4 hours.

Hydrogen-induced-cracking tests were made on five weldments of the commercial high-strength structural steel heat treated to the hard condition. Cracks were found in three weldments. Several cracks were found in the weld metal after charging for 7-3/4 hours in a butt joint (Specimen FT2), and some of

them extended into the base plate without further charging. A few short cracks were found after 16-1/2 hours of charging another butt joint (Specimen FT3), and one of them extended to the edge of the specimen after charging for 24 hours. A longitudinal crack was found in the back surface of the bottom plate in the fillet weld (Specimen AT-F1).

SAE 4340 Steel. A hydrogen-induced-cracking test was conducted on one weldment made in SAE 4340 steel in the as-rolled condition. No cracks were observed after charging for 14 hours.

Several very short cracks in the heat-affected zone were observed after hydrogen charging for 2 hours on Specimen R5 made in SAE 4340 steel oil quenched and tempered at 1000 F. The initial cracks grew and the number of cracks increased when hydrogen charging was continued. A system of transverse cracks, as shown in Figure 7, was obtained after hydrogen charging for 6-3/4 hours. One pair of cracks in the central part of the specimen, shown in Figure 7, grew quite long after hydrogen charging was stopped.

On Specimen R4 made in SAE 4340 steel oil quenched and tempered at 750 F, a set of cracks, about 1-1/2 inches long on both sides of the crack (the crack in one side was curved), was observed after hydrogen charging for 30 minutes. A number of very short cracks were formed in the heat-affected zone while the hydrogen-induced-cracking test was continued. The crack pattern obtained after hydrogen charging for 6 hours was similar to that shown in Figure 7. A pair of long transverse cracks in the central part of the specimen grew after hydrogen charging was stopped.

A system of transverse cracks was found after 1 hour of hydrogen charging of Specimen P4-3 made in SAE 4340 steel oil quenched and tempered at 600 F. The crack pattern was similar to that obtained on butt joints made in SAE 4340 steel oil quenched and tempered at 500 F.

Hydrogen-induced-cracking tests were conducted on 25 welded specimens made in SAE 4340 steel oil quenched and tempered at 500 F. Extensive cracks were observed in all specimens except one (Specimen D6) which had been mechanically stress relieved by loading to 80 percent of the yield stress. For example, Figures 8a and b show crack patterns obtained on Specimen 042, a simple butt joint. During the hydrogen charging test, the d-c generator was turned off at 5-minute intervals to inspect the specimen surface for cracking. Fine lines which appeared to be cracks, were observed in the heat-affected zone parallel to the weld after hydrogen charging for about 20 minutes. No systematic cracks, however, were observed until the specimen was charged for 45 minutes. A system of transverse cracks was observed after hydrogen charging for 46 to 47 minutes. The photograph in Figure 8a shows the specimen in the container after hydrogen charging for 50 minutes. Transverse cracks and longitudinal cracks along the heat-affected zone were obtained in this time. Hydrogen charging was continued for 2-1/4 hours when some of the cracks started to extend as shown in Figure 8b. Figures 8a and b show that few new cracks were formed if hydrogen charging was continued longer than 50 minutes. Some of the original cracks did extend during the additional charging time.

Figure 9 shows the crack pattern obtained on Specimen R2, another simple butt joint made in SAE 4340 steel oil quenched and tempered at 500 F. Several transverse cracks were observed after hydrogen charging for 40 minutes. The hydrogen charging was continued for 10 more minutes until systematic cracks

Fig. 8a. *Crack pattern after hydrogen-induced-cracking test for 50 minutes.*
Crack patterns observed on a simple-butt joint made from SAE 4340
steel oil quenched and tempered at 500 F (Specimen 042).

were obtained, then the specimen was placed in a furnace at 400 F for 2 hours
to allow hydrogen to diffuse from the specimen. Transverse and longitudinal
cracks were obtained in the heat-affected zone. No appreciable change of crack
pattern was observed after baking. Apparently, sufficient hydrogen was removed
from the specimen to stop delayed cracking.

        The above mentioned experimental results clearly show that the tendency
of a weldment for hydrogen-induced cracking is affected by the properties of the
base plate. As the tensile strength of the base plate increases, more extensive
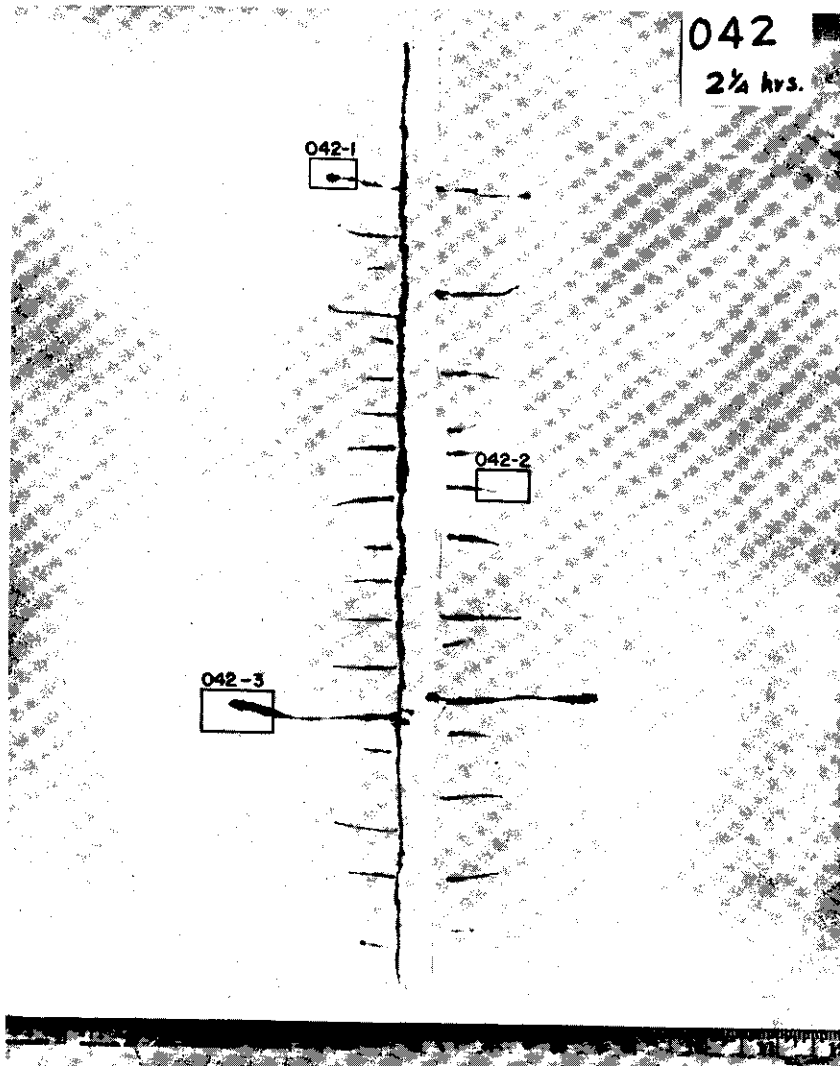cracks are formed in a shorter period of hydrogen charging.

Fig. 8b. Crack pattern after hydrogen-induced-cracking test for 2-1/4 hours.
Specimens 042 - 1, 042 - 2, and 042 - 3 were taken for metallographic
examinations of fracture surfaces.

Figures 6 through 9 show that the typical crack pattern in butt joints
was composed of transverse cracks in areas near the weld. These transverse cracks
were apparently caused by the high-tensile-longitudinal residual stresses that
were present in the vicinity of the weld. As shown clearly in Figure 9, the
lengths of cracks were uniform in the central portion of the weld but they grad-
ually decreased in length in regions several inches from the edge of the plate,
and there were no cracks near the plate edge. The results indicate that longi-
tudinal residual stresses are less significant in regions near the plate edge.

Effect of Plate Thickness. A limited study was made of the effect of
weldment plate thickness on the tendency for hydrogen-induced cracking. Hydrogen-
induced-cracking tests were made on heavy weldments up to 2 inches thick in mild
steel and HY-80 steel. Very small cracks were produced in the heat-affected zone
in Specimen GM1, a 2-inch-thick large butt joint in mild steel, while no cracks
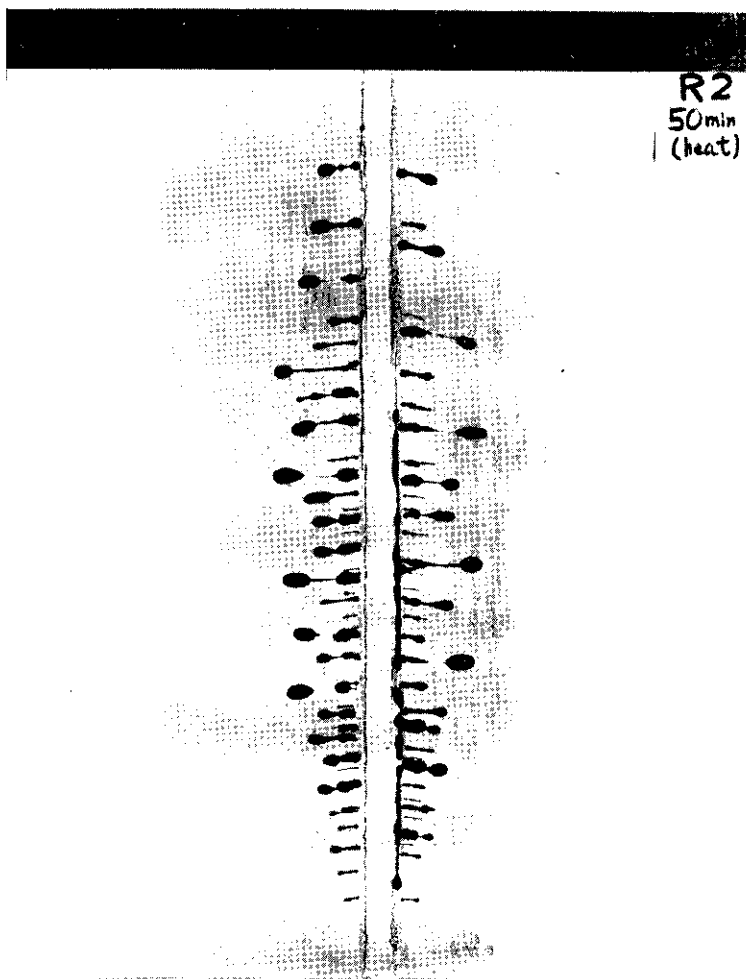
R2
50min
(heat)

Fig. 9. Crack pattern in a simple-butt joint made from SAE 4340 steel oil quenched and tempered at 500F (Specimen R2) after hydrogen-induced-cracking test for 50 minutes. After the test, the specimen was heated in a furnace at 400 F for two hours.

were observed in other mild-steel specimens except Specimen TM2 which was cooled to -30 F after hydrogen charging. On HY-80 steel specimens, cracks were found in Specimens GH1 (2 inches thick) and PH-2 (1-1/2 inches thick), while no cracks were observed in other specimens 1/2 inch thick. These results showed that cracks were more pronounced in heavy weldments than in weldments made from thinner plates. The effect of plate thickness, however, was not great.

Experimental Results, Part 2 Hydrogen-Induced Crack Patterns Obtained on Various Weldments Prepared in Heat-Treated SAE 4340 Steel

Hydrogen-induced-cracking tests were conducted on 25 weldments made in SAE 4340 steel oil quenched and tempered at 500 F. Different weldment designs and different welding procedures were used to produce a variety of residual-stress distributions.
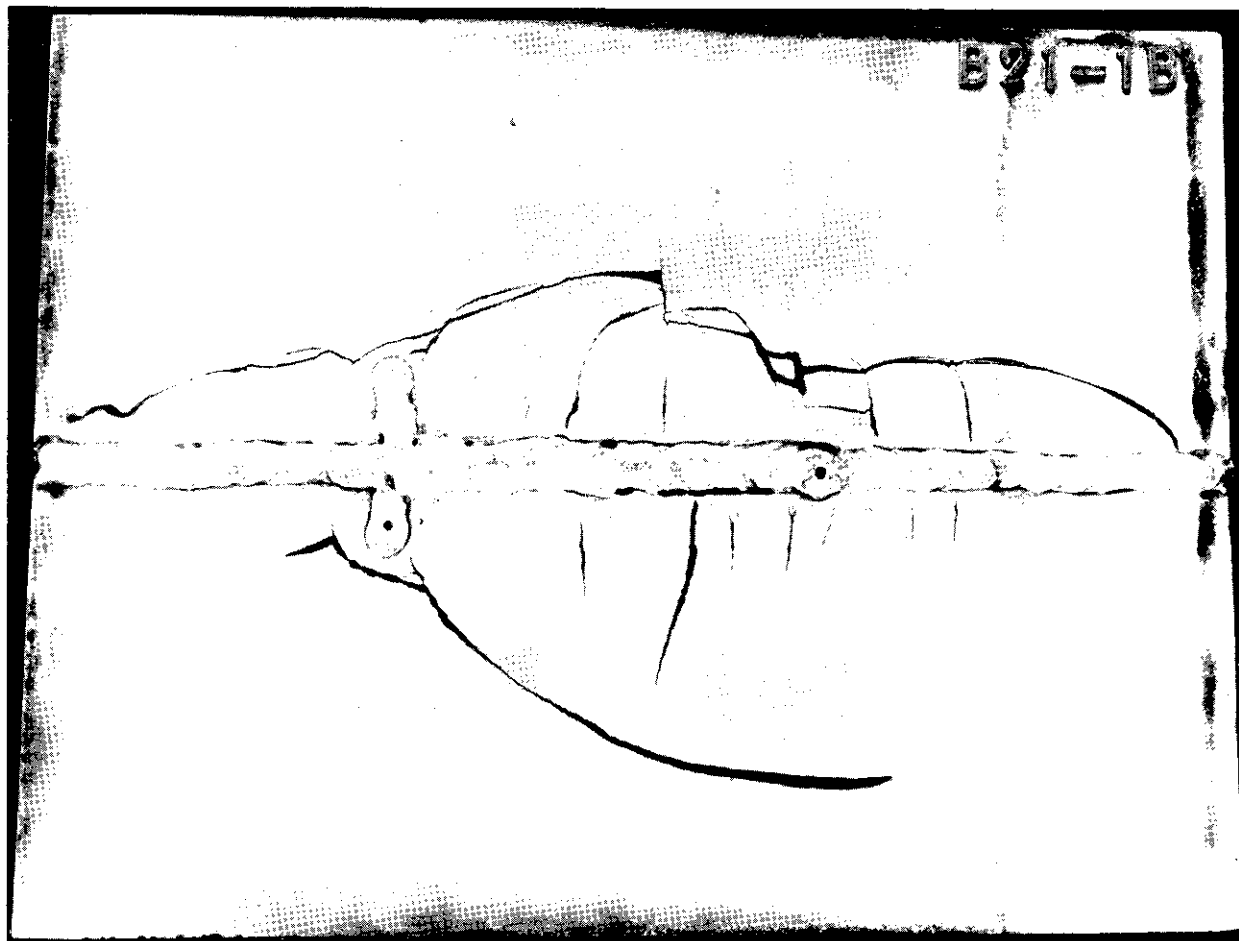
Fig. 10.   Crack pattern in Specimen B21 - 1.   Back surface.

Simple Butt Joints Welded With Different Processes. Hydrogen-induced-cracking tests were conducted on 9 simple butt joints ranging from 1/2 by 12 by 16 inches to 5/8 by 26 by 38 inches in size; 7 joints were welded with E15016 electrodes, 1 with the inert-gas metal-arc process, and 1 with the Narrow-Gap process. In all welds systematic transverse cracks were observed in the base plate in regions near the weld; no cracks were observed in the welds themselves. Longitudinal cracks along the heat-affected zone were found in Specimens 042 and R2.

Table 3 shows the average crack lengths observed in the middle part of butt joints. They include the weld metal about 1/2 inch wide, but long cracks which were produced during prolonged hydrogen charging or after the hydrogen charging was completed are excluded. The average crack lengths were 2 to 3 inches in 12- by 16-inch joints made with the shielded-metal-arc process (E15016 electrodes) and the inert-gas metal-arc process. The average crack length was about 4 inches in Specimen T42, a butt joint 5/8 by 26 by 38 inches in size made with E15016 electrode. This indicates that the tension zone of longitudinal residual stress is wider in the large weldment than in 12- by 16-inch welds. The average crack length was only about 1-1/2 inches in Specimen T43N, a butt joint 5/8 by 21 by 38 inches in size welded with the Narrow-Gap process, after hydrogen charging for 15 minutes. The result indicates that the tension zone of residual stresses
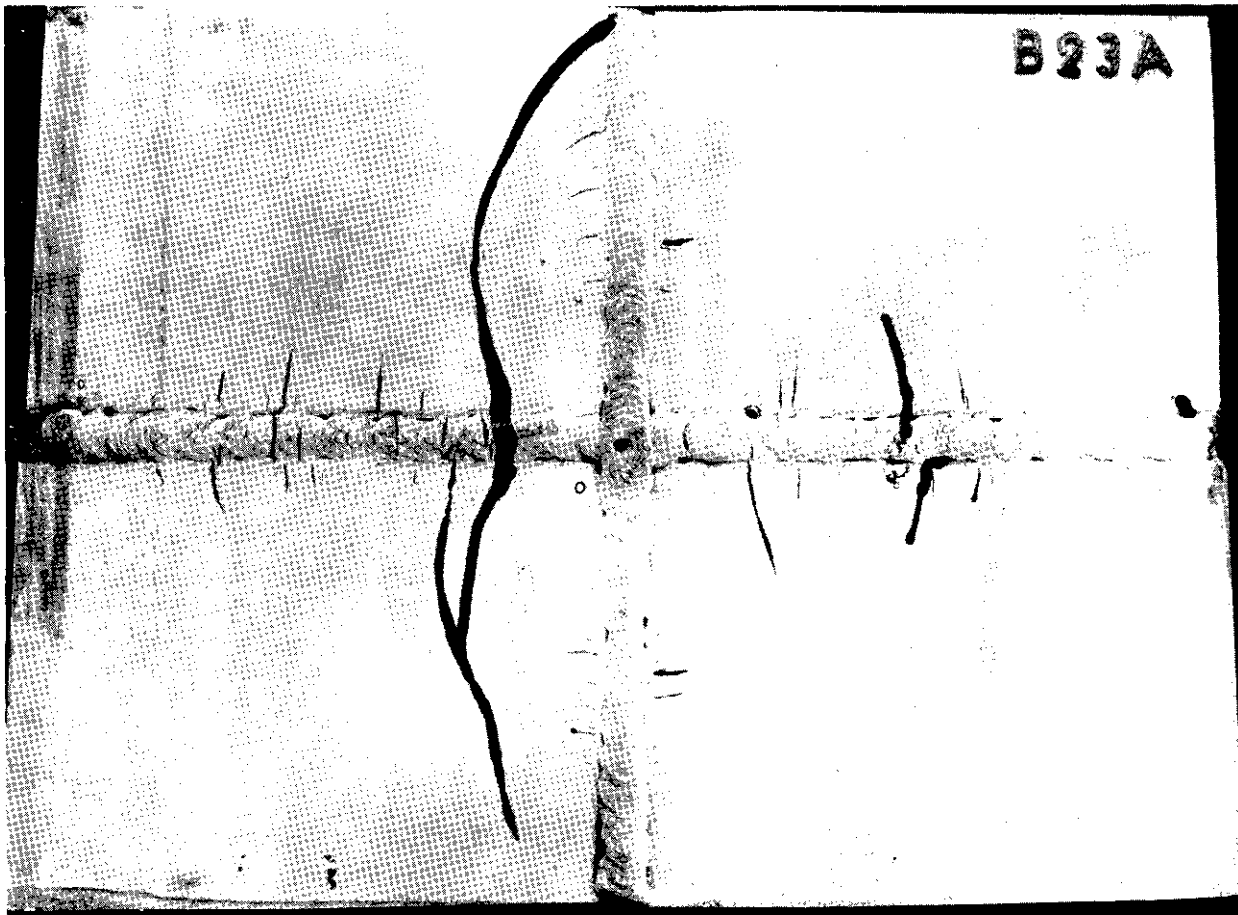
Fig. 11.   Crack pattern in cross-butt joint.

produced by the Narrow-Gap process is narrower than that produced by the ordinary shielded-metal-arc process, and that the maximum residual stresses produced by the both processes are probably comparable.

Complex Butt Joints and Circular-Groove Weld.   Hydrogen-induced cracks were obtained in three weldments:

> (1)   Butt joint with repair welding (Specimen B21-1), Figure 10
>
> (2)   Cross-butt joint (Specimen B23), Figure 11
>
> (3)   Circular-groove weld (Specimen B32), Figure 12.

Transverse cracks were obtained in longitudinal and transverse butt welds in Specimens B21-1 and B23.   There was a long parabolic crack starting from one end of the repair weld in Specimen B21-1.   In Specimen B23, a long crack was obtained parallel to the transverse weld.   This weld was made after the longitudinal weld was completed.   A long crack parallel to the weld also was obtained in Specimen B21-1.

In Specimen B32, the major crack was a circular one surrounding the groove weld.   The specimen also contained a system of radial cracks on one surface.
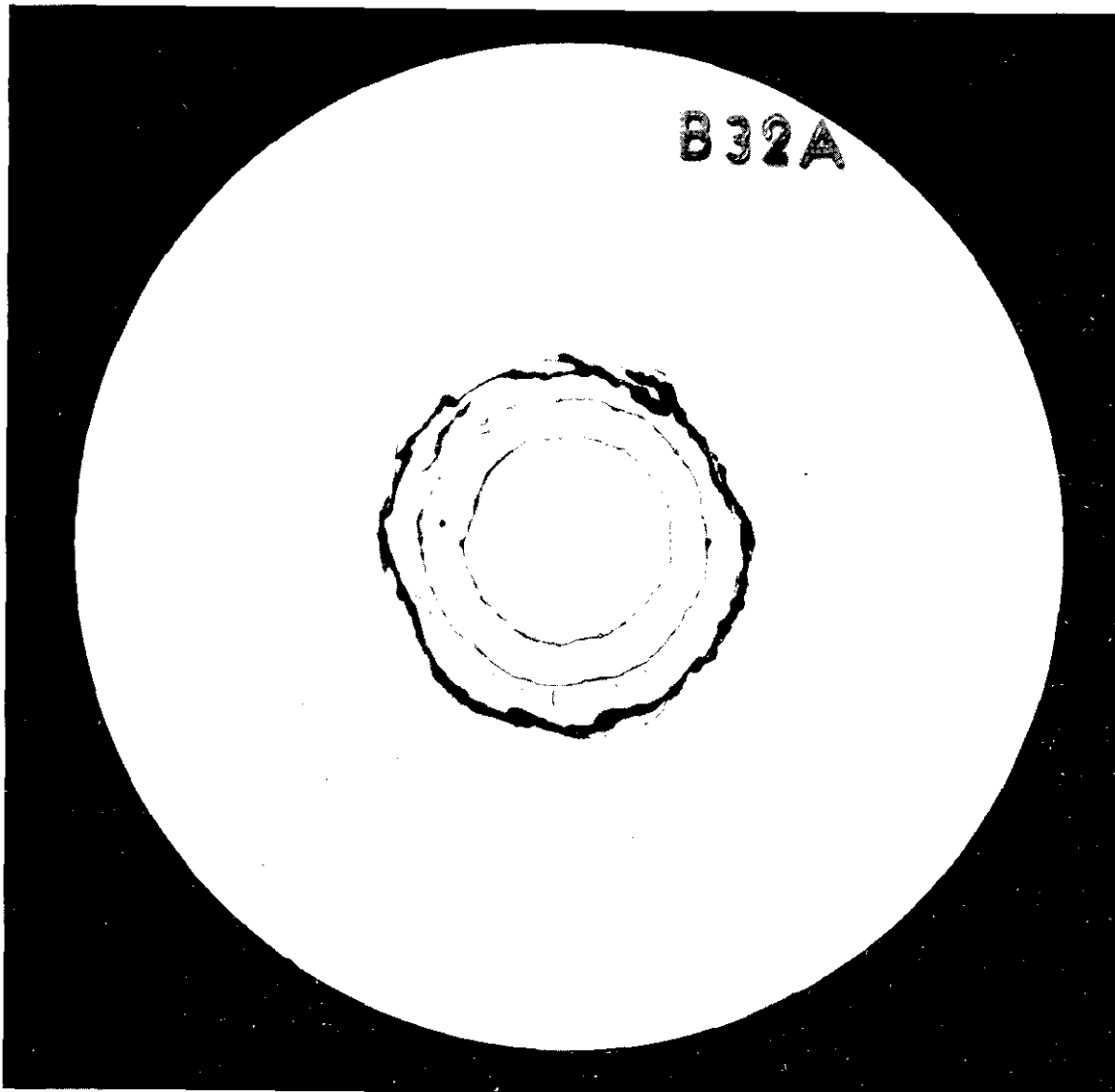
Fig. 12.   Crack pattern in circular-groove weld.

Fillet Welds. Hydrogen-induced cracks were obtained in four fillet-welded specimens made with different procedures:

(1)   Heavy, continuous welding (Specimen A4-F1), Figure 13

(2)   Light, continuous welding (Specimen A4-F2), Figure 14

(3)   Heavy, intermittent welding (Specimen A4-F3), Figure 15

(4)   Light, intermittent welding (Specimen A4-F4), Figure 16.
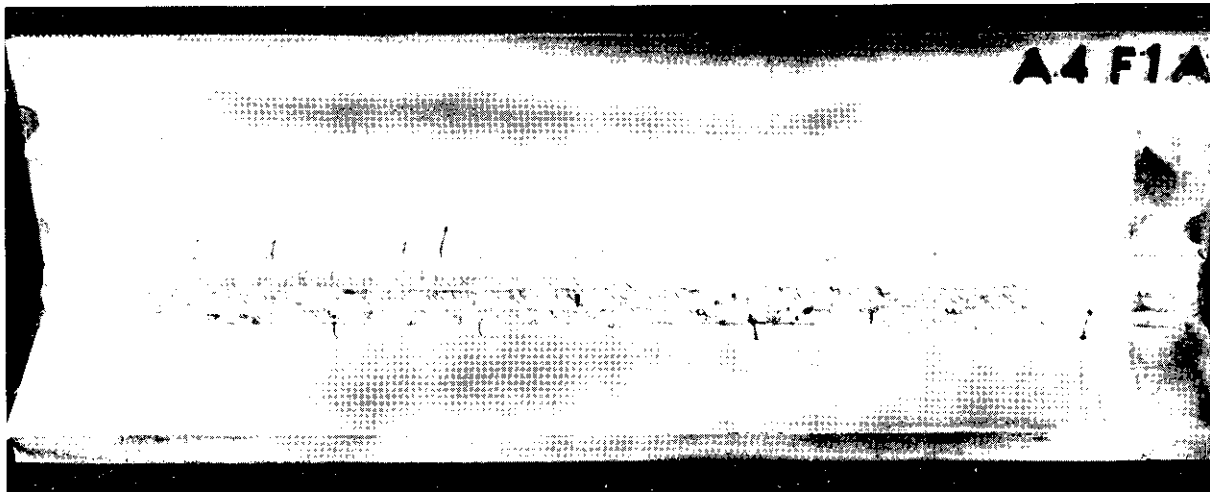
a. *Front side*

b. *Back side*

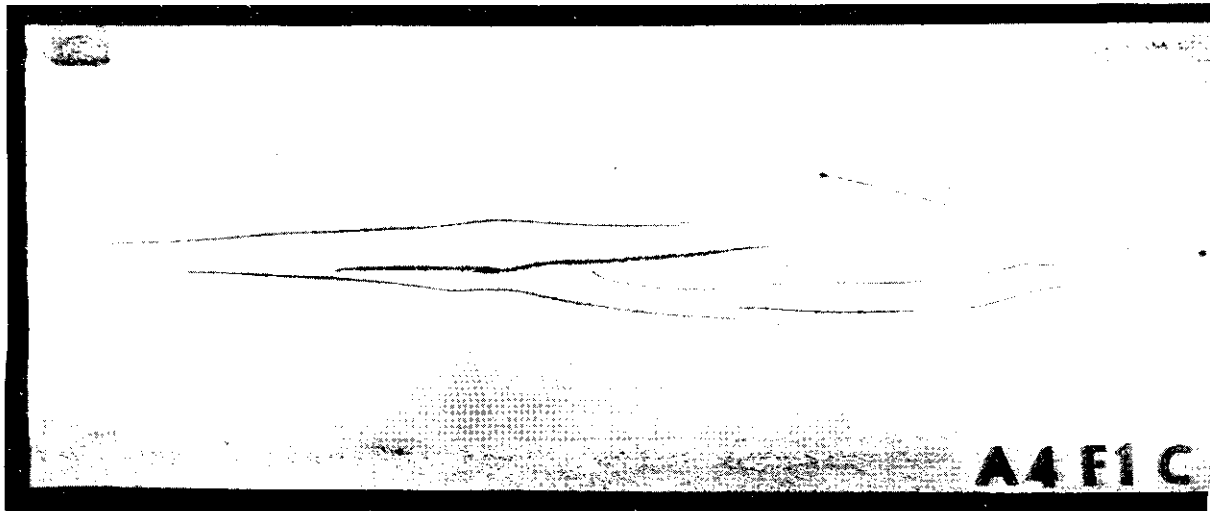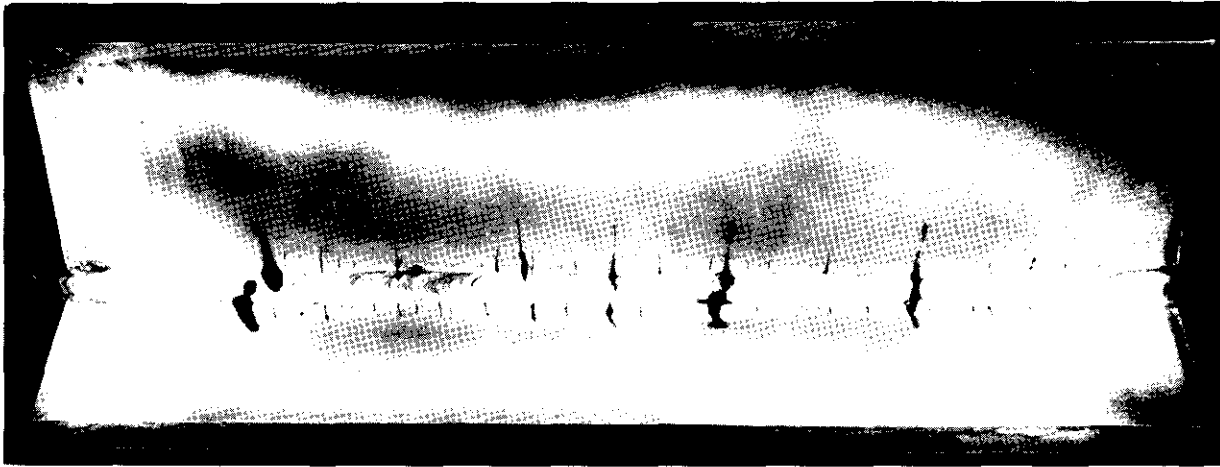*Fig. 13.   Crack pattern in heavy, continuous fillet-weld
Specimen made with SAE 4340 steel.*

There was a series of short cracks transverse to the welding direction
on the welded side in the specimens welded by the continuous-welding procedure,
as shown in Figures 13a and 14a.   The transverse cracks consisted of two different
sets of cracks.   One was shorter and rather closely spaced, and the other, longer
and more widely spaced.   Different crack patterns were obtained on the unwelded
back surface.   Transverse cracks on the back surface of the light-continuous weld
appear to correspond to the longer, more widely spaced cracks on the welded side,
as shown in Figure 14b.   In the heavy-continuous-weld specimen several longitudinal
cracks were found on the back surface, as shown in Figure 13b.

In the heavy-intermittent-weld specimen, curved cracks were observed
at the ends of each fillet weld, as shown in Figure 15a.   Curved cracks around
the fillet weld also were observed on the back surface (Figure 15b).   Tiny trans-

a. Front side
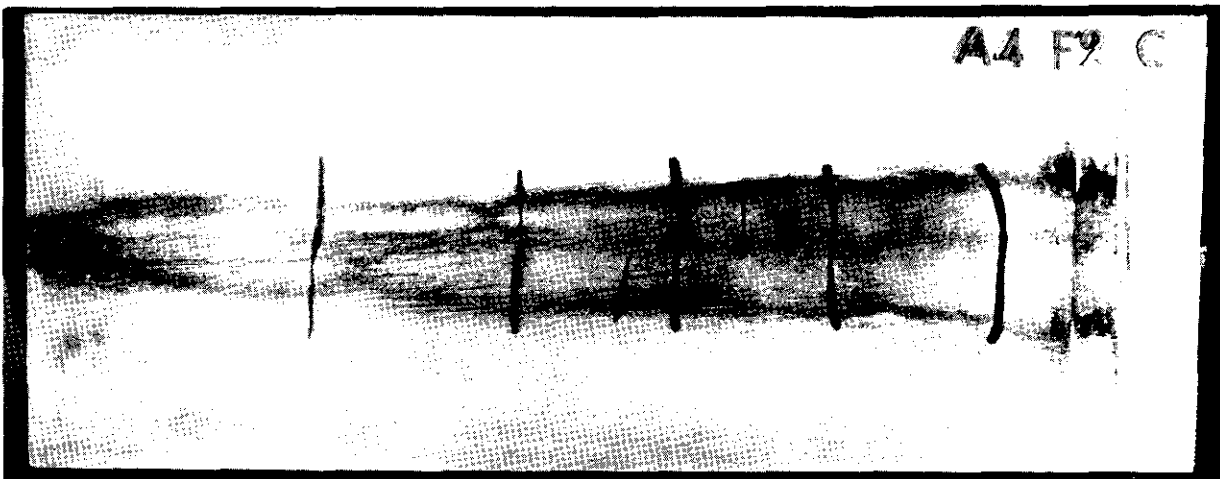
b. Back side

Fig. 14. *Crack pattern in light, continuous fillet-weld Specimen made with SAE 4340 steel.*

verse cracks alongside the fillet welds were found on the front surface, and longitudinal cracks connecting the curved cracks were found on the back surface. In the light-intermittent-weld specimen, both curved cracks at the ends of the welds and transverse cracks were found, as shown in Figure 16. However, these cracks were not so predominant as those observed in other specimens. This appears to be a result of the lower residual stress in the specimen made with a minimum of welding.

Complex Structures. Figures 17 and 18 show hydrogen-induced crack patterns obtained on complex structures.

Short transverse cracks were found along all fillet welds. The transverse cracks consisted of two different series, short, closely spaced cracks, and longer, more widely spaced ones. The transverse cracks also were found on the back surface of the bottom plate, as shown in Figure 17b. These corresponded
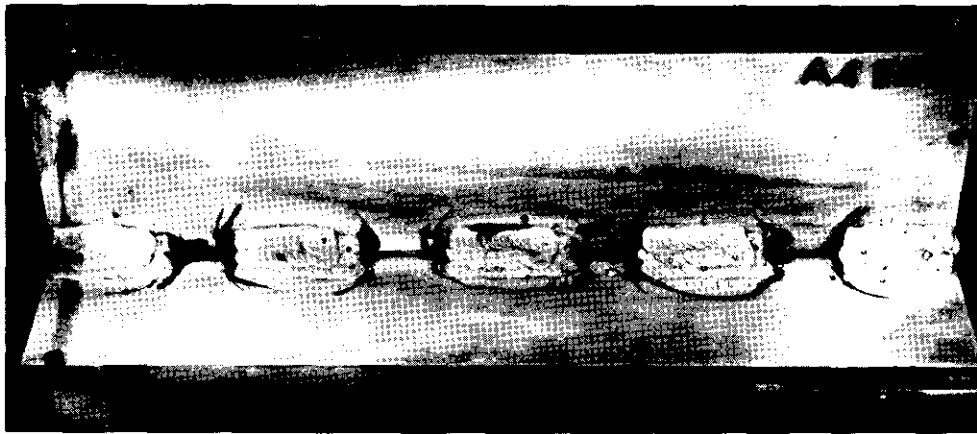
a.   Front side
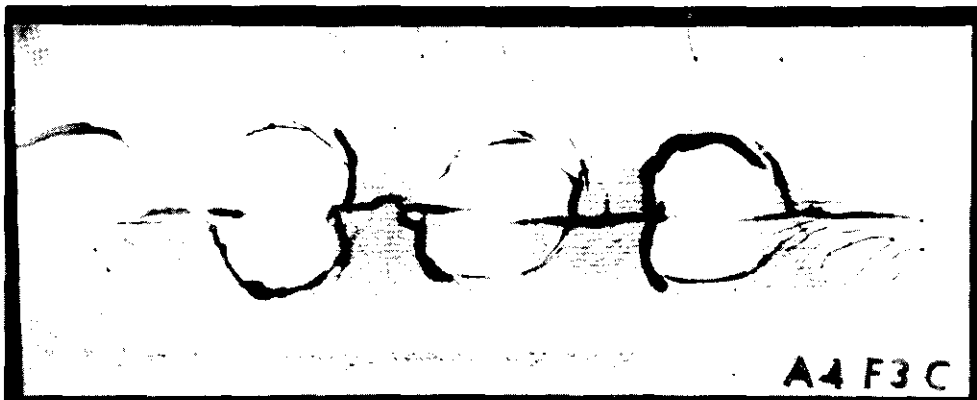
b.   Back side

*Fig. 15.   Crack pattern in heavy, intermittent fillet-weld
Specimen made with SAE 4340 steel.*

approximately to the cracks which had wider spacing on the front surface.   The
average lengths of transverse cracks measured on the back surface of the bottom
plate were:

Locations	Average Length of Cracks, inch
Specimen B11, under longitudinal frame	2.2 (see Figure 17b)
Specimen B11, under transverse frames	1.8
Specimen B12, under longitudinal frame	2
Specimen B12, under transverse frames with cut-outs	1 (only a few cracks)
Specimen B13, under longitudinal frame with cut-outs	2
Specimen B13, under transverse frames with cut-outs	1 (only a few cracks)
Specimen 3C42, under longitudinal frame	2

As shown in this tabulation, transverse cracks were more predominant in fillet
welds between the longitudinal (through) frame and the bottom plate than in fillet
welds between the transverse (interrupted) frame and the bottom plate.   The
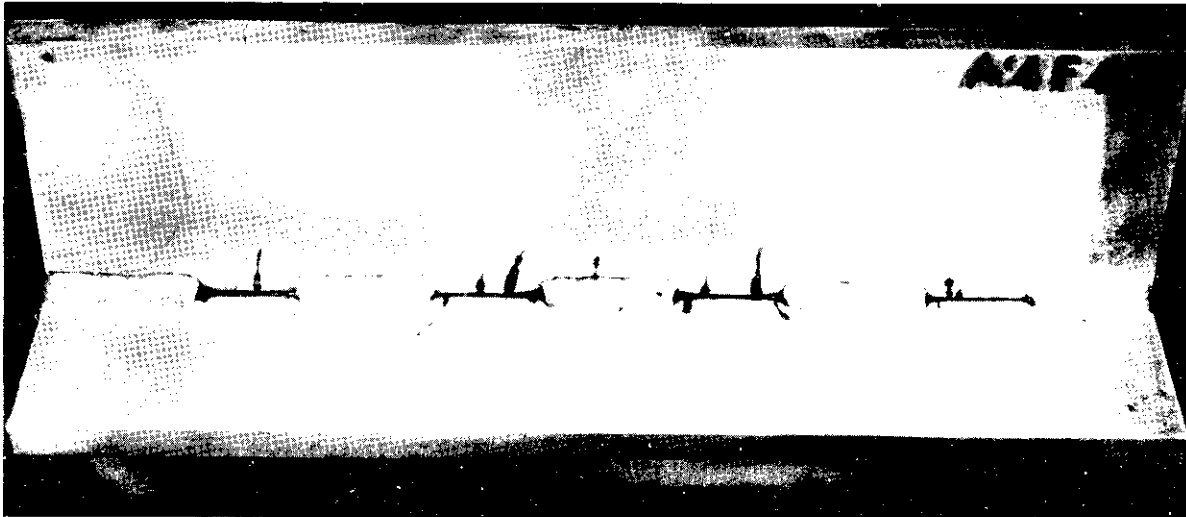
a. Front side

b. Back side

Fig. 16. Crack pattern in light, intermittent fillet-weld
Specimen made with SAE 4340 steel.

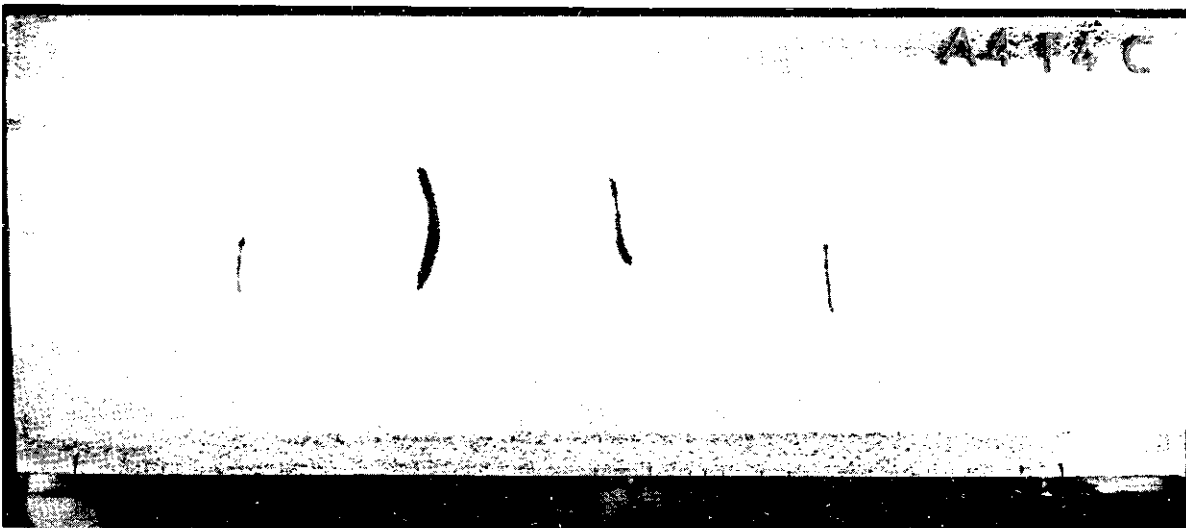decrease in number of transverse cracks in these welds may be caused by release
of residual stresses as a result of the formation of other types of cracks in the
vicinity of these welds.

Parabolic cracks were found in the vicinity of every structural dis-
continuity. These cracks were much longer than the transverse cracks, and they
appeared in the plate to which the edge of another plate was joined.

In the region near the intersection of the longitudinal and transverse
frames, slightly curved, radial cracks were found at the center of the cutout
(Specimens B12 and B13, see Figure 18), while a slightly curved crack parallel to
the weld was found in the longitudinal plate in Specimen B11.
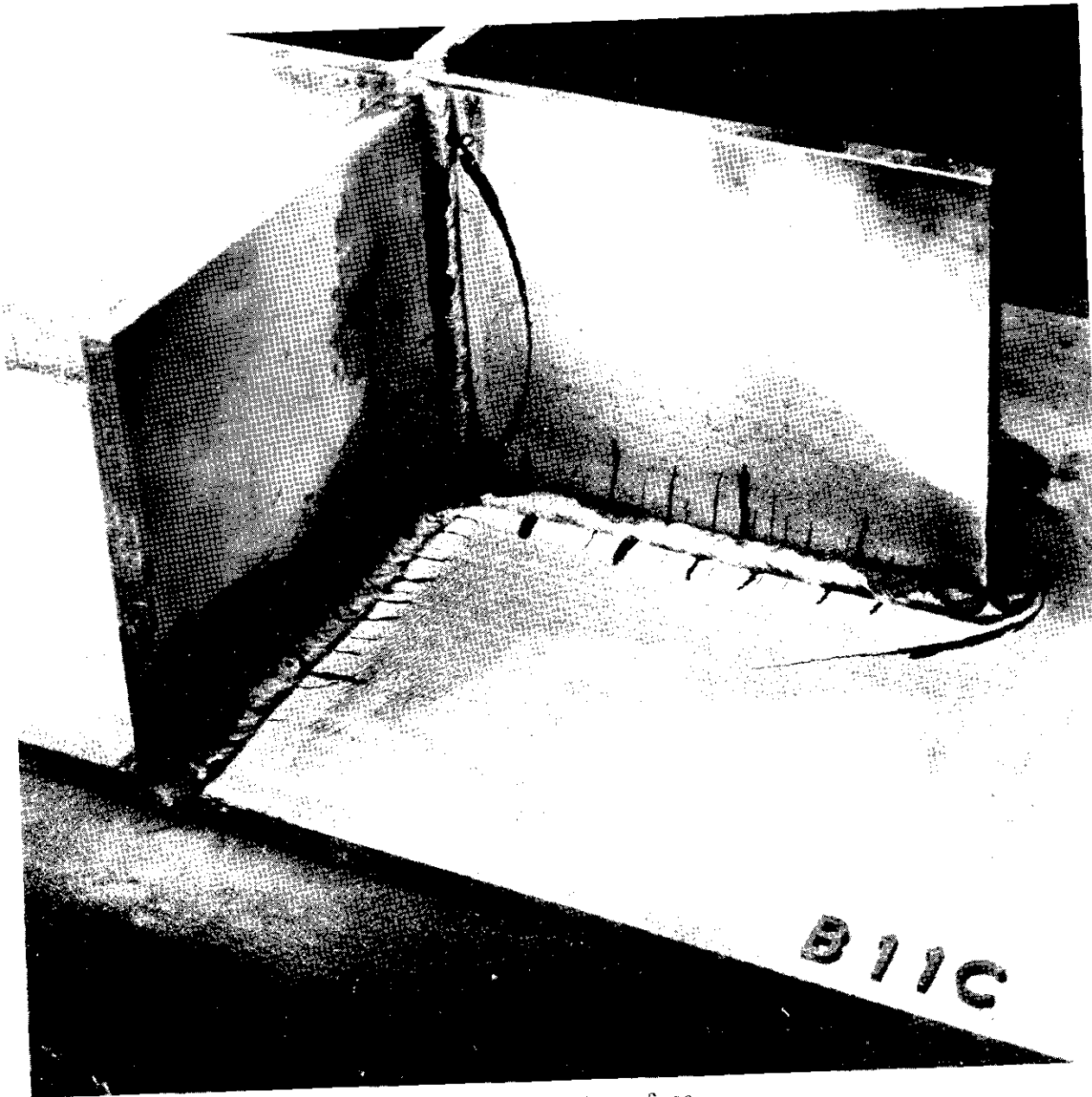
a. Front surface

Fig. 17. Crack pattern in complex-structure specimen with directly intersecting frames.

Effect of Mechanical Stress Relieving. Hydrogen-induced-cracking tests were made on five bead-on-plate specimens which had been partially stress relieved by loading up to different stress levels. Figures 19a, b, and c show hydrogen-induced crack patterns obtained in Specimens D8, D4, and D6, respectively. Regularly spaced transverse cracks were obtained in the as-welded specimen and the specimens which had been loaded to 20 and 40 percent of the yield stress. In the specimen loaded to 60 percent of the yield stress, the interval of cracks was
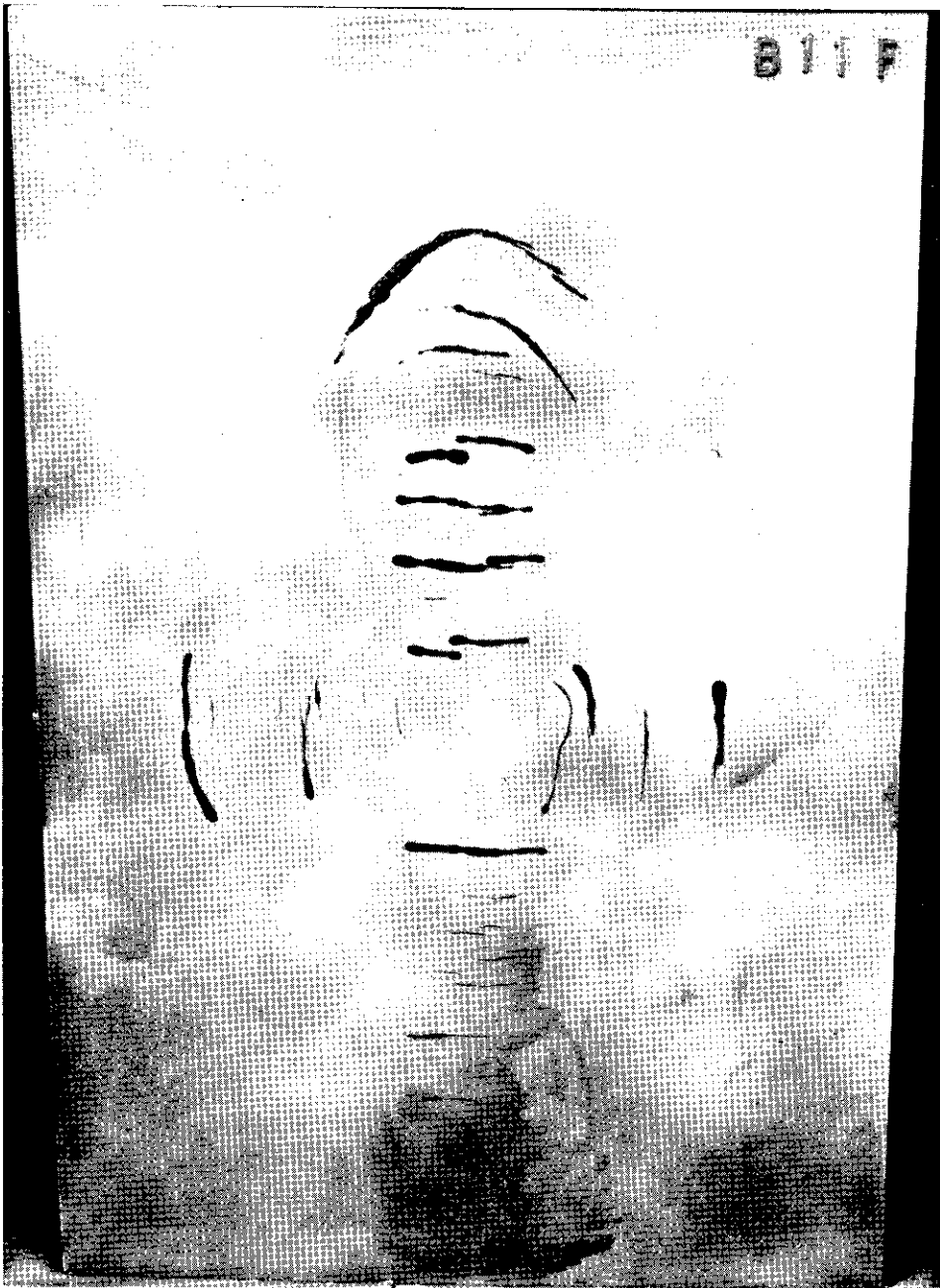
b. Back surface

Fig. 17. (Continued)

wider than that of cracks in as-welded specimens and specimens stress relieved to a lower level. Transverse cracks were not found in the specimen which had been loaded to 80 percent of the yield stress. The results indicate that hydrogen-induced cracks are stress sensitive rather than plastic-strain sensitive.
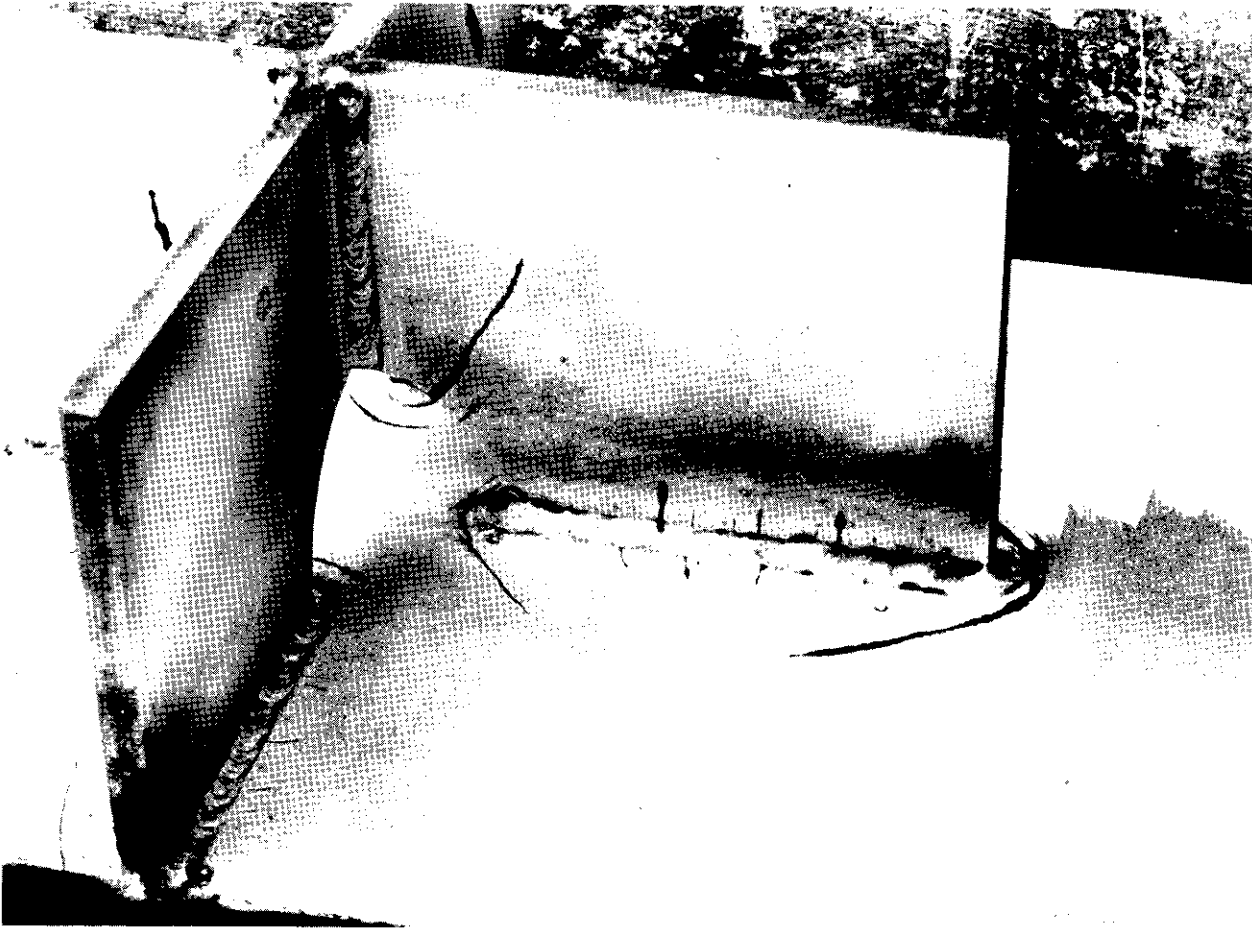
Front surface

*Fig. 18.   Crack pattern in complex-structure specimen with
serrated transverse and longitudinal plates.*

Hydrogen-Induced-Cracking Tests on Press-Fit Specimens

Hydrogen-induced-cracking tests were conducted on five press-fit
specimens made in SAE 4340 steel and in the commercial high-strength structural
steel.

Experimental Methods

Four ring specimens, 3/8 inch thick, 2-1/2 inches in inner diameter,
and 10-7/8 to 11 inches in outer diameter, were made from SAE 4340 steel oil
quenched from 1550 F and tempered at 500 F for 1 hour. A ring specimen, 3/8 inch
thick, 2-1/2 inches in inner diameter, and 10 inches in outer diameter, was made
in the commercial high-strength structural steel water quenched from 1650 F and
tempered at 350 F for 1 hour (the "hard condition").
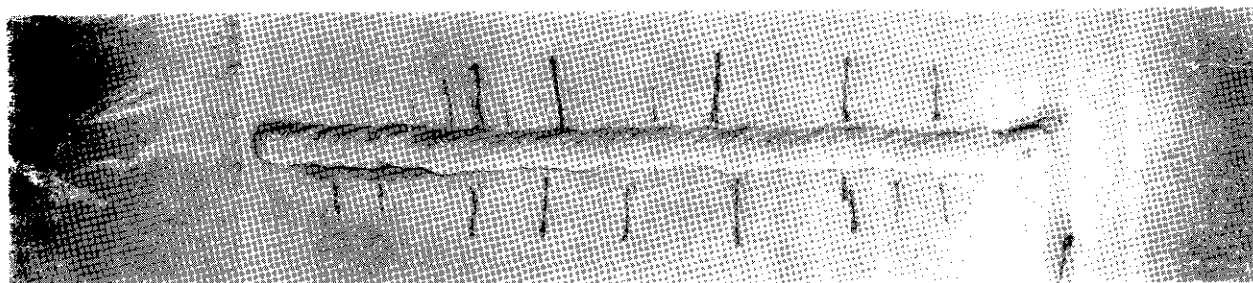
a.   *As welded, Specimen D8*
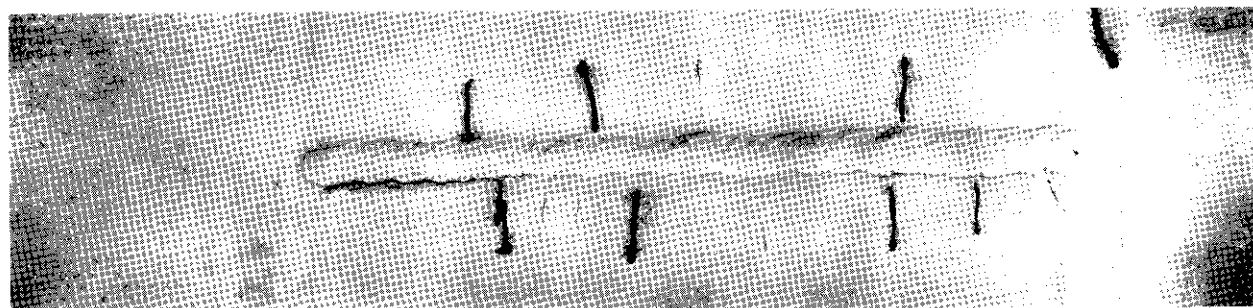
b.   *Loaded to 40 percent of yield, Specimen D4*

c.   *Loaded to 80 percent of yield, Specimen D6*

Fig. 19.   *Hydrogen-induced crack patterns in mechanically
stress-relieved specimens.*

Tapered pins 2-1/2 inches in diameter and 3 inches long were made of heat-treated SAE 4340 steel. The pin had a taper of 1/2 degree. The same taper was machined on the inner circle of the specimens.

Figure 20 shows procedures for making the press-fit specimens from heat-treated SAE 4340 steel. In Specimens K1, K2, and K4, a tapered pin was pressed into the specimen. Magnitudes of stresses introduced varied from one specimen to another. In preparing Specimen K3, a tapered pin was pressed into the specimen, and a ring was pressed onto the specimen. The outer ring was used in an attempt to produce compressive stresses in areas near the outer edge of the specimen. The outer ring, 10-7/8 inches in inner diameter, 14 inches in outer diameter, was made of mild steel. The outer diameter of the specimen was 10-7/8 inches. The inner surface of the outer ring was tapered, as was the outer circumference of the specimen.
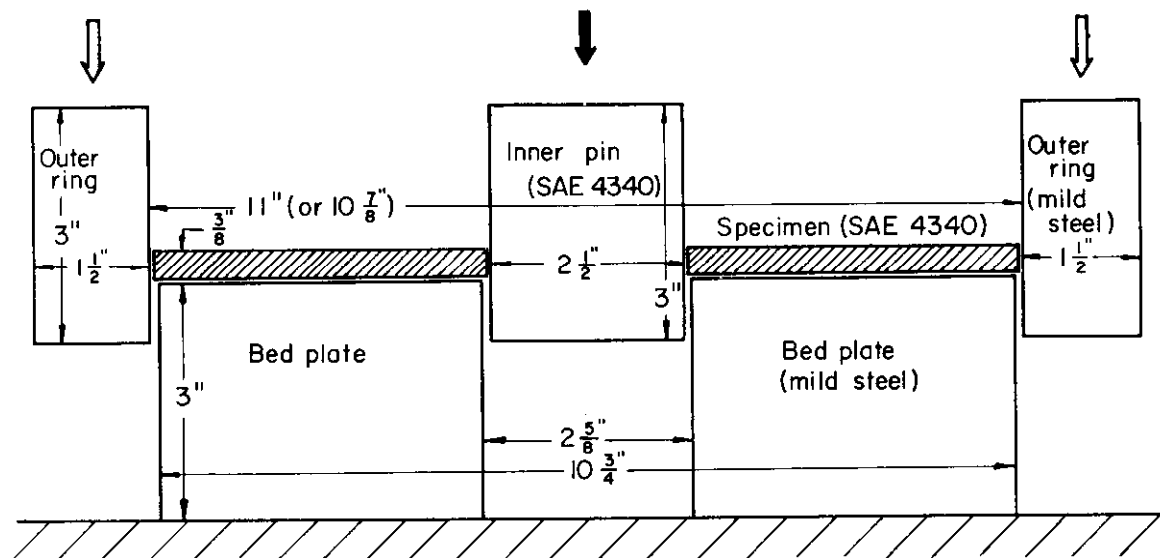
Fig. 20. *Procedures for making a press-fit specimen*
(Heat-treated SAE 4340 steel).

Strain gages (mostly 1/8-inch gage length) were mounted on both surfaces of the specimens to measure strains caused by the press fitted pins. The locations of strain gages varied from one specimen to another. The gages were covered with synthetic rubber and wax. After pins were pressed into the specimens, the specimens were charged with hydrogen. The hydrogen-charging conditions were as follows:

	Current, amperes	Charging Time, hours
Specimen K1	150	3
Specimen K2	150	3
Specimen K3(a)	150	4
Specimen K4	75	5-1/2
Specimen LT1	77	20

(a) The surface of the outer ring was covered by wax and a plastic tape.

Specimens K4 and LT1 were hydrogen charged in the container which had transparent walls. Other specimens were charged in the barrel.

Strain release due to the formation of cracks during the hydrogen-induced-cracking test was measured with several of the gages on Specimens K3, K4, and LT1.

Mathematical Analysis on Stress Distributions in Press-Fit Specimens

A mathematical analysis was made of the stress distribution in the press-fit specimens. When two sets of uniform pressure, P_1 and P_2, are applied along the inner and the outer edge of a ring region, stress components are given by Equation (1)[13]:

$$\sigma_\theta = \left[\frac{\varkappa^2 - \eta}{1 - \varkappa^2} + \frac{1 - \eta}{1 - \varkappa^2} \cdot \frac{1}{\rho^2} \right] P_1$$

$$\sigma_r = \left[\frac{\varkappa^2 - \eta}{1 - \varkappa^2} - \frac{1 - \eta}{1 - \varkappa^2} \cdot \frac{1}{\rho^2} \right] P_1 \qquad (1)$$

where

$$\eta = \frac{P_2}{P_1} \ , \ \frac{1}{\varkappa} = \frac{r_2}{r_1} \ , \ \rho = \frac{r}{r_1} \ ,$$

and

σ_θ = circumferential stress

σ_r = radial stress

r_1 = radius of inner circle ($\sigma_r = -p_1$ at $r = r_1$)

r_2 = radius of outer circle ($\sigma_r = -p_2$ at $r = r_2$)

r = ordinate of a point.

The circumferential stress at the inner circle, $\sigma_{\theta 1}$ is ($\rho = 1$):

$$\sigma_{\theta 1} = \frac{1 + \varkappa^2 - 2\eta}{1 - \varkappa^2} \cdot P_1 \ . \qquad (2)$$

Various stress distributions can be produced in the ring region by changing the two pressures, p_1 and p_2.

Experimental Results

Strain Distributions. Strain distributions observed on Specimens K1 and K3 are shown in Figures 21(a) and (b), respectively. Since radial strains were compressive, $-\epsilon_r$ was plotted in the figures. Similar results were obtained on other specimens.

The analysis given in the preceding section shows that the following relationships exist between the circumferential stress at the inner circle $\sigma_{\theta 1}$ and strain components ϵ_θ and ϵ_r for specimens where only inner pins were pressed ($\eta = 0$):

a. Specimen Kl, SAE 4340 Steel ($\sigma_{\theta l}$ = 136,000 psi)   b. Specimen K3, SAE 4340 Steel ($\sigma_{\theta l}$ = 98,000 psi)
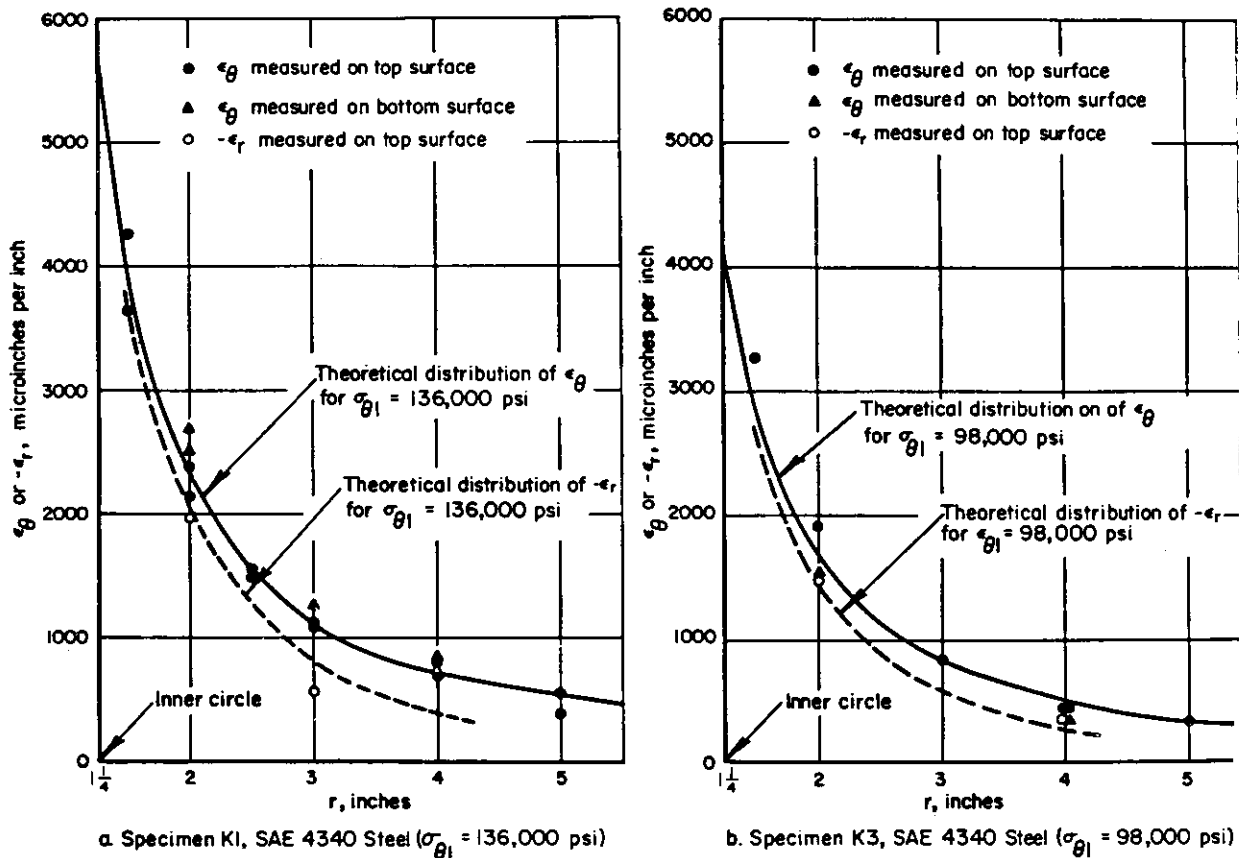
Fig. 21.   Strain distributions in press-fit specimens.

$$\sigma_{\theta 1} = E\epsilon_{\theta} \cdot \frac{1 + \varkappa^2}{(1 - \nu)\,\varkappa^2 + (1 + \nu)\,\dfrac{1}{\rho^2}}$$

$$\sigma_{\theta 1} = -E\epsilon_{r} \cdot \frac{1 + \varkappa^2}{(1 - \nu)\,\varkappa^2 - (1 - \nu)\,\dfrac{1}{\rho^2}} \tag{3}$$

where

    ϵ_{θ} = circumferential strain

    ϵ_{r} = radial strain

    E = Young's modulus

    ν = Poisson's ratio.

From the group of strain values measured at various locations, calculated values of $\sigma_{\theta 1}$ for Specimens Kl, K2, K4, and LT1 were:
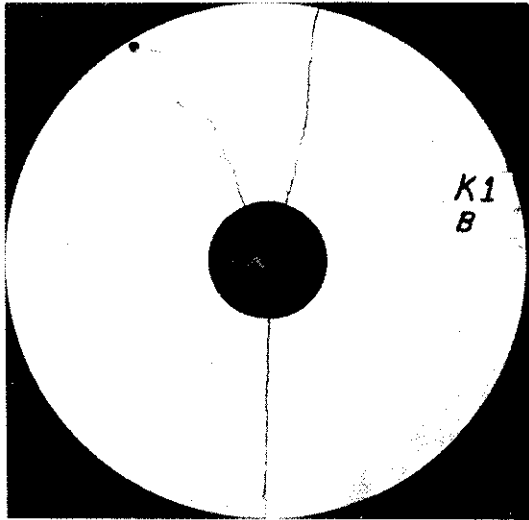
a. Specimen K1, $\sigma_{\theta 1}$ = 136,000 Psi,
    Tested for 3 hours.
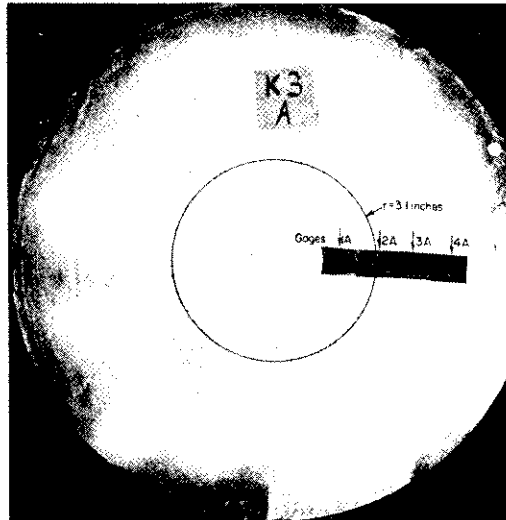
c. Specimen K3, $\sigma_{\theta 1}$ = 98,000 Psi,
    Tested for 4 hours.
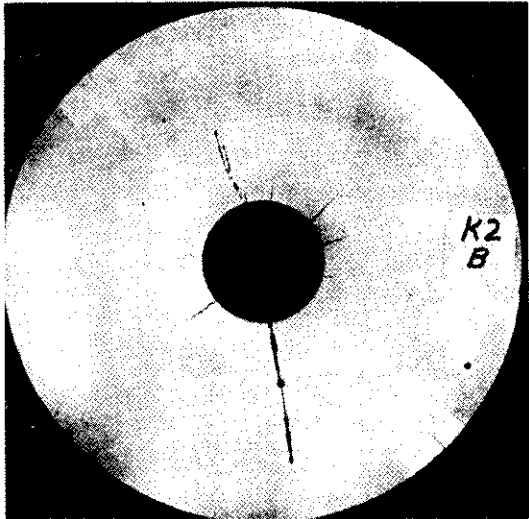
b. Specimen K2, $\sigma_{\theta 1}$ = 68,000 Psi,
    Tested for 3 hours.
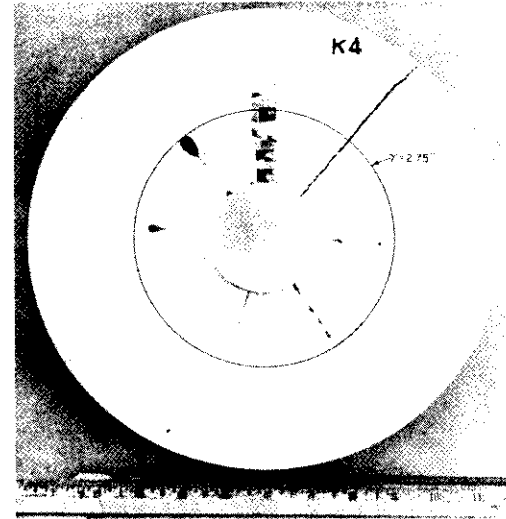
d. Specimen K4, $\sigma_{\theta 1}$ = 81,000 Psi,
    Tested for 5-1/2 hours.

Fig. 22.   Crack patterns in press-fit specimens made from
            SAE 4340 steel oil quenched and tempered at 500 F
            after hydrogen-induced-cracking test.

$\sigma_{\theta 1}$ = 136,000 psi for Specimen K1

$\sigma_{\theta 1}$ =   68,000 psi for Specimen K2

$\sigma_{\theta 1}$ =   81,000 psi for Specimen K4

$\sigma_{\theta 1}$ =   90,000 psi for Specimen LT1.

Theoretical distributions of ϵ_θ and ϵ_r were then calculated using the above values of $\sigma_{\theta 1}$ and were compared with measured strain values. The theoretical strain distributions and measured strain values coincided very well, as shown in Figure 21a.

Strain distributions obtained on Specimen K4 are shown in Figure 21b. At a low-stress level compressive stresses were produced by the outer ring; however, the outer ring had little effect on stress distributions at higher maximum stresses. The outer ring was made with mild steel, and this may have kept it from working effectively in pressing the specimen made with heat-treated SAE 4340 steel. The theoretical stress distributions shown in Figure 10b were obtained assuming that $\eta = 0$. The value of $\sigma_{\theta 1}$ was estimated as:

$$\sigma_{\theta 1} = 98,000 \text{ psi for Specimen K3.}$$

Results of Hydrogen-Induced-Cracking Test. Figures 22a through d show the crack patterns obtained in SAE 4340 specimens (K1 through K4). Complete fracture occurred in Specimen K1, where residual stresses were high ($\sigma_{\theta 1}$ = 136,000 psi). Systems of radial cracks were obtained in Specimen K2 ($\sigma_{\theta 1}$ = 68,000 psi) and in Specimen K3 ($\sigma_{\theta 1}$ = 98,000 psi). In Specimen K4 ($\sigma_{\theta 1}$ = 81,000 psi), a similar system of radial cracks was formed after hydrogen charging for 5-1/2 hours; however, a crack extended after the hydrogen-induced-cracking test was over and the specimen fractured completely.

In Specimen LT1 made from a commercial high-strength heat-treated structural steel, several short cracks were obtained after hydrogen charging for 13-1/2 hours. Hydrogen charging was continued for 20 hours. After the charging was stopped, a crack extended and the specimen fractured completely.

Change of Strains During Hydrogen-Induced-Cracking Test. Figure 23 shows the change of strains during hydrogen-induced-cracking test observed on four gages mounted on Specimen K3[*]. The locations of the gages are shown in Figure 22c.

On Gage 1A located close to the pin (r = 1.5 inches), the strain began to decrease after several minutes of hydrogen charging. The strain decreased steadily for about 3 hours, after which no appreciable further decrease was observed. The strain decreased from 3270 microinches per inch at the initial stage to 668 microinches per inch after 4 hours of charging (reduction of strain: 80 percent).

On Gage 2A (r = 2 inches), a pronounced reduction of strain was observed after hydrogen charging for about 25 minutes. The strain decreased steadily for the whole test period. The reduction of strain for 4 hours was 64 percent.

---

[*] The temperature of the electrolyte increased 12 F during hydrogen charging. The correction for the temperature change of the measured values has been made.
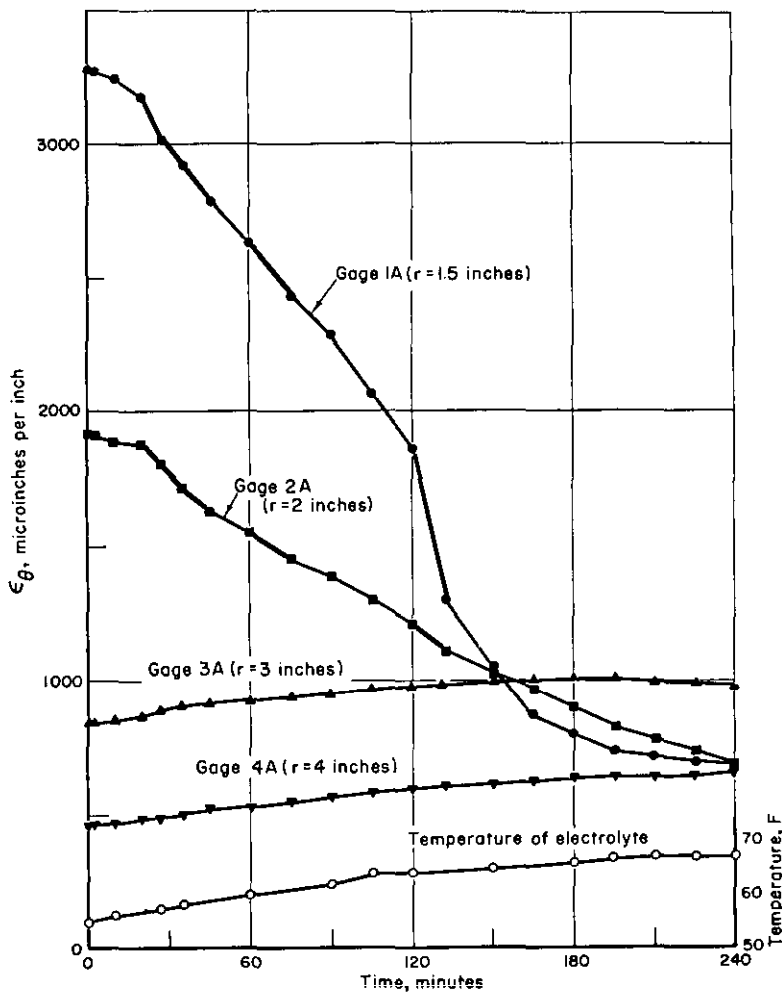
Fig. 23. Change of strains during hydrogen-induced-cracking test on a press-fit specimen. (K3).

On Gages 3A (r = 3 inches) and 4A (r = 4 inches) increases of strains were observed; however, a very slight reduction of strain was observed on Gage 3A after 3 hours of hydrogen charging. This may indicate that the cracks reached the point r = 3 inches in the final stage of hydrogen charging but that the cracks did not penetrate much further.

On Specimen K4, appreciable strain changes were first observed after hydrogen charging for 2 hours. The reductions (percent) of residual stresses after hydrogen charging for 5-1/2 hours were:

69 percent reduction on Gage 1A (r = 1.5 inches)

28 percent reduction on Gage 2A (r = 2 inches)

Slight increase on Gage 3A (r = 3 inches).

On Specimen LT1, no appreciable changes of strains were observed during hydrogen charging for 20 hours. Apparently the formation of several short cracks did not cause appreciable reduction in residual stresses.

TABLE 4. SUMMARY OF PROCEDURES AND RESULTS OF STRESS-
CORROSION-CRACKING TESTS ON WELDED SPECIMENS.

Specimen Code Number	Plate Thickness	Material	Type of Specimens and Welding Techniques	Duration of Testing, hours			Results
				Last Checking Time Before Cracking	First Checking Time After Cracking	Total Testing Time	
			1. MILD STEEL				
FM5	1/2	ABS Class B	12" x 16" butt joint, submerged-arc process	230	--	230	No crack
FM7	1/2		12" x 16" butt joint, E6010	400	--	400	No crack
C1	3/4		12" x 16" butt joint, E6010	48	72	240	Two transverse cracks (Figure 24a)
C2	3/4		Slit-groove weld, E6010	201	--	201	No crack
C3	3/4		Circular-groove weld, E6010	49	73	273	Three radial cracks (Figure 24b
			2. HIGH-STRENGTH STEELS				
FH1	1/2	HY-80	12" x 16" butt joint, E10016	25-1/2	68	224	One transverse crack
FT1		Commercial high-strength structural steel	12" x 16" butt joint, E10016 and E12015	--	23-1/2	31	Systematic transverse cracks (Figure 25)
F-1		SAE 4340	12" x 16" butt joint, MIG process	11	29	180	Several transverse cracks (Figure 26)
F43	1/2	SAE 4340	12" x 16" butt joint, MIG process	--	7 to 24(a)	12 to 29(a)	Several transverse cracks
F-8			12" x 16" butt joint, E15016	181-1/2	205-1/2	325-1/2	One long crack

a) The electric-power source was acting after testing for 7 hours, but the power-source failure was found at 24 hours after testing. Stress-corrosion-cracking test was conducted for 5 more hours. Therefore, the effective testing time was longer than 12 hours but shorter than 29 hours.

Stress-Corrosion-Cracking Tests on Weldments

Stress-corrosion-cracking tests were conducted on 10 weldments.

Experimental Methods

The following welded specimens were used:

(1) Five specimens made in mild steel including three simple butt joints (Specimens FM5, FM7, and C1), one slit-groove weld (Specimen C2), and one circular-groove weld (Specimen C3)
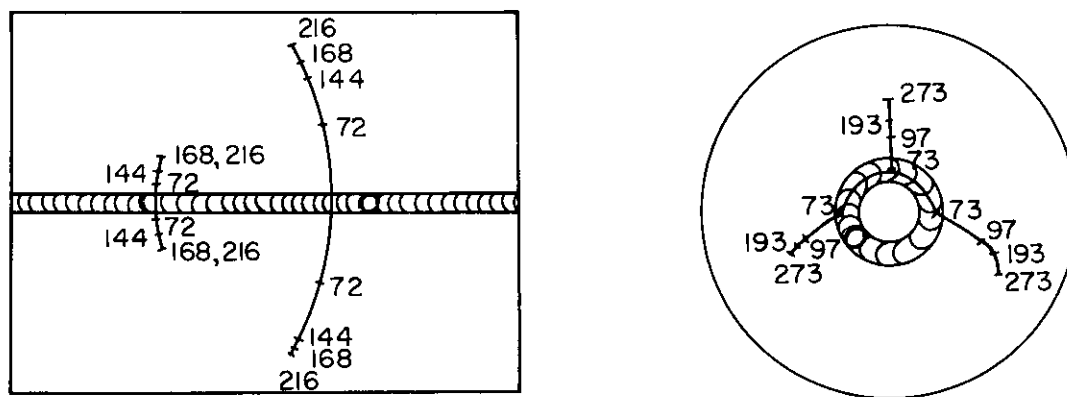
a. *Simple butt joint, Specimen C1*   b. *Circular-groove weld, Specimen C3*

*Fig. 24.   Growth of stress-corrosion cracks in mild-steel
specimens.   The numbers in the figure show the
duration of stress-corrosion-cracking test in
hours.*

(2) Five specimens made in high-strength steels including:

    a. One simple butt joint in HY-80 steel (Specimen FH1)
    b. One simple butt joint in the commercial high-strength structural
        steel heat treated in the hard condition (Specimen FT1)
    c. Three simple butt joints in SAE 4340 steel oil quenched from
        1550 F and tempered at 500 F for 1 hour (Specimens 41, 43, and
        48).

The specimens were immersed in a boiling aqueous solution consisting of
60 percent $Ca(NO_3)_2$ and 4 percent NH_4NO_3. After testing for a certain period,
the specimens were inspected for cracking.

Experimental Results

Results of the stress-corrosion-cracking tests are summarized in Table 4
and discussed briefly in the following.

Mild-Steel Specimens. Cracks were found in two out of the five speci-
mens tested. In these specimens cracks did not occur during the first 48 hours
of testing. Cracks first appeared after about 72 hours of testing. They grew
gradually thereafter, as shown in Figure 24. Cracks were not observed, however,
in the other specimens even though they were tested 201 to 400 hours.

High-Strength-Steel Specimens.   Cracks were found in all specimens made
with high-strength steels.

In the HY-80 steel specimen, one transverse crack about 5 inches long
was observed after 68 hours of testing. As testing continued, the crack gradually
extended; one side of the crack extended into two cracks.
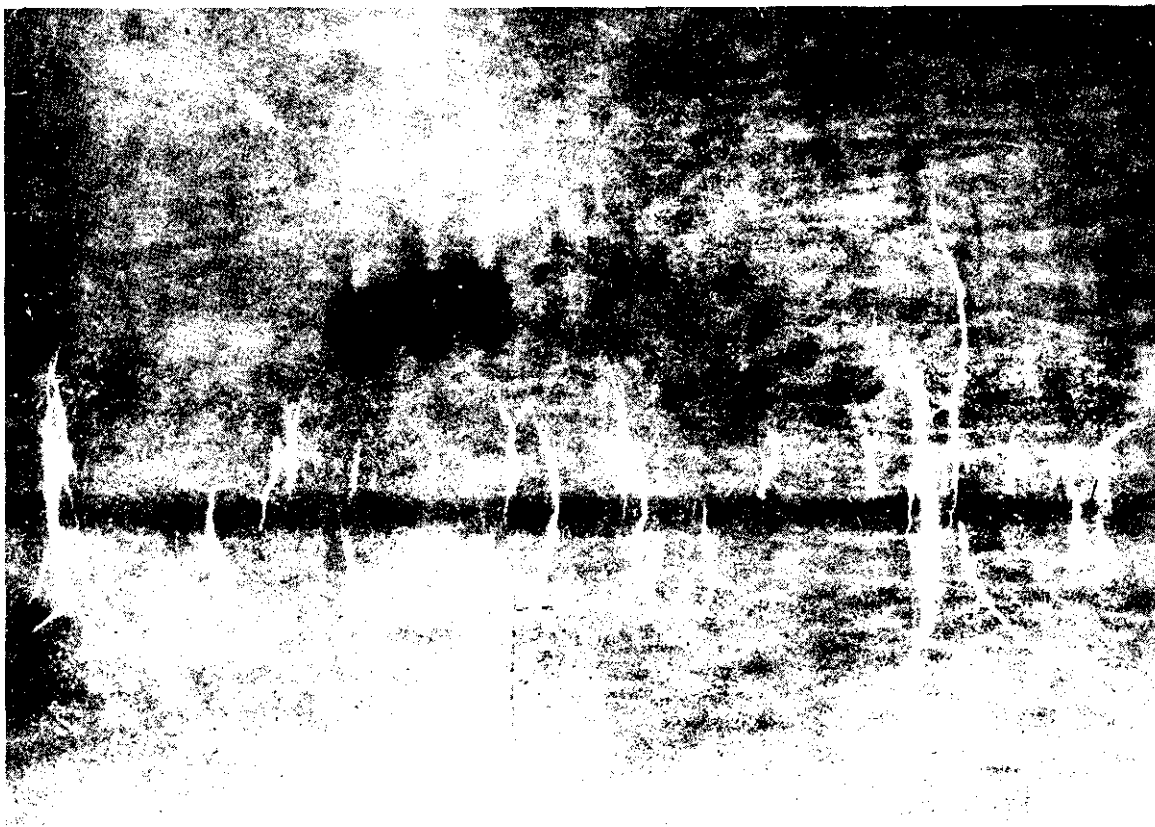
Fig. 25.   Radiograph of simple butt joint (Specimen FF1) of commercial high-
strength, heat-treated structural steel treated to "hard condition"
after stress-corrosion-cracking test for 31 hours.   .04 X

A fairly systematic crack pattern was obtained in the specimen made with
the commercial high-strength structural steel, as shown in Figure 25.   The crack
pattern was similar to that produced in SAE 4340 steel specimens which were
hydrogen charged (Figures 8 and 9).   The cracks were first observed after testing
for 23-1/2 hours, the cracks apparently occurred at some time between 0 and 23-1/2
hours of testing.

Cracks also were found in SAE 4340 steel specimens.   In Specimen F41,
cracks were first observed after 29 hours of testing (the crack occurred at some
time between 11 and 29 hours of testing), and these gradually extended (Figure 26).
In Specimen F43, cracks were first found after 7 to 24 hours of testing, and
extended greatly in the ensuing 5 hours of testing.   The cracks observed in
Specimens F41 and F43 are very similar.   However, a different crack pattern was
obtained in Specimen F48.   In this specimen, one long crack was first observed
after 205-1/2 hours of testing.   This extended gradually as the test was contin-
ued; finally another crack was observed after 325-1/2 hours of testing.
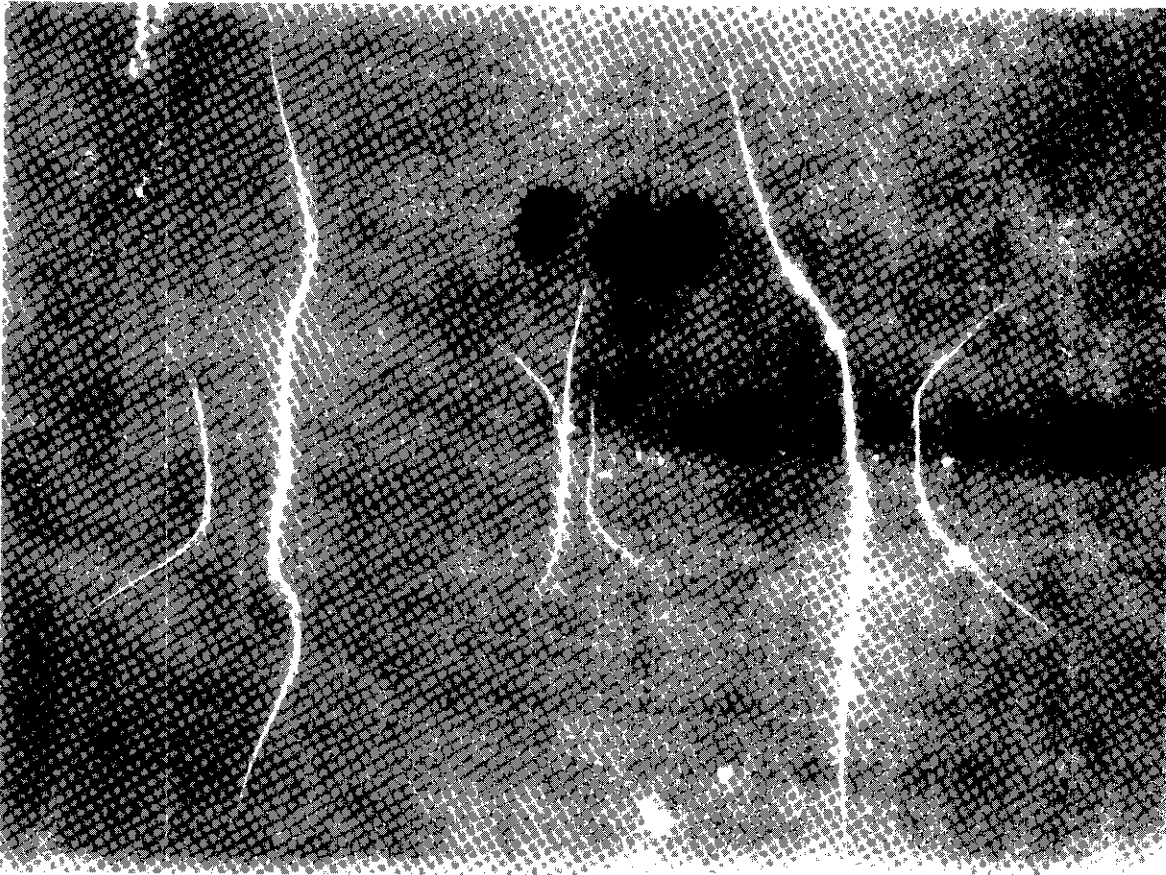
Fig. 26. Radiograph of simple butt joint (Specimen F41) of heat-treated SAE 4340 steel after stress-corrosion-cracking test for 180 hours. .04 X

Metallographic Examinations of Cracks

Metallographic examinations were made of sections cut through cracks to characterize the mode of cracking.

Experimental Methods

A number of sections were cut from areas which contained cracks produced by the hydrogen-induced-cracking technique and the stress-corrosion-cracking technique. The sections were taken from the following specimens:

Specimens with Hydrogen-Induced Cracks

4 sections from Specimen FT2 - commercial high-strength structural steel water quenched and tempered at 350 F

7 sections from Specimen P4-3) SAE 4340 steel oil quenched and
6 sections from Specimen F49) tempered at 500 F
3 sections from Specimen 042)

Specimens with Stress-Corrosion Cracks

6 sections from Specimen FT1 - commercial high-strength structural
steel water quenched and tempered
at 350 F.

6 sections from Specimen F43 - SAE 4340 steel oil quenched and
tempered at 500 F.

Figure 8b shows locations of Sections 042-1, 042-2, and 042-3 taken from
Specimen 042. All sections were cut in such a way that the tips of the cracks
could be examined. Metallographic examinations were made on the center plane
(middle of the plate thickness) of the sections.

Experimental Results

Figures 27a, b, c, and d are photomicrographs of cracks. On the speci-
mens made in the commercial high-strength structural steel, different modes of
fracture were found between hydrogen-induced cracks and stress-corrosion cracks.
Hydrogen-induced cracks were transgranular, while stress-corrosion cracks were
intergranular, as shown in Figures 27a and b, respectively. On the SAE 4340
steel specimens, both hydrogen-induced cracks and stress-corrosion cracks were
intergranular, as shown in Figures 27c and d.

Measurements of Residual Stresses by
Stress-Relaxation Techniques

Measurements of residual stresses by stress-relaxation techniques using
strain gages were made on 8 weldments in mild steel and SAE 4340 steel.

Experimental Methods

Specimens. The following welded specimens were prepared:

(1) Three mild-steel specimens -

Specimen OM1, butt joint, 1/2 by 12 by 16 inches

Specimen TM1, butt joint, 5/8 by 24-1/4 by 38 inches

Specimen 3CM, complex welded structure

(2) Five specimens made from SAE 4340 steel oil quenched from 1550 F
and tempered at 500 F

Specimen R1, butt joint, 1/2 by 12 by 16 inches

Specimen S1, butt joint, 3/4 by 12 by 16 inches

Specimen S2, butt joint, 3/4 by 18 by 32 inches

Specimen T41, butt joint, 5/8 by 24-1/2 by 38 inches

Specimen 3C41, complex welded structure.
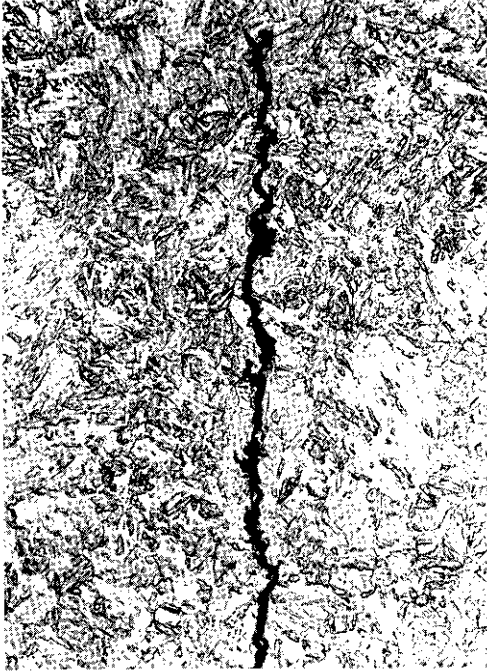
a. Commercial high-strength, heat-treated
   structural steel after hydrogen-
   induced-cracking test.   (396 X)

b. Commercial high-strength, heat-treated
   structural steel after stress-
   corrosion-cracking test.   (396 X)
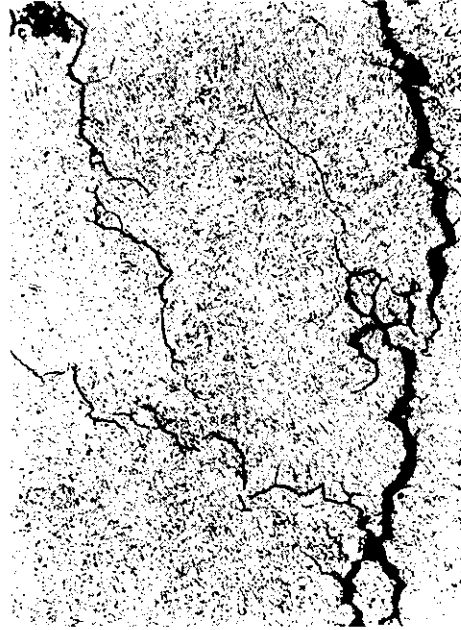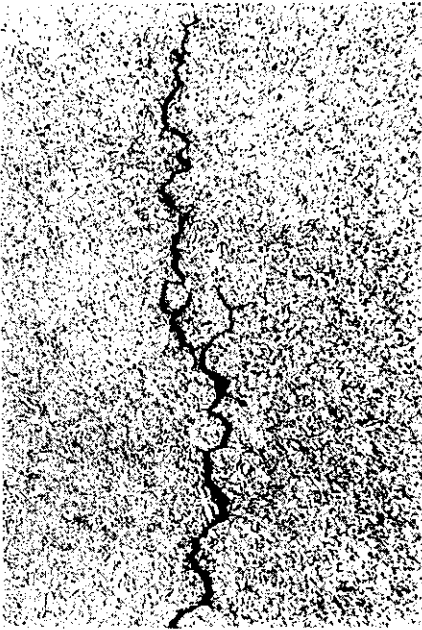
c. Heat-treated SAE 4340 steel after
   hydrogen-induced-cracking test.
   (396 X)

d. Heat-treated SAE 4340 steel after
   stress-corrosion-cracking test.
   (396 X)

Fig. 27.   Sections through cracks.
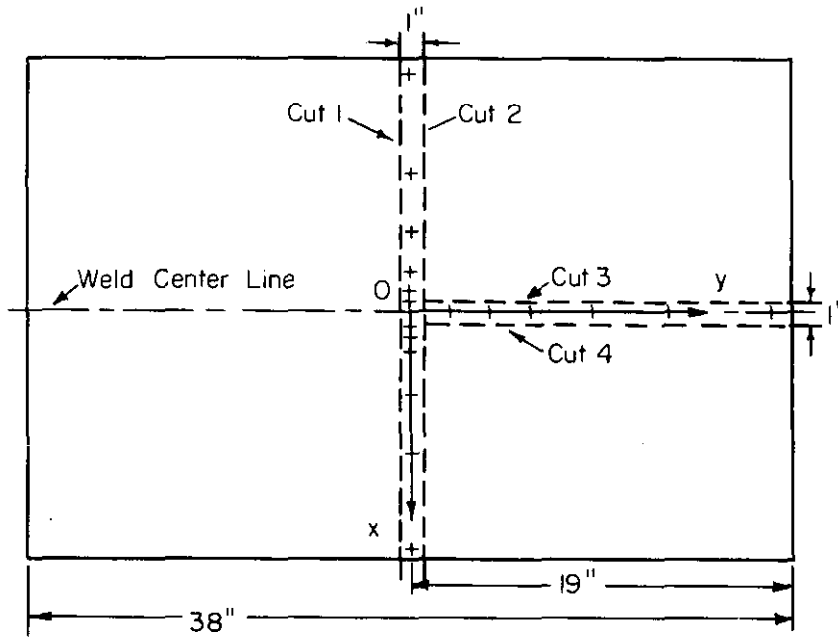
a. *Large-size butt joint*
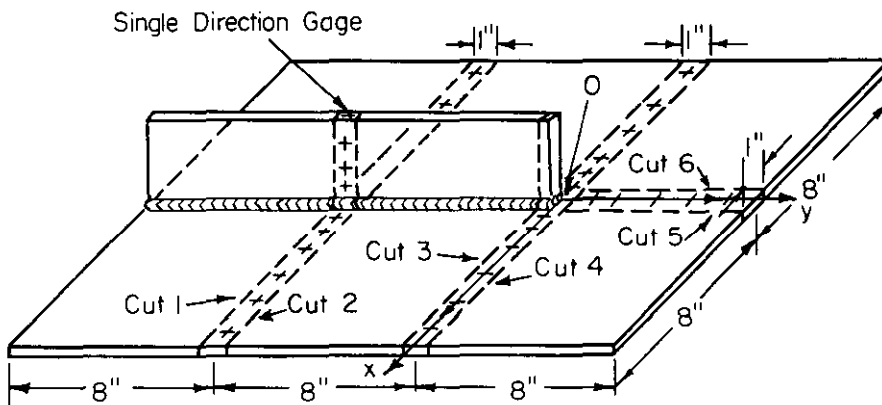
b. *Complex welded structure*

Fig. 28. *Location of strain gages and sequence of cuts for determination of residual stresses by stress-relaxation technique. Strain gages were mounted on both surfaces of plates.*

All of the specimens were welded with covered electrodes, E6010 electrodes for the mild-steel weldments and E15016 electrodes for the SAE 4340 steel weldments. Specimens OM1 and R1 were made from 5/8-inch plates and ground to 1/2 inch thick after welding. On Specimens TM1 and T41, weld reinforcements were ground to form flush specimen surfaces. On Specimen S2, the reinforcement was removed from a 3 inch length of the weld so that strain gages could be mounted on the weld metal.
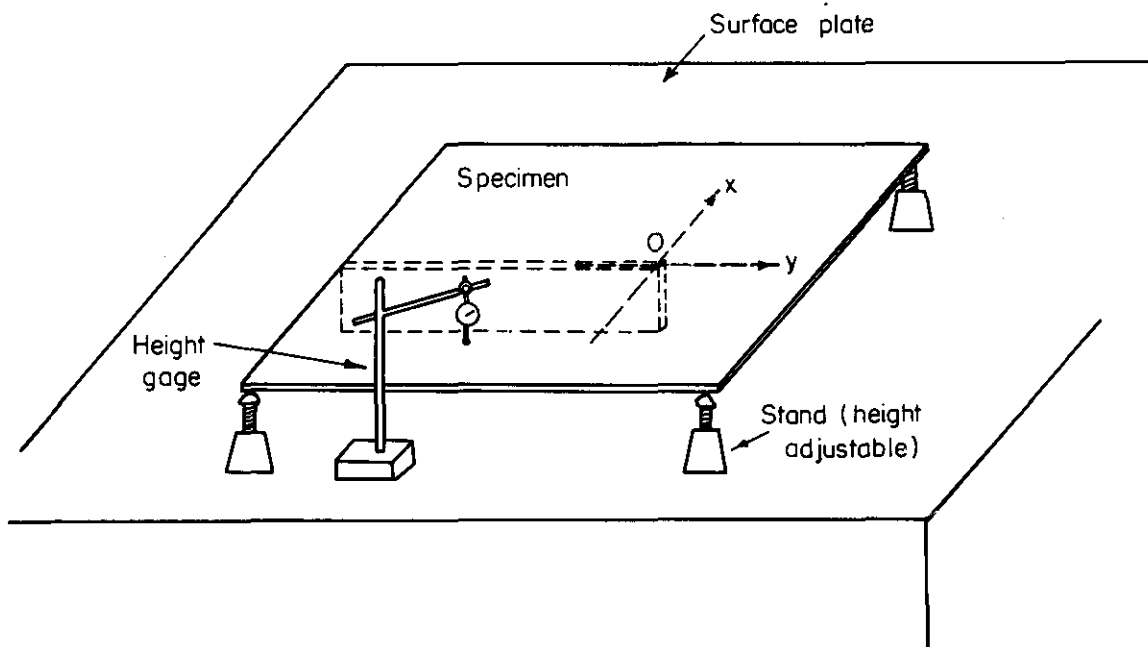
Fig. 29. *Method of measuring distortion of complex welded structure.*

The weld reinforcement was not removed on Specimen S1. These procedures were used to investigate the effect of the grinding operation on results of the residual-stress measurement. On complex structures (Specimens 3CM and 3C41), specimen surfaces were ground before welding but no grinding was done after welding.

Techniques for Measuring Residual Stresses. Figure 28a shows locations of strain gages on the 38-inch-long butt joints (Specimens TM1 and T41). Strain gages were mounted on the specimen surface along two lines: the transverse line passing the center of the weld (the x-axis) and the longitudinal line on the weld metal (the y-axis). On the other butt joints (Specimens OM1, R1, S1, and S2), strain gages were mounted on the specimen surface along the transverse line only. Figure 28b shows locations of strain gages on the complex structures.

Metal-film gages with 1/8-inch gage length were used. Most of the gages were two-direction gages mounted so that one component was parallel and the other perpendicular to the weld line. Strain gages were mounted on both surfaces of the specimen except in areas near the fillet welds of the complex structures (gages were mounted on the back surface of the bottom plate under the fillet welds). Rubber and plastic coatings were used to protect gages during machining.

One-inch-wide strips containing gages were cut from the specimens with a grinding wheel. Liquid coolant was used to prevent undesirable temperature rise in the specimens during cutting. The cutting sequences are shown in Figures 28a and b (Cuts 1 to 6). The values of strain release due to cutting were measured and residual stresses were determined.
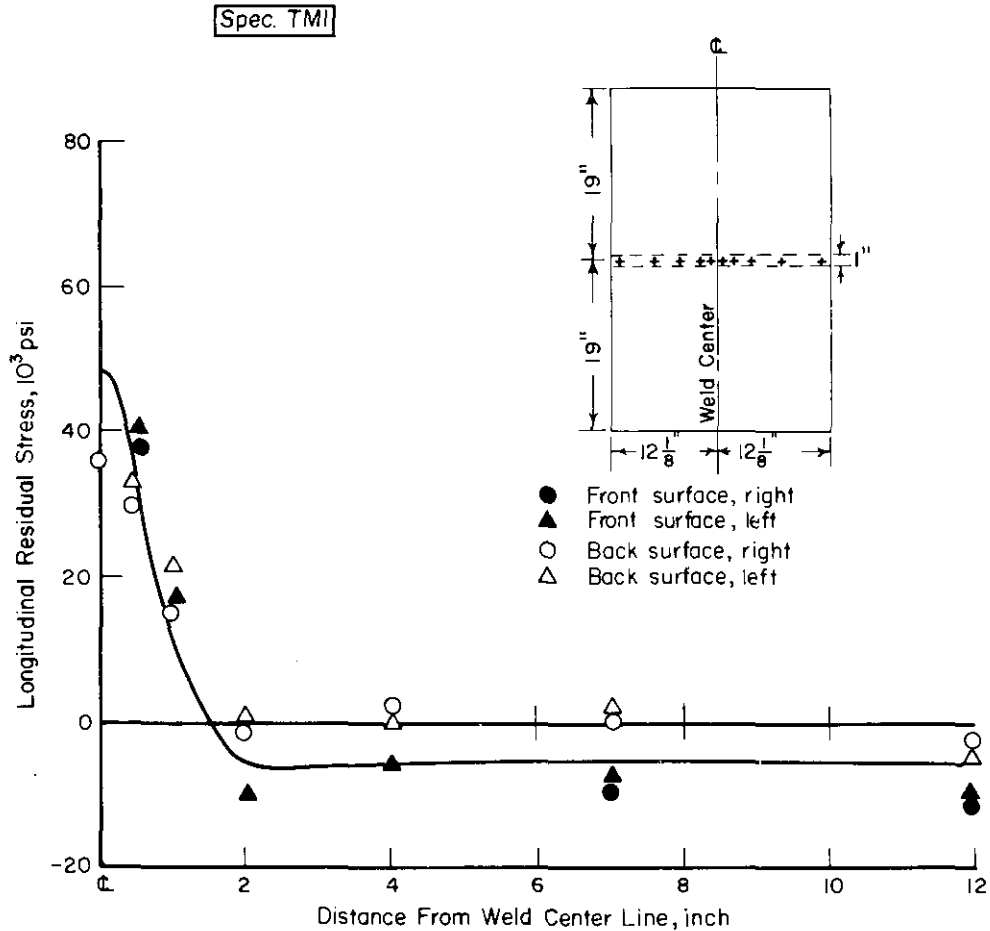
Fig. 30. *Transverse distribution of longitudinal residual stresses in 38-inch-long butt joint made with mild steel.*

<u>Measurement of Distortions</u>. Measurements were made of distortions caused by welding of complex welded structures, Specimens 3CM, 3C41, and 3C42.[*] As shown in Figure 29, the specimen was placed on four adjustable height stands on a surface plate with the bottom plate up. Distances between the surface plate and various locations on the back surface of the bottom plate of the complex structure were measured with a height gage. The distortion measurements were made before the measurements of residual stresses by stress-relaxation techniques or the hydrogen-induced-cracking tests.

Experimental Results

<u>Butt Joints</u>. Figure 30 and 31 show distributions of longitudinal residual stress (σ_y) along the transverse line passing the center of the weld (the x-axis) of the 38-inch-long butt joints in mild steel and SAE 4340 steel,

---

[*] Specimen 3C42 was used for the hydrogen-induced-cracking test.
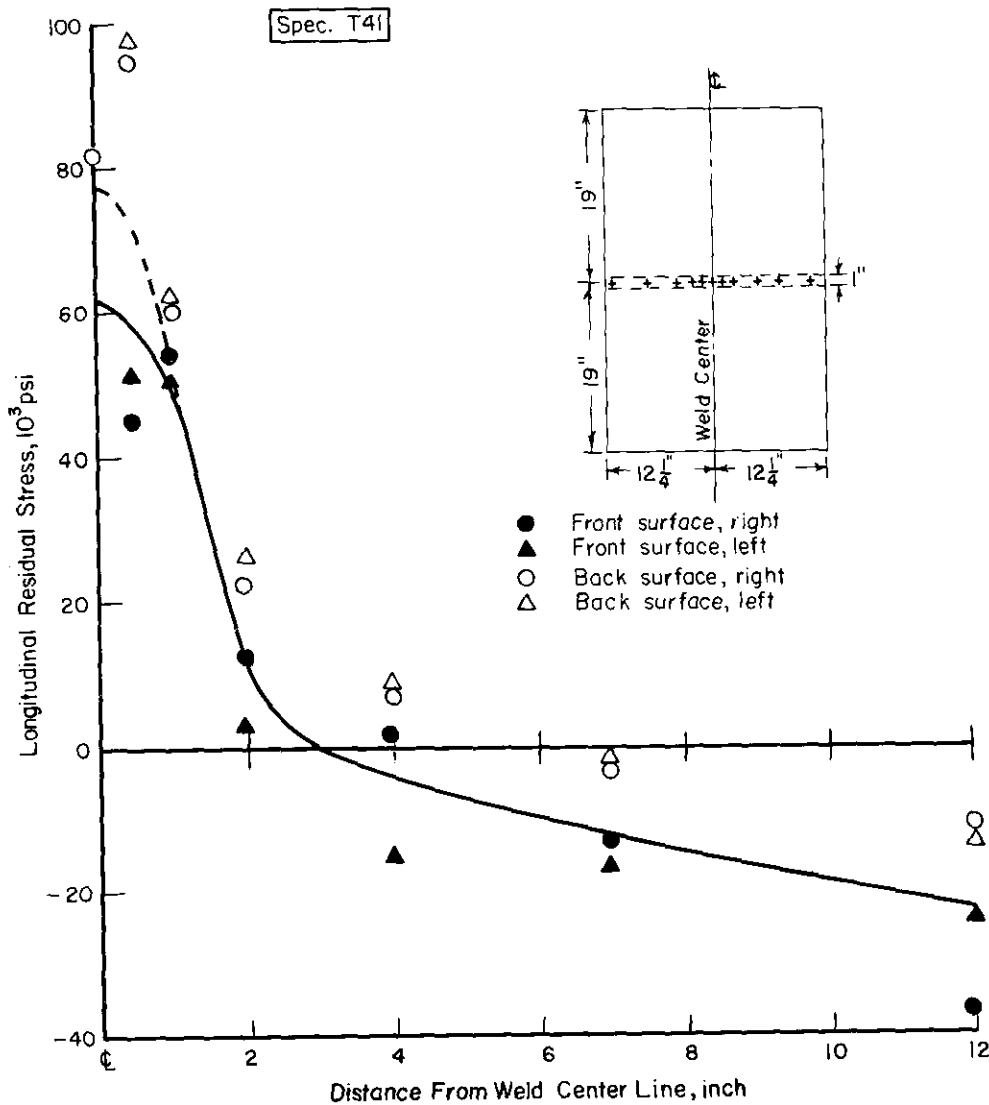
Fig. 31. *Transverse distribution of longitudinal residual stresses in 38-inch-long butt joint made with heat-treated SAE 4340 steel.*

respectively. In both specimens, high-tensile residual stresses were observed in regions near the welds and compressive stresses were observed in regions away from the welds.

Figure 32 shows distributions of longitudinal residual stress along the weld centerline of the 38-inch-long butt joints. In the SAE 4340 steel specimen, stresses on the top and bottom surfaces were quite different indicating that substantial longitudinal distortion occurred. However, distributions of the mean stress were quite similar for the two specimens tested. Residual stresses were low in regions near the edge of the plate. The longitudinal residual stress reached maximum values when the distance from the edge was more than 7 inches for the mild-steel joint and 9 inches for the SAE 4340 steel joint. The results obtained in this research on the mild-steel joint agree very well with those obtained by DeGarmo, et al.[14]
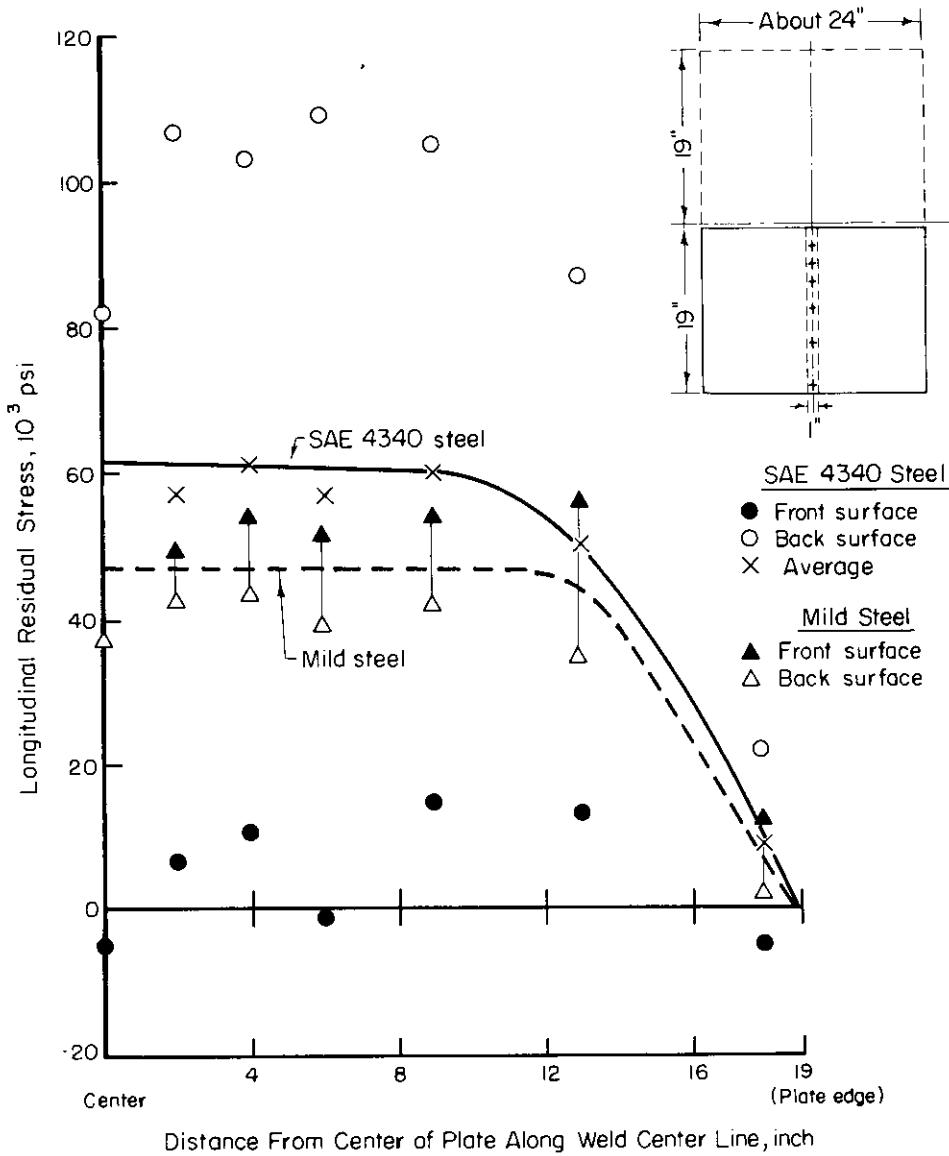
Fig. 32. *Distribution along weld center line of longitudinal residual stresses in 38-inch-long butt joints made with SAE 4340 steel and mild steel.*

Figure 30 through 32 show that distributions of residual stresses in the two butt joints were quite similar; the SAE 4340 steel joint had somewhat higher stresses than had the mild-steel joint. On the basis of the data shown in these figures, values of the maximum (mean) stress at the weld center, σ_0,

TABLE 5. SUMMARY OF RESULTS OF RESIDUAL-STRESS MEASUREMENTS

Specimen Code Number	Type of Steel	Joint Type (Specimen Size)	Maximum Stress in or near the Weld, σ_0, (approximately) psi	Width of Residual-Stress Tension Zone b, in	$K_w = \sqrt{\frac{\pi}{2}}\, \sigma_0 \sqrt{b}$
OM1	Mild Steel	Butt joint[a] 1/2 by 12 by 16 inches	60,000	4	151,000
TM1		Butt joint[b] 5/8 by 24 by 38 inches	50,000	3	109,000
3CM		Complex welded structure (bottom plate: 7/16 by 16 by 24 inches)	45,000[e]	3[e]	98,000
R1	SAE 4340	Butt joint[a] 1/2 by 12 by 16 inches	51,000	3	111,000
S1		Butt joint[c] 3/4 by 12 by 16 inches	52,000	3	113,000
S2		Butt joint[d] 3/4 by 18 by 32 inches	45,000[f]	3	98,000
T41		Butt joint[b] 5/8 by 24 by 38 inches	61,000	6	188,000
3C41		Complex welded structure (bottom plate: 7/16 by by 16 by 24 inches)	75,000[e]	2.5[e]	149,000

Notes:
(a) The specimens were ground for 5/8 inch to 1/2 inch thick.
(b) Weld reinforcements were ground to form flash specimen surfaces.
(c) Weld reinforcement was not ground.
(d) Weld reinforcements were ground partially.
(e) Values for the transverse section through the center of the longitudinal frame.
(f) Estimated value.

and the width of the tension zone of residual stress, b, were determined.* These values are shown in Table 5 along with values of σ_0 and b determined on other butt joints and complex structures. The maximum stress, σ_0, ranged from 45,000 to 61,000 psi, and the width of tension zone of residual stresses, b, ranged from 3 to 6 inches for butt joints.

---

* The maximum mean stress, σ_0, is not the maximum measured data which was close to 100,000 psi on Specimen T41, but it is the estimated value of residual stress at the midthickness at the center of the weld (x=y=o). In analyzing Figure 31, it is reasonable to estimate that σ_0 of Specimen T41 was about 78,000 psi as indicated by the dotted curve. However, in analyzing both Figures 31 and 32, σ_0 is estimated to be about 61,000 psi as indicated by the solid lines.
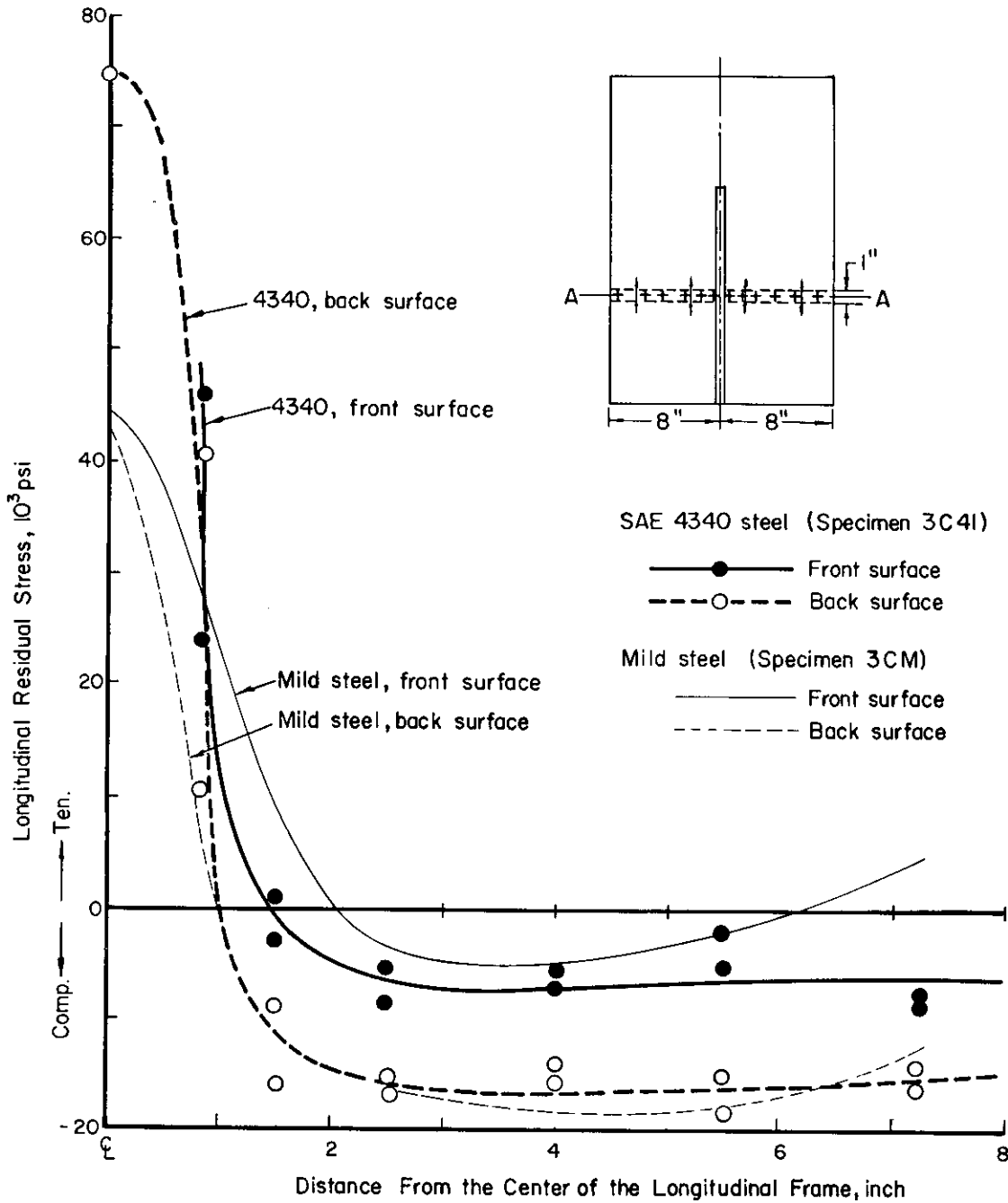
a. *Distribution of longitudinal residual stresses in the bottom plate along line AA.*

Fig. 33. Distributions of residual stresses in complex welded structures.

Transverse residual stresses (σ_x) in butt joints also were determined. Transverse stresses were tensile in regions near the weld and decreased gradually as the distance from the weld increased (σ_x must be zero at the plate edge).
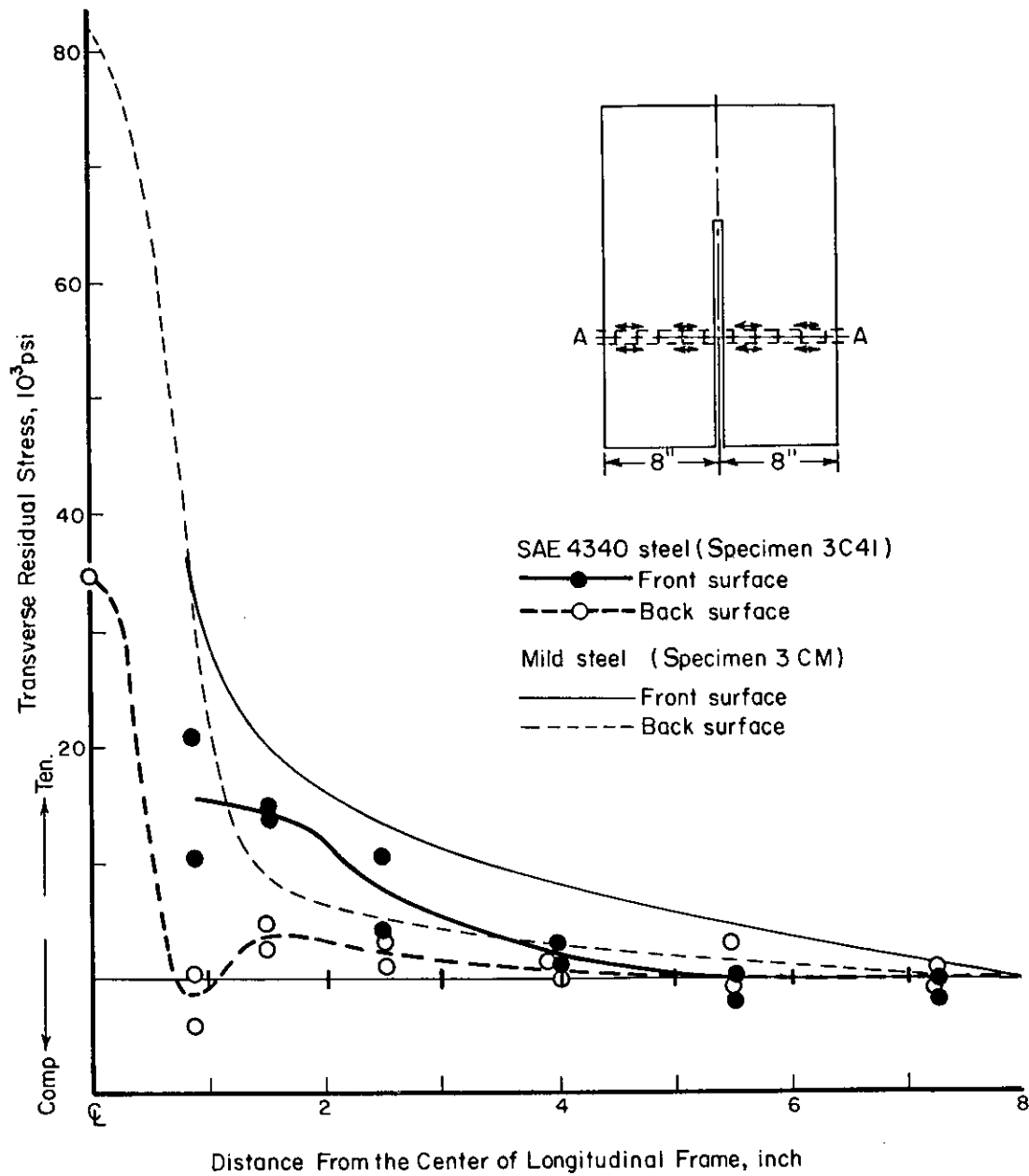
b. Distributions of transverse residual stresses in the bottom plate along line AA.

Fig. 33. (Continued).

Values of the transverse stress at the weld center were around 20,000 psi for most butt joints tested, considerably lower than the maximum longitudinal residual stresses.

The most important finding obtained in this investigation is that residual stresses in butt joints in SAE 4340 steel were similar to those in mild steel despite the considerable differences in the yield strengths of the base plates and the weld metals. It was expected that tensile residual stresses
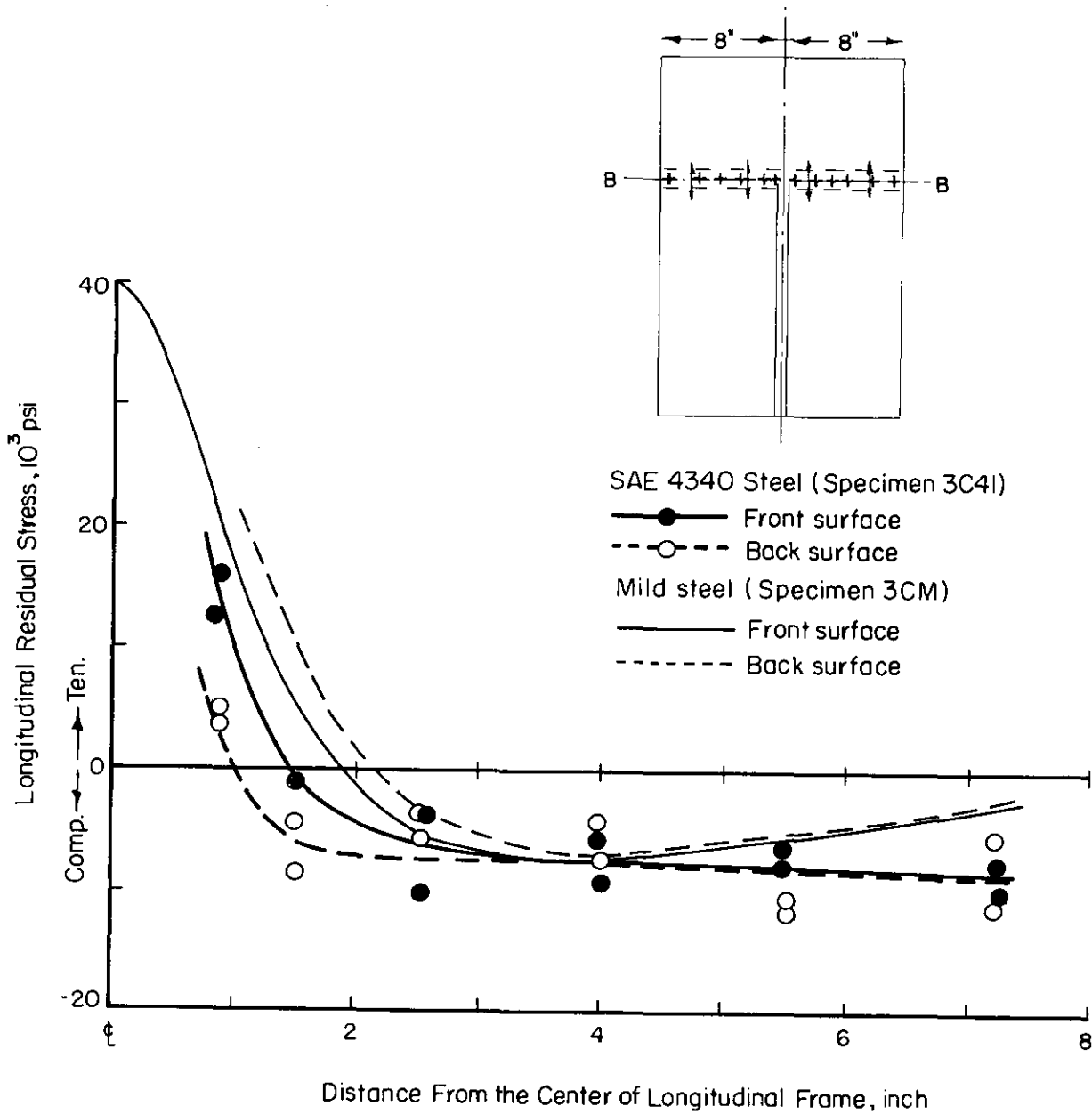
c. Distributions of longitudinal residual stresses in the bottom plate along line BB.

Fig. 33.   (Continued).

approaching the yield stress of the weld metal would be observed in areas near the weld--around 50,000 psi for mild-steel specimens and 150,000 psi for SAE 4340 steel specimens. The results obtained in the mild-steel specimens were as expected. However, the maximum stresses observed in SAE 4340 steel specimens
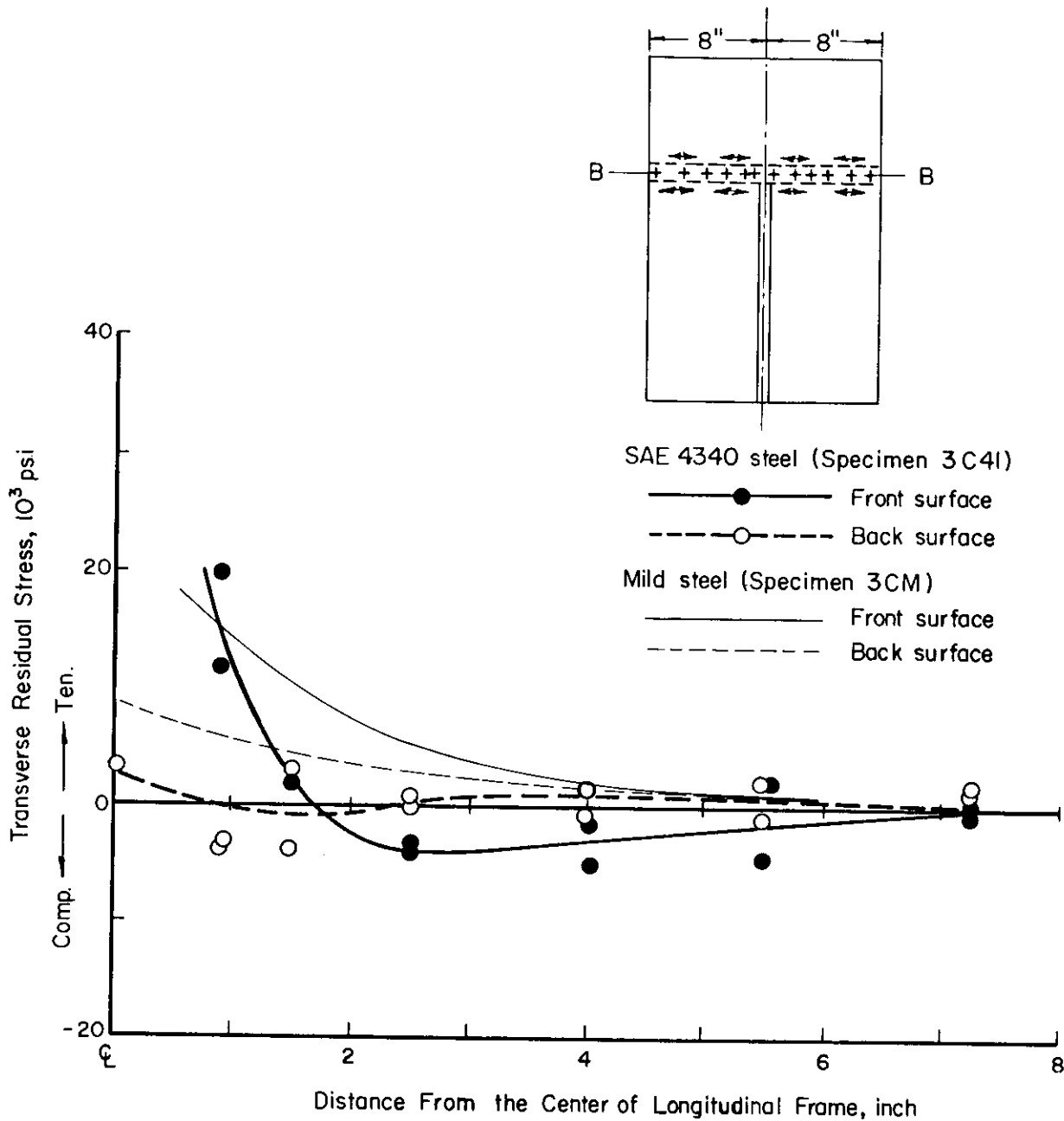
d. *Distributions of transverse residual stresses in the bottom plate along line BB.*

Fig. 33. *(Continued).*

were much lower than expected. Although some measured data were higher (see Figure 32), the average stresses in the weld metal were much lower than the yield stress of the E15016 weld metal. Table 5 shows that the differences in the grinding operations on the weld reinforcement had little effect on the maximum stress. The results indicate that the low values of residual stresses in the
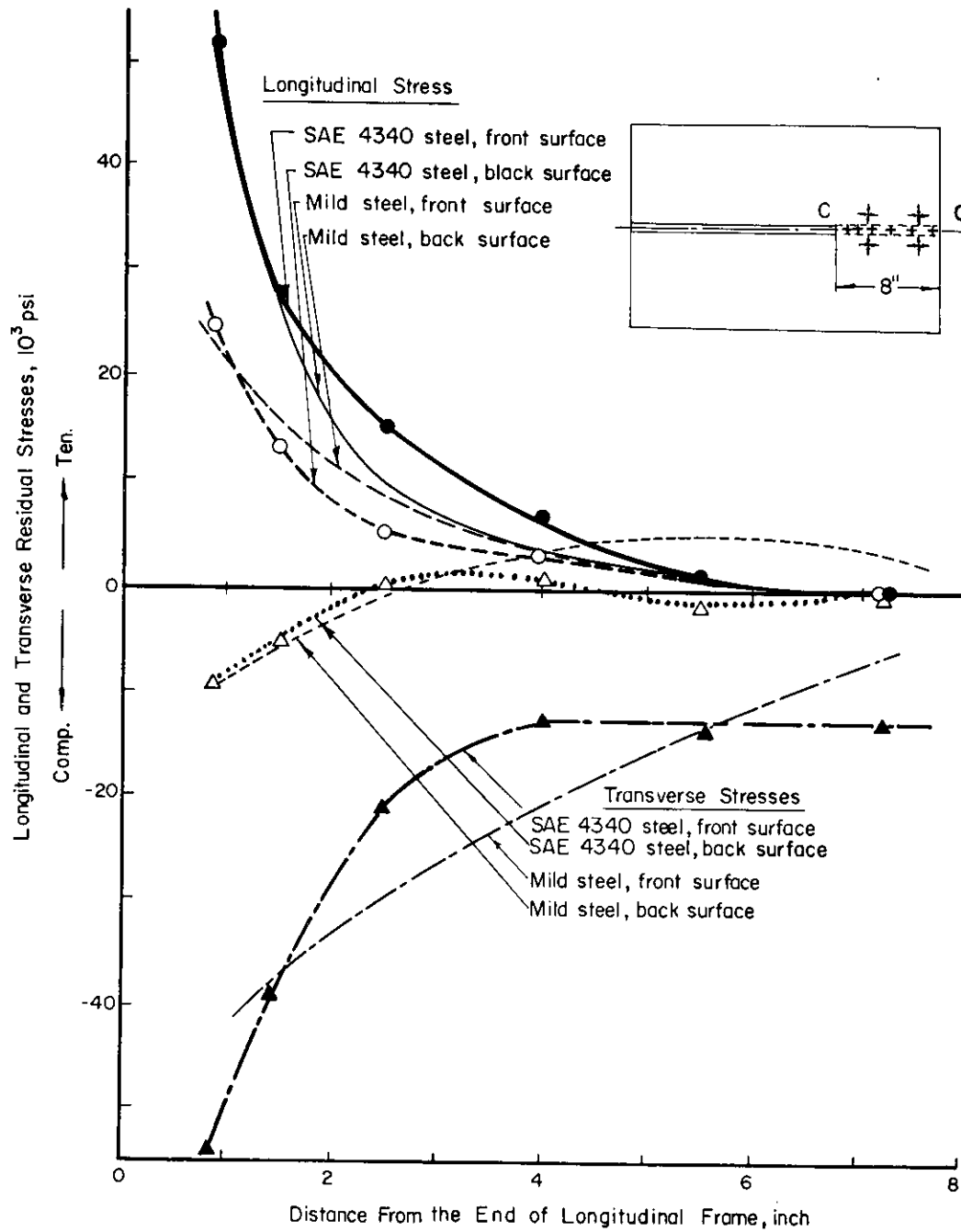
e. *Distance of longitudinal and transverse residual stresses in the bottom plate alloy line CC.*

Fig. 33.   (Continued).

SAE 4340 steel weldments were not due to the fact that some specimens were ground after welding.
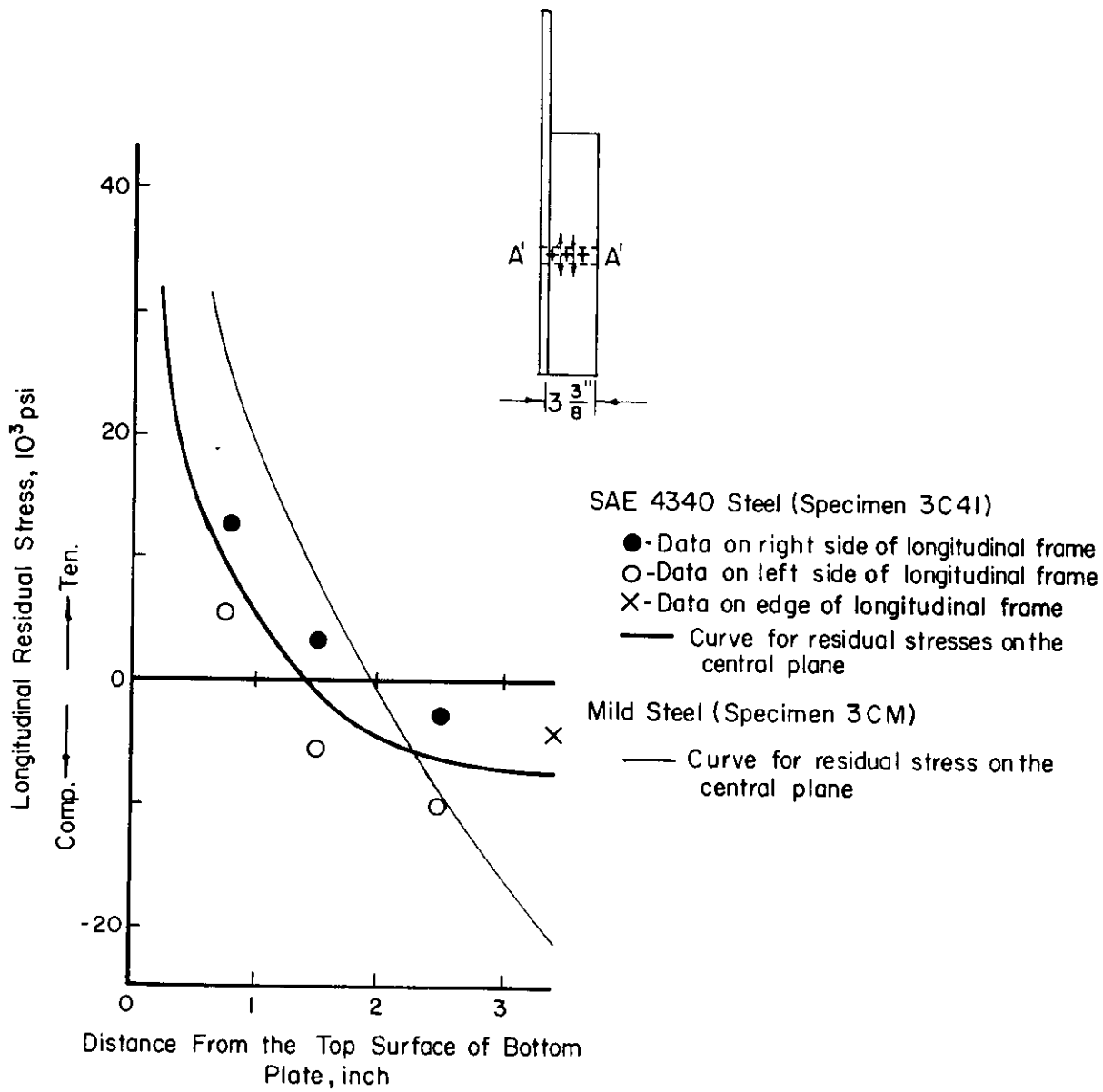
f. Distribution of longitudinal residual stresses in the longitudinal frame along line A'A'.

Fig. 33.   (Continued).

Complex Welded Structures. Figures 33a through f show distributions of residual stresses in two complex welded structures, one made from mild steel and the other from SAE 4340 steel. Measured data obtained on both surfaces of the SAE 4340 steel specimen (3C41) and curves determined by these data are shown; while curves determined by measured data only are shown for the mild steel specimen (3CM). Figures 34 and 35 show weld distortions on Specimens 3CM and 3C41,

a. Transverse distribution of distortion, δ
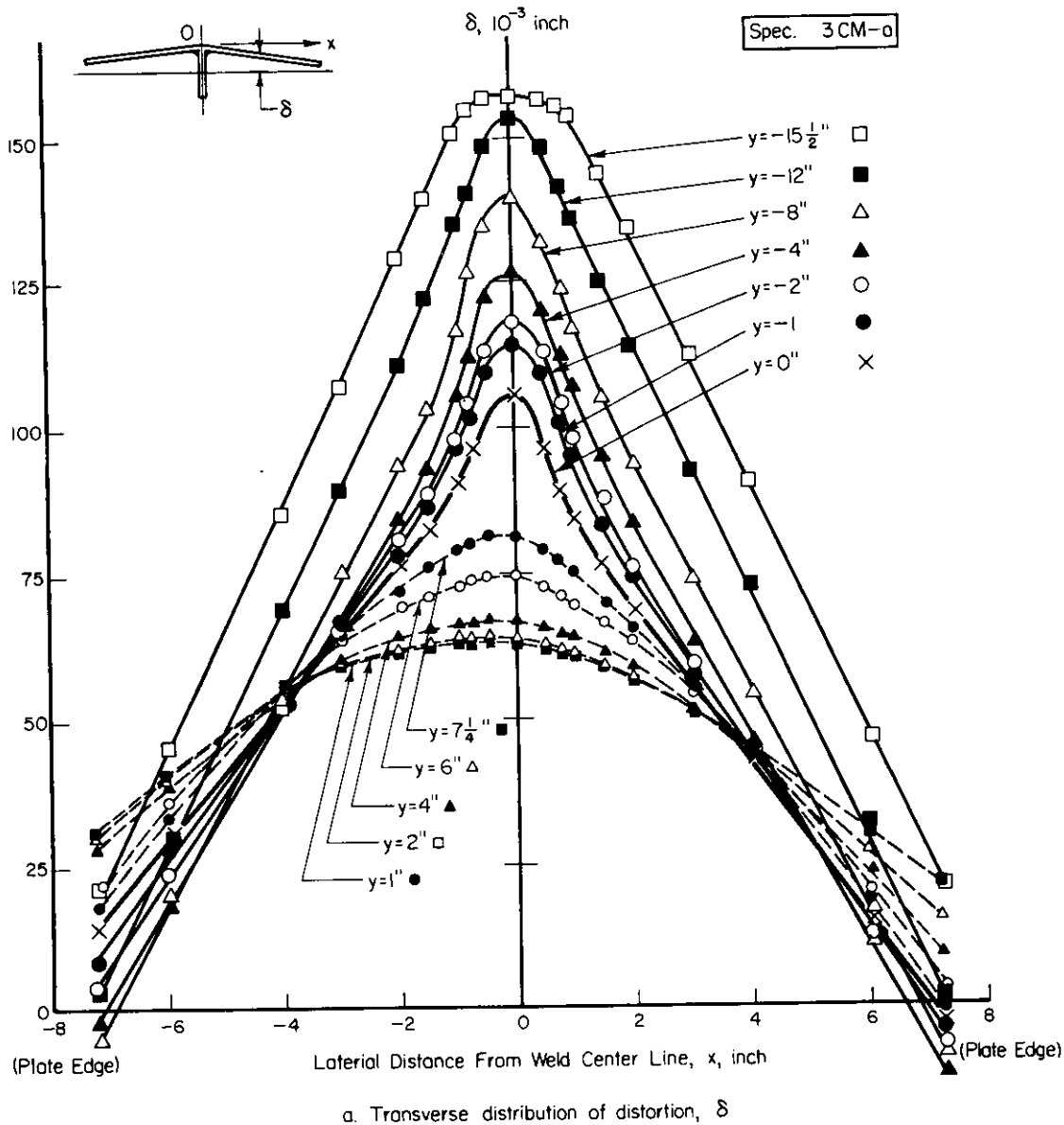
Fig. 34. Distortion due to welding of Specimen 3CM (Complex structure, mild steel).

respectively.*   Figures 34a, and 35a show distributions of distortions along various transverse sections, y = 0, 1, 2, --- inches; y = 0 means the end of the longitudinal frame.   Figures 34b and 35b show distributions of distortions along various longitudinal sections, x = 0, 1, 2, --- inches; x = 0 means the center of the longitudinal frame.

* The weld distortions on Specimen 3C42 were similar to those on Specimen 3C41.
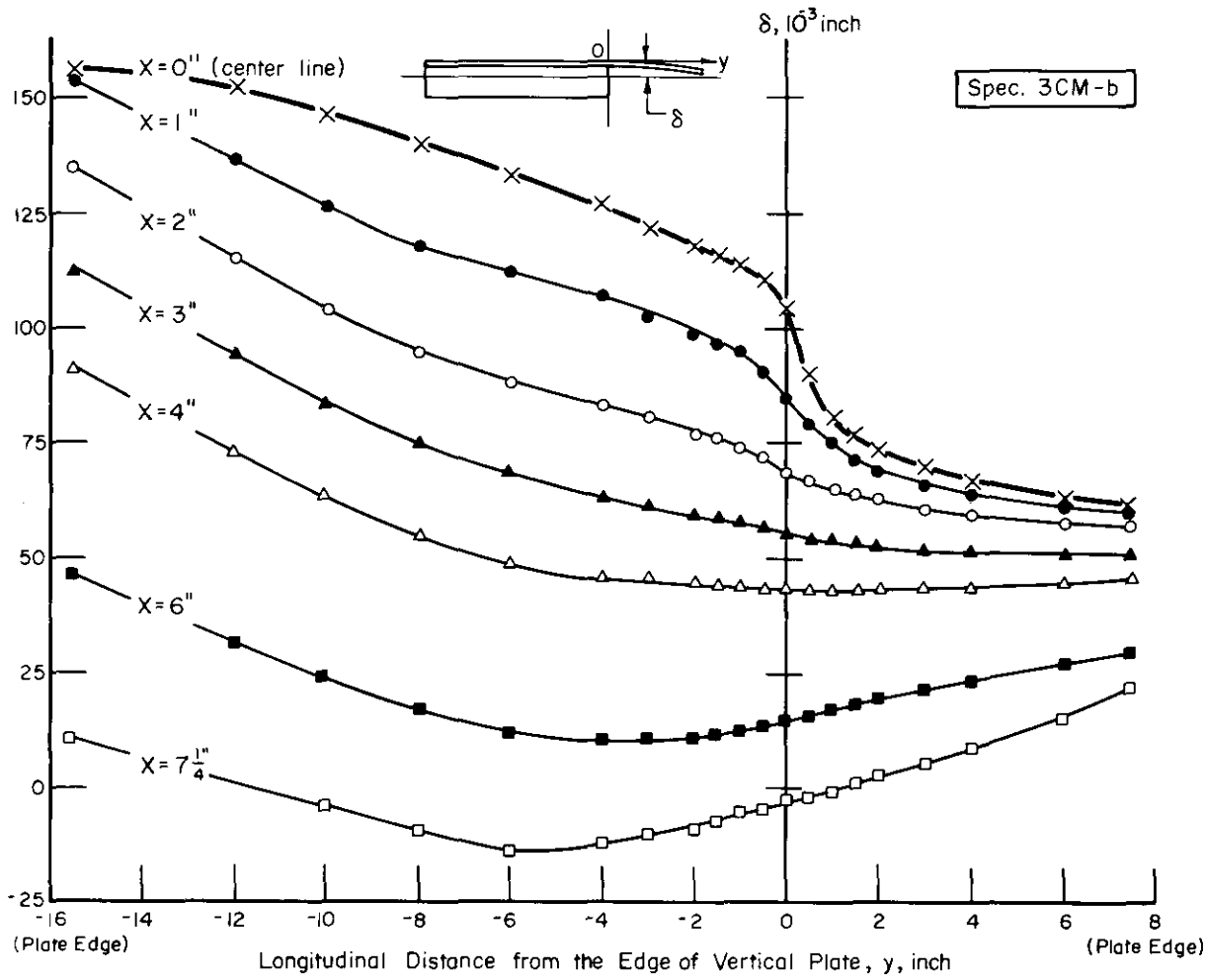
b. Longitudinal distribution(+Xside) of distortion,δ

Fig. 34. (Continued).

Figure 33a shows the distributions of longitudinal residual stresses in the bottom plate along Line AA, perpendicular to the weld line passing the center of the longitudinal frame. On both SAE 4340 steel and mild-steel specimens, high tensile residual stresses were observed in regions near the weld and compressive stresses in regions away from the weld. Values of the maximum residual stress, σ_0, and the width of tension zone of residual stress, b, were:

	σ_0	b
Mild-steel specimen	45,000 psi	3.0 inches
SAE 4340 steel specimen	75,000 psi	2.5 inches

These values also were shown in Table 5. Compressive residual stresses in regions away from the weld were greater on the back surface than on the front surface indicating that the bottom plate was bent--convexly looking from the front-surface

Spec. 3C41-a

a. Transverse distribution of distortion, δ
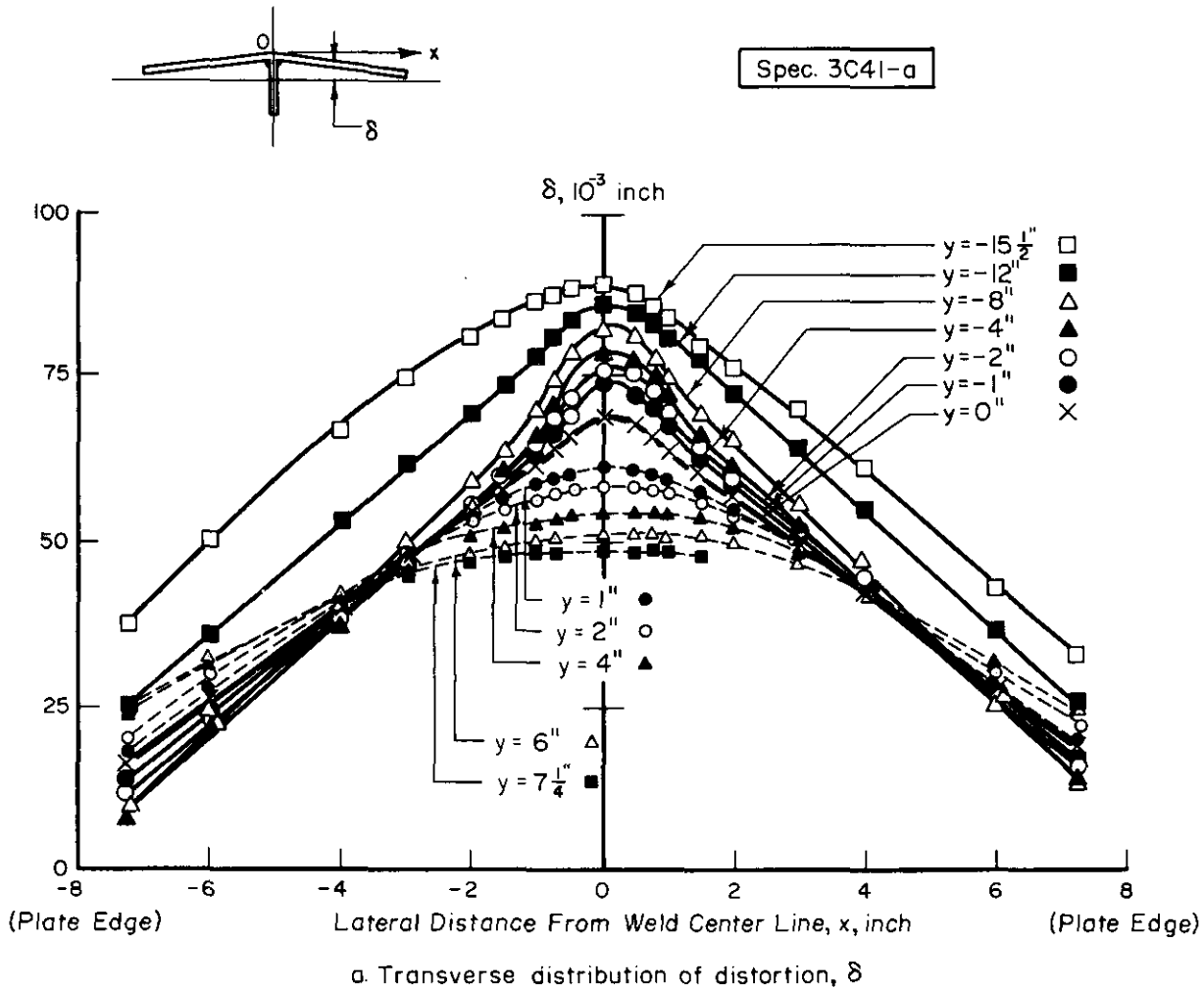
Fig. 35. Distortion due to welding of Specimen 3C41 (Complex structure, SAE 4340 steel).

side. Longitudinal distributions of distortions are shown in Figures 34b and 35b. In regions near Line AA (y = -8 inches), the bottom plates were slightly bend to convex forms looking from the front-surface side of the bottom plate.

Figure 33b shows the distribution of transverse residual stresses along Line AA. High-tensile stresses were produced in regions near the weld and they decreased gradually as the distance from the weld increased. Concentrated high-tensile stresses on the back surface near the weld were due to the angular change cuased by the fillet welding. As shown in Figures 34a and 35a, the bottom plates were bent severely in regions near the welds causing high-tensile stresses in the transverse direction on the back surface of the bottom plate.

Figure 33c shows distributions of longitudinal residual stresses in the bottom plate along Line BB, perpendicular to the weld line passing the end of the longitudinal frame. Tensile stresses were produced in regions near the weld and compressive stresses in regions away from the weld. In regions away from the

b. Longitudinal distribution (+ X side) of distortion, δ
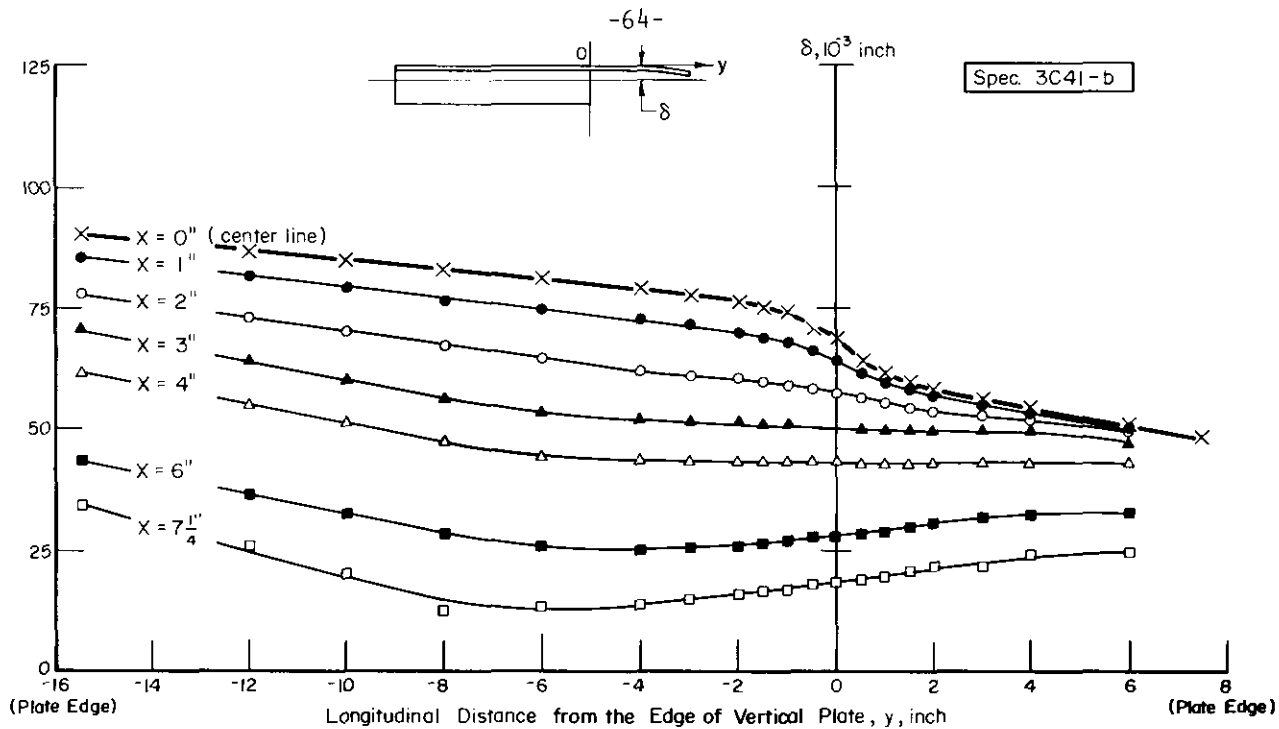
Fig. 35. (Continued).

weld, stresses on both surfaces were almost identical. As shown in Figures 34b and 35b, longitudinal distortions of the bottom plate changed from convex to concave (looking from the front-surface side) in regions near the end of the longitudinal frame, or y = o. The results indicate that longitudinal bending stresses in these areas were minor.

Figure 33d shows distributions of transverse residual stresses along Line BB. Residual stresses were relatively low.

Figure 33e shows distributions of longitudinal and transverse residual stresses in the bottom plate along Line CC, a longitudinal line passing through the center of the longitudinal frame. Longitudinal stresses were tensile large in regions near the end of the longitudinal frame decreasing with increasing distance from the weld. The results indicate that the longitudinal residual stresses were primarily due to longitudinal shrinkage of the weld. Transverse stresses were compressive in large values in regions near the weld decreasing with increasing distance from the weld. This indicates that transverse stresses were primarily caused by transverse shrinkage of the weld. When the weld shrinks in the transverse direction, the weld will be subjected to tensile stresses in that direction by the surrounding material; while compressive stresses in the transverse direction will be produced in the surrounding material so that the tensile stresses in the weld (x = o, y<o) and the compressive stresses in the plate (x = o, y>o) are balanced. Significant differences existed between transverse stresses on the front surface and those on the back surface. This is because the bottom plates were bent in the transverse direction to concave forms looking from the front-surface side, as shown in Figures 34a and 35a.

Figure 33f shows distributions of longitudinal residual stresses in the longitudinal frame along Line A'A', perpendicular to the weld line passing the center of the longitudinal frame. Data obtained on both sides of the frame were

somewhat different indicating that the longitudinal frame was slightly bent in the lateral direction. High-tensile stresses were produced in regions near the weld and compressive stresses in regions near the top edge of the frame. Figures 34b and 35b show that the bottom plate under the frame x = o was bent longitudinally in a concave form looking from the front surface indicating that considerably high compressive stresses could be produced in regions near the top edge of the frame.

Figures 33 through 35 show that distributions of residual stresses and distortions were quite similar in distribution in complex structures made in mild steel and SAE 4340 steel. Little difference was found between the magnitude of residual stresses in the two weldments. The magnitude of the distortions in the mild-steel specimen were considerably higher than those in the SAE 4340 specimens. This is probably because the mild-steel specimen was welded without preheating, while the SAE 4340 steel specimens were welded with 400 F preheat and interpass temperature.

ANALYTICAL INVESTIGATIONS

Objectives

In the experimental hydrogen-induced-cracking tests on welded and press-fit specimens it was found that:

(1) Crack patterns were affected by properties of the material,

(2) Crack patterns were affected by the magnitude and distribution of residual stresses.

Investigations were made to establish analytical relationships among the residual-stress distribution, properties of the material, and the crack pattern. Attempts also were made to apply findings obtained in the analytical investigations to the interpretation of experimental results.

General Theory of the Crack Pattern
Produced by Residual Stresses

Background

The Griffith theory has been widely used as a fundamental statement of the mechanism of fracture in a brittle material and has been applied by many investigators to various types of brittle fracture.[15-17] The modified Griffith theory developed by Irwin and others is often called fracture mechanics theory, and it is widely applied to the fractures of high-strength steels and nonferrous materials.[18-20]

In the Griffith-Irwin fracture mechanics theory, the stability of a crack in a solid is discussed. If a straight crack of length $\ell = 2a$ occurs in an infinite plate (of uniform thickness) subjected to uniform tensile stress, σ, the elastic strain energy stored in the plate decreases but additional energy is required to produce the new surfaces. Therefore, the decrease in the total energy in the plate (per unit thickness), U, is expressed as follows:

$$U = W_e - W_s = \frac{\pi \ell^2 \sigma^2}{4E} - 2\rho\ell \qquad (4)$$

where

W_e = decrease in elastic strain energy
W_s = energy required to produce the new surface
ρ = amount of energy required to produce a surface of unit area*
E = Young's modulus.

---

* In case of a metal, the value of ρ is mostly plastic work, as has been pointed out by Felbeck and Orowan.[21]

The crack is unstable if $\frac{\partial U}{\partial \ell} > 0$. In other words, the crack will propagate when (1) the stress σ exceeds the critical stress, σ_{cr} (for given values of ℓ and ρ or (2) the crack length exceeds the critical crack length, ℓ_{cr}, as follows:

$$\sigma > \sigma_{cr} \equiv \sqrt{\frac{4\rho E}{\pi\ell}}$$

$$\ell > \ell_{cr} \equiv \frac{4E\rho}{\pi\sigma^2} \tag{5}$$

In fracture mechanics theory, the critical stress-intensity factor, K_c, and the critical crack-extension force, G_c, are widely used for characterizing the material property sometimes called fracture toughness, as follows:

$$G_c = 2\rho = \frac{K_c^2}{E} \tag{6}$$

Unstable fracture occurs when the stress-intensity factor, K, exceeds the critical stress-intensity factor K_c of the material, as follows:

$$K \equiv \sqrt{\pi a} \cdot \sigma > K_c \tag{7}$$

General Theory of Crack Pattern

An attempt has been made to develop a general crack pattern theory produced in a solid containing residual stresses by modifying the Griffith-Irwin fracture mechanics theory. However, there is a basic difference between subjects discussed in this crack pattern theory and ordinary fracture-mechanics theory. In the crack pattern theory, the major concern is to determine the crack pattern that is stable. In fracture mechanics theory, on the other hand, the major concern is to determine the condition for the occurrence of unstable fracture. Another important problem in the crack pattern theory is that it is essential to assume that residual stresses are not uniformly distributed in the solid. The crack may be curved, and there may be more than one crack.

When a crack occurs in a solid containing residual stresses, new surfaces appear and the residual stresses that existed in regions near the crack are partially released. If the decrease in residual stress strain energy due to the strain release is greater than the energy required to produce the new surfaces, a crack will form since the total energy of the solid decreases due to the occurrence of the crack.

General view

Detail of crack opening
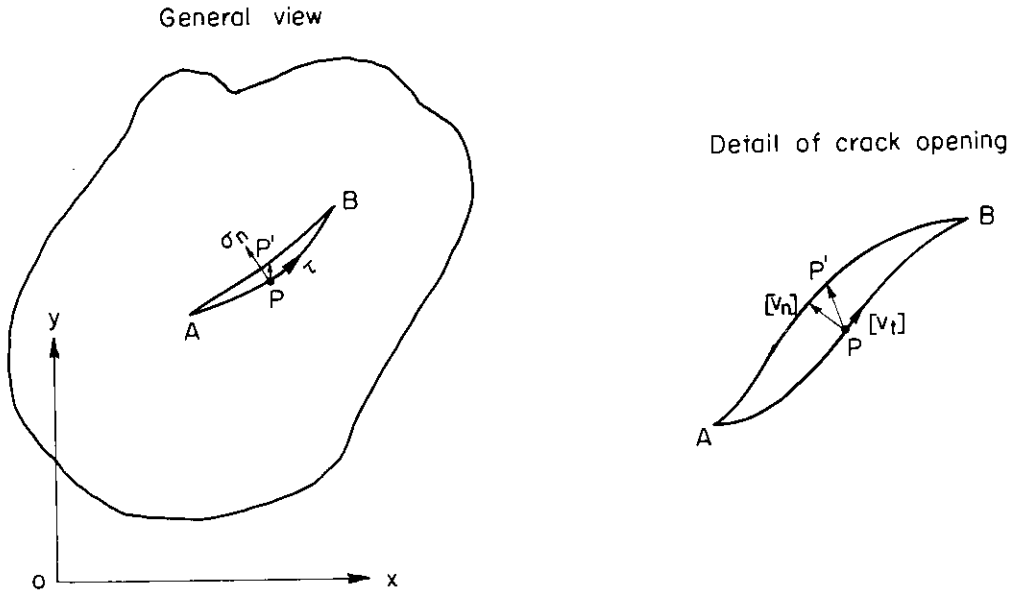
Fig. 36. Occurrence of a crack in a body containing residual stress.

a. Different crack paths
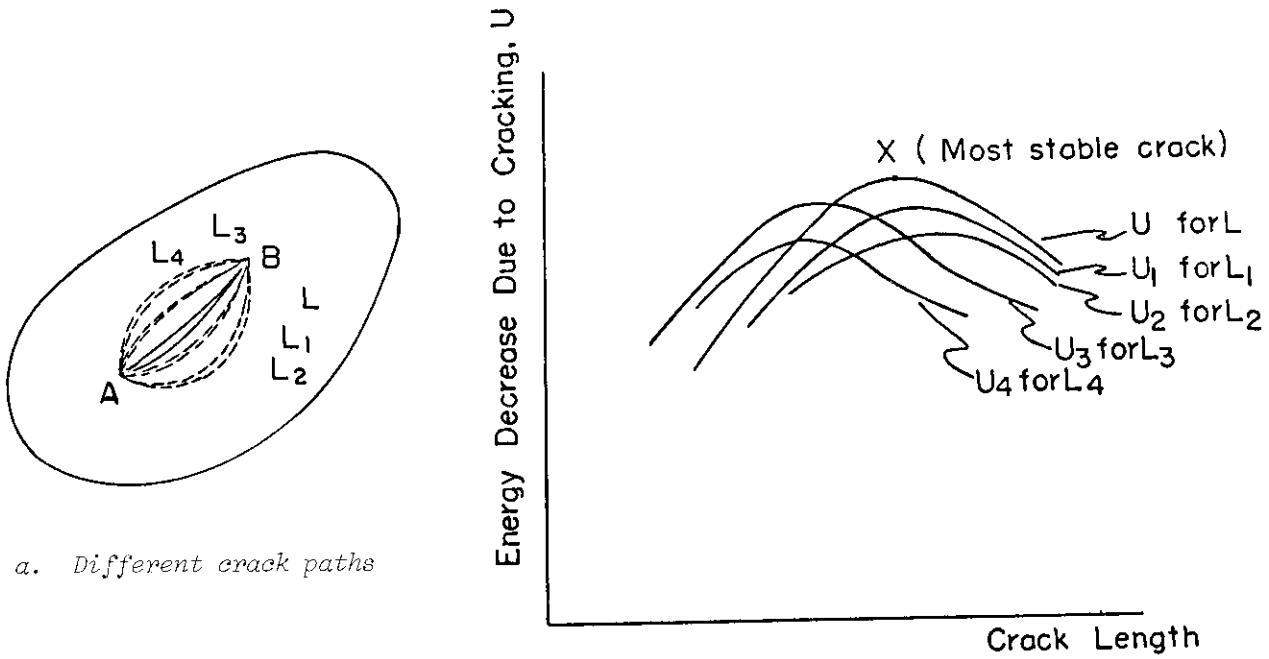
b. Changes of energy decrease due to cracking, U, for cracks which have different paths and different lengths

Fig. 37. Determination of the most stable crack.

The increase of surface energy depends on the properties of the material and is considered to be proportional to the surface area of the crack. When a crack of length ℓ (between A and B in Figure 36) occurs in a plate of uniform thickness, the increase of surface energy per unit plate thickness, W_s, is given by:

$$W_s = 2\rho\ell$$

$$= 2\rho \int_A^B ds \tag{8}$$

where

ρ = amount of energy required to produce a surface of unit area

$ds = \sqrt{dx^2 + dy^2}$ = line element.

The major characteristics of the changes of residual stresses that take place during the formation of the crack are:

(1) Since residual stresses are released due to cracking, the stress changes are considered to be elastic even when the pre-existed residual stresses are caused by plastic deformation*

(2) As the crack surface will remain free from stress after cracking, the normal and shearing stresses that were acting along the crack will be fully released.

Consequently, the decrease in elastic-strain energy of residual stresses per unit thickness due to the occurrence of the crack, W_e, can be determined from knowing (1) the residual stresses that were acting along the crack before cracking and (2) the relative displacement of both sides of the crack or the crack opening, as follows**:

$$W_e = \int_A^B 1/2 \left\{ \sigma_n[\nu_n] + \tau[\nu_t] \right\} ds \tag{9}$$

---

* Even when a material is in the plastic state, the strain change during unloading is elastic.

** In many applications, the relative displacement along the crack, $[\nu_t]$, is considerably smaller than that in the normal direction, $[\nu_n]$. In such cases the second term in Equation (9) can be neglected.

where

> σ_n, τ = normal and shearing residual stresses, respectively,
> that were acting along the crack
>
> $[\nu_n]$, $[\nu_t]$ = relative displacements of both sides of the crack
> in the normal and tangential directions,
> respectively.

The decrease in the total energy of the system, U, is:

$$U = W_e - W_s \tag{10}$$

Since the stress changes due to cracking are considered to be elastic, the relationships between the residual stress along the crack, (σ_n, τ), and the crack opening, $([\nu_n], [\nu_t])$, can be determined analytically as a problem of the theory of elasticity. Masubuchi and Martin[22] have conducted an analysis of stress changes due to the formation of a crack. Consequently, the decrease in total energy, U, can be calculated when the path of the crack and the residual stresses that were acting along the crack are known.

The stability of a crack is now considered. First of all, the value of U must be positive if a crack is to form. However, there may be many different crack paths between two points, A and B, as shown by L_1, L_2, $\cdots$, in Figure 37(a), which may satisfy the above condition. Different values of energy decrease U_1, U_2, $\cdots\cdots$, will be produced by these different crack paths. One crack path may result in a larger value of U than another crack path does. The crack path that produces the largest decrease in total energy is likely to be the preferred path between A and B. The crack also will extend as long as U is increased by the increase in crack length $\left(\dfrac{\partial U}{\partial \ell} > 0\right)$. The crack will stop when $\dfrac{\partial U}{\partial \ell} = 0$. The above mentioned conditions are shown schematically in Figure 37(b). Relationships between the length of crack and energy decrease, U, are shown for different crack paths. The crack path (including crack length) which correspond to Point X is more stable than other paths.

The discussion so far has been about a crack between A and B. The analysis can be extended to a group of cracks. The crack pattern that produces the maximum value of U is the one that is most likely to occur.

The above analysis shows that the unique solution for crack pattern can be obtained by calculating the maximum value of an integral of a function determined by residual stresses and properties of the material. The analysis, unfortunately, shows that the reverse process is mathematically indeterminate. The unique solution of residual-stress distribution cannot be determined from the knowledge of crack pattern because of indeterminate coefficients associated with the integration of unknown functions. Nevertheless it is apparent that the knowledge of crack pattern provides valuable information on the residual-stress distribution. A comparison of crack patterns obtained in specimens made with different designs and different welding procedures will provide qualitative information on how the design and procedure variables affect

the residual-stress distribution. Analytical investigations are sometimes quite useful for properly interpreting the crack pattern. Further analyses have been made of the following simple crack patterns:

> (1) Transverse cracks which appeared in most of the welds
>   in the experimental work
>
> (2) Circular and radial cracks in radially symmetric stress
>   fields.

Analyses for Transverse Cracks in Welds

Introduction

It was found in the experimental investigations that typical hydrogen-induced cracks are short transverse cracks adjacent to the weld. This type of crack, which occurs in almost every hydrogen charged weld, is a result of the longitudinal tensile residual stresses that are always present in the vicinity of a weld. Transverse cracks are most predominant in simple-butt joints, as shown in Figures 8 and 9.

Results of experimental hydrogen-induced-cracking tests of welds made in various steels have shown that properties of the material have definite effects on the crack pattern, as shown in Figures 6 through 9. When the material was embrittled badly by hydrogen charging, extensive cracks were formed. If the material was embrittled less, the cracks became less predominant or cracks became shorter and more widely spaced. When the material was tougher than some limit, no cracks were produced during or after hydrogen charging.

The typical transverse cracks observed in most weldments consisted of short parallel cracks of about equal length spaced at about equal intervals. The results indicate that the distribution of longitudinal residual stresses has the following characteristics:

> (1) High tensile stresses exist in narrow regions on
>   both sides of the weld
>
> (2) The distribution of residual stresses along the weld
>   is uniform except in regions near the end of the weld.

These characteristics have been proved in the measurements of residual stresses as shown in Figures 31 and 32.

On the basis of the experimental finding, analyses have been made for cracks in an infinite plate caused by the residual stresses as shown by Curve AA in Figure 38(a). It is assumed that residual stresses in the y-direction $\sigma_{yo} = f(x)$ vary along the x-direction but are uniform in the y-direction. Two types of transverse cards were analyzed:

> (1) A straight single crack, as shown in Figure 38(b)
>
> (2) Parallel cracks with equal length and equal spacing,
>   as shown in Figure 38(c).

Curve AA : Aibitrary distribution

Curve BB : $\sigma_{yo} = \sigma_o \left\{ 1 - \left(\frac{x}{f}\right)^2 \right\} e^{-\frac{1}{2}\left(\frac{x}{f}\right)^2}$

Curve CC : $\sigma_{yo} = \sigma_o \left\{ 1 - \left(\frac{x}{f}\right)^2 \right\}$
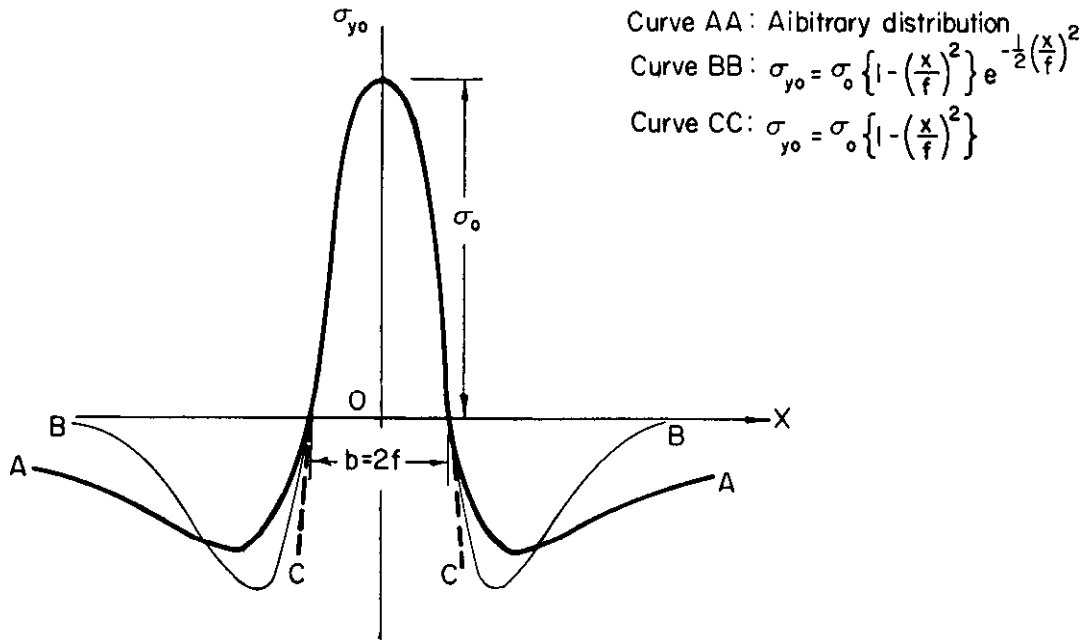
a. *Distributions of longitudinal residual stress δyo.*
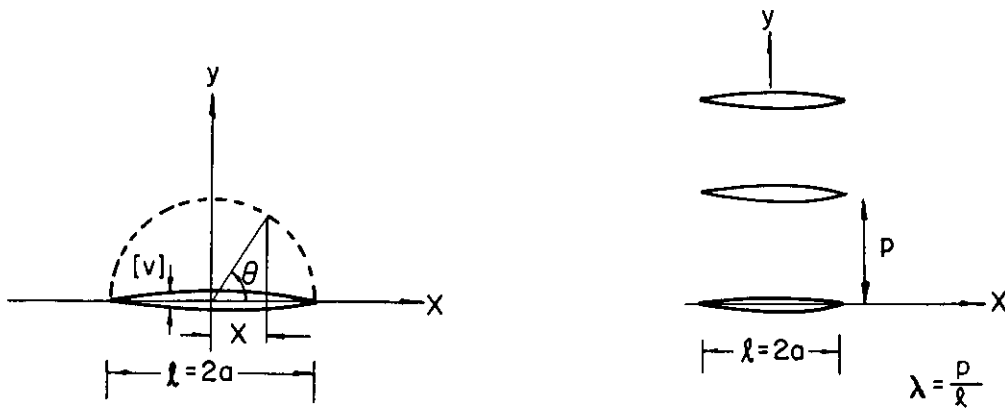
b. *Straight single crack*   c. *Parallel cracks*

Fig. 38. *Residual stresses* $\sigma_{yo} = f(x)$ *and transverse cracks.*

Analysis for a Straight Single Crack

Fundamental Equations. The analysis of a straight single crack in an arbitrary stress field has already been made by investigators including Masubuchi[23,24], and Barenblatt[25]. The following describes the analysis made by Masubuchi.

First, the residual stresses that existed along the crack before cracking are expressed by a modified Fourier series as follows:

$$\sigma_{yo} = f(x) = \frac{E}{2\ell} \sum_{n=1}^{\infty} n \, B_n \frac{\sin n\theta}{\sin \theta}$$

where

  E = Young's modulus
  $\ell = 2a$ = crack length
  θ = parameter which expresses the position x, $\cos \theta = \frac{x}{a}$.

$$B_n = \text{coefficient} = \frac{4\ell}{\pi E} \cdot \frac{1}{n} \int_0^{\pi} \sigma_{yo} \sin n\theta \cdot \sin \theta \, d\theta \qquad (11\text{-}1)$$

For a given stress distribution, σ_{yo}, and crack length, ℓ, a series of coefficients B_1, B_2, B_3, ····· can be determined by conducting the integrations given in Equation (11-1) from $\theta = 0$ (x = a) to $\theta = \pi$ (x = -a).

The opening of the crack in the y-direction, $[v]$, also can be expressed in a Fourier series as follows:

$$[v] = \sum_{n=1}^{\infty} A_n \sin n\theta \qquad (12)$$

Equation (12) satisfies the condition that the crack must be closed at both ends of the crack; i.e., $[v] = 0$ at $x = \pm a$ or $\theta = 0$ and π. According to Masubuchi's analysis, the two sets of coefficients are identical in case of a straight single crack:[24]*

$$A_n = B_n.$$

Then the strain energy released by the occurrence of the single crack, W_e, is:

---

* The following relation exists between σ_{yo} and $[v]$:

$$\sigma_{yo} = \frac{E}{4\pi} \int_{-a}^{a} \frac{1}{x - x'} \left(\frac{d[v]}{dx} \right)_{x'} dx'$$

σ_{yo} and $[v]$ given in Equations (11) and (12) satisfy the above relation when $A_n = B_n$.

$$W_e = \int_{-a}^{a} \frac{1}{2} \sigma_{yo} [v] \, dx$$

$$= \frac{E}{8} \frac{\pi}{2} \left[\sum_{n=1}^{\infty} n \, B_n^2 \right] \qquad (13)$$

The decrease in total energy, U, caused by the occurrence of the crack is:**

$$U = W_e - 2\rho\ell \qquad (14)$$

A crack will occur when the total energy decreases as the result of the formation of the crack, or $U > 0$. The stable crack length will be determined by the following condition:

$$\frac{\partial U}{\partial \ell} = 0$$

Numerical Analyses for Mathematically Expressed Stress Distributions. Numerical analyses have been made on stress distributions mathematically expressed by two equations as follows:

(1) Modified parabolic stress distribution

$$\sigma_{yo} = \sigma_o \left\{ 1 - \left(\frac{x}{f} \right)^2 \right\} e^{-1/2 \left(\frac{x}{f} \right)^2} \qquad (15)$$

(2) Parabolic stress distribution

$$\sigma_{yo} = \sigma_o \left\{ 1 - \left(\frac{x}{f} \right)^2 \right\} \qquad (16)$$

** The strain energy release due to the occurrence of a crack in a plate under uniform tension, Equation (4), can be obtained as a simple example of the analysis presented here. Under uniform stress σ, $B_1 = \frac{2\ell}{E} \sigma$, $B_2 = B_3 = \cdots = 0$, in Equation (12). Thus, $W_e = \frac{E}{8} \cdot \frac{\pi}{2} \left(\frac{2\ell}{E} \sigma \right)^2 = \frac{\pi \ell^2}{4E} \sigma^2$.

TABLE 6. SUMMARY OF NUMERICAL ANALYSES OF TRANSVERSE CRACKS PRODUCED IN AN INFINITE PLATE CONTAINING RESIDUAL STRESSES EXPRESSED BY MATHEMATICAL EQUATIONS.

Conditions	1. Single Crack, Modified Parabolic Stress Distribution (length, ℓ)	2. Single Crack, Parabolic Stress Distribution (length, ℓ)	3. Parallel Cracks, Parabolic Stress Distribution (length, ℓ; pitch, p)
Residual stresses[a], σ_{yo}	$\sigma_{yo} = \sigma_o \left\{ 1 - \left(\frac{x}{f}\right)^2 \right\} e^{-1/2 \left(\frac{x}{f}\right)^2}$	$\sigma_{yo} = \sigma_o \left\{ 1 - \left(\frac{x}{f}\right)^2 \right\}$	$\sigma_{yo} = \sigma_o \left\{ 1 - \left(\frac{x}{f}\right)^2 \right\}$
Coefficient, Bn	For n = even $\quad B_n = 0$ For n = odd $\quad B_n = \frac{4\ell}{E} \sigma_o b_n$ $b_n{}^{(c)} = \sum\limits_{m=o}^{\infty} Q_{nm} \left(\frac{\ell}{b}\right)^{2m}$ $Q_{nm} = (-1)^m \frac{2m+1}{2^{m+1}} \cdot \frac{(2m)!}{m! \left(m + \frac{n+1}{2}\right)! \left(m - \frac{n-1}{2}\right)!}$	$B_1 = \left\{ 1 - \frac{1}{4}\left(\frac{\ell}{b}\right)^2 \right\} \left(\frac{\sigma_o}{E}\right) 2\ell$ $B_3 = -\frac{1}{12}\left(\frac{\ell}{b}\right)^2 \left(\frac{\sigma_o}{E}\right) 2\ell$ $B_2 = B_4 = B_5 = B_6 = \cdots\cdots = 0$	$B_1 = \left\{ 1 - \frac{1}{4}\left(\frac{\ell}{b}\right)^2 \right\} \left(\frac{\sigma_o}{E}\right) 2\ell$ $B_3 = -\frac{1}{12}\left(\frac{\ell}{b}\right)^2 \left(\frac{\sigma_o}{E}\right) 2\ell$ $B_2 = B_4 = B_5 = B_6 = \cdots\cdots = 0$
Enery decrease per crack[b] U or $U_1 = \pi \left(\frac{\sigma_o}{E}\right)\left(\sigma_o f^2\right) F(\mu,\xi)$	$F(\mu,\xi) = 4\xi^2 \left(\sum\limits_{n=1}^{\infty} n b_n{}^2 \right) - 2\mu\xi$	$F(\mu,\xi) = \xi^2 - \frac{1}{2}\xi^4 + \frac{1}{12}\xi^6 - 2\mu\xi$	$F(\mu,\xi) = \xi^2 g(\xi) - 2\mu\xi$ $g(\xi) = \gamma_{11} - \frac{1}{2}\left(\gamma_{11} + \frac{\gamma_{13}}{3}\right)\xi^2$ $\quad + \frac{1}{8}\left(\frac{\gamma_{11}}{2} + \frac{\gamma_{13}}{3} + \frac{\gamma_{33}}{6}\right)\xi^4$ [d]
Energy decrease per length in y-direction $\bar{U} = \frac{\pi}{2}\left(\frac{\sigma_o}{E}\right)\left(\sigma_o f\right)\cdot H(\mu,\lambda,\xi)$			$H(\mu,\lambda,\xi) = \frac{1}{\lambda}\left\{ \xi\cdot g(\xi) - 2\mu \right\}$

Notes: (a) σ_o = maximum residual stress in the weld center, b = 2f = width of the the tension zone of residual stress.

(b) $\xi = \frac{\ell}{b}$.

(c) Values of b_n for various values of n and $\xi = \frac{\ell}{b}$ are shown in Table A-1 in Appendix.

(d) Values of γ_{nj} are shown in Table A-3.

where

σ_o = maximum stress at the weld center
b = 2f = width of the tension zone of residual stress.

The stress distribution given by Equation (15) is shown by Curve BB in Figure 38(a) which represents the residual-distribution in a weld with reasonable accuracy.* Curve CC in Figure 38(a) shows the stress distribution given by Equation (16); this distribution can be used for an approximate analysis of short transverse cracks.

Table 6 summarizes results of mathematical analyses for the above two stress distributions. Values of coefficient B_n are determined by Equation (11-1). Then the decrease in total energy, U, can be calculated by Equation (13) and (14). Here, U is expressed as follows:

$$U = \pi \left(\frac{\sigma_o}{E}\right)\left(\sigma_o f^2\right) F (\mu, \xi) \tag{17}$$

U is determined by two constants σ_o and f which characterize the maximum stress and the width of tension zone, respectively, and a dimensionless function F (μ, ξ). F (μ, ξ) is a function of two dimensionless parameters μ and ξ. The parameter ξ is the ratio of crack length, ℓ, to the width of tension zone of residual stress, b; and μ is the ratio of the critical crack length, ℓ_{co}, of the material for the stress level σ_o to the width of tension zone, b, as follows:

$$\xi = \frac{\ell}{b} = \frac{a}{f} \tag{17-1}$$

$$\mu = \frac{\ell_{co}}{b} = \left(\frac{K_c}{K_w}\right)^2 \tag{17-2}$$

$$\ell_{co} = \frac{4}{\pi} \frac{E\rho}{\sigma_o^2} = \frac{2}{\pi} \left(\frac{K_c}{\sigma_o}\right)^2 \tag{17-3}$$

$$K_w = \sqrt{\frac{\pi}{2}} \, b \, \sigma_o \tag{17-4}$$

where K_c is the critical stress-intensity factor of the material, see Equation (6). K_W is a parameter determined by the residual-stress distribution, and it may be called the "effective stress-intensity factor of the weldment". When the material has greater fracture toughness the value of the parameter μ increases, therefore, μ is called the "relative toughness of the weldment".

The expressions of $F(\mu, \xi)$ for the above two stress distributions are:

(1) For the modified parabolic stress distribution**:

$$F(\mu,\xi) = 4\xi^2 \left(\sum_{n=1}^{\infty} n\, b_n \right)^2 - 2\mu\xi \qquad (18)$$

where

$$b_n = \sum_{m=o}^{\infty} Q_{nm}\, (\xi)^{2m} \qquad (18-1)$$

$$Q_{nm} = (-1)^m \frac{2m+1}{2^m+1} \cdot \frac{(2m)!}{m!\left(m + \frac{n+1}{2}\right)!\left(m - \frac{n-1}{2}\right)!} \qquad (18-2)$$

(2) For the parabolic stress distribution:

$$F(\mu,\xi) = \xi^2 - \frac{1}{2}\xi^4 + \frac{1}{12}\xi^6 - 2\mu\xi \qquad (19)$$

Equation (17) indicates that the dimensionless function $F(\mu, \xi)$ determines the stable crack pattern. In other words, for a given value of μ, the most stable crack length is determined as the ξ value that gives the maximum value of $F(\mu, \xi)$.

Figure 39 shows values of $F(\mu, \xi)$ for various values of μ and ξ for the modified parabolic and the parabolic residual-stress distribution. For both stress distributions, values of $F(\mu, \xi)$ are negative when ξ is close to zero indicating that a certain additional energy is required to initiate a crack, since the <u>decrease</u> of energy is discussed here. The amount of additional energy is small when the weldment is brittle (when the μ-value is small).

** Table A-1 in Appendix shows values of bn for various values of n and ξ. The calculations were carried out on a computer by M. S. Edwards and M. Tikson of the Systems Engineering Division of Battelle.
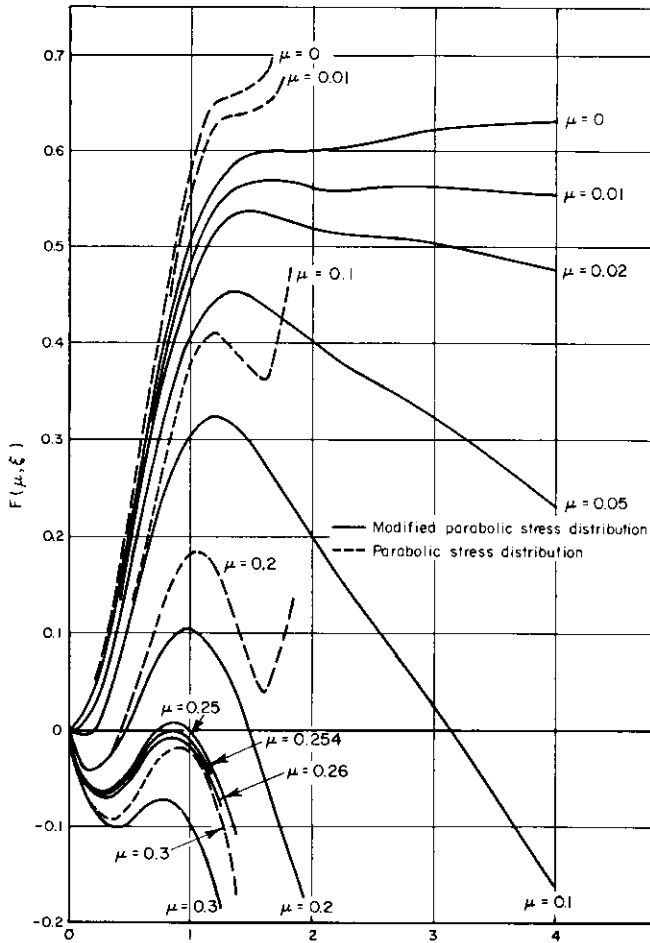
Fig. 39. Curves of $F(\mu, \xi)$ for modified parabolic and parabolic residual-stress distributions.

The value of ξ which gives the maximum value of F (μ, ξ) determines length of the most stable crack for a given μ-value. For $\mu = 0.1$, for example, F (μ, ξ) becomes maximum at around $\xi = 1.2$; in other words, the length of the most stable crack length is about 1.2 times the width of the tension zone of residual stress. As the μ-value increases, the values of F (μ, ξ) become greater and they decrease very slowly after passing the maximum point at around $\xi = 1.4$. This means that when the material is brittle (small μ value) cracks occur easily and are likely to extend to long cracks. When the μ-value is large, on the other hand, a crack is likely to remain at the most stable crack length.

As the μ-value increases the value of F (μ, ξ) decreases, and it becomes negative when the μ-values becomes larger than a certain value. This means that a stable crack will not occur because of residual stress alone when the toughness of a weldment exceeds a certain limit. The critical value of μ is 0.254 for the modified parabolic stress distribution, while the critical value for the parabolic stress distribution is 0.29. Figure 39 also shows that curves of F (μ, ξ) for the two stress distributions are fairly similar in the range $\xi = 0$ to 1.4. This indicates that the analysis for a parabolic stress distribution provide a good approximation for short cracks formed in the tension zone of residual stress.

Analysis for Parallel Cracks

When an infinite plate contains residual stresses $\sigma_{yo} = f(x)$, which vary along the x-direction but are uniform in the y-direction, as shown by Curve AA in Figure 38(a), parallel cracks with equal length, ℓ, and equal interval, p, can be formed, as shown in Figure 38(c).

Fundamental Equations. An arbitrary residual-stress distribution, $\sigma_{yo} = f(x)$, can be expressed by Equation (11), and the crack opening, [v], also can be expressed by Equation (12). However, coefficient B_n and A_n are not identical in this case, but they are related as follows[*]:

$$A_n = \sum_{j=1}^{\infty} \gamma_{nj} B_j \tag{20}$$

where γ_{nj} is an inverse matrix of matrix β_{nj}:

$$\beta_{nj} = \alpha_{nj} + \delta_{nj} \tag{20-1}$$

$$\alpha_{nj} = \left(\frac{2}{\pi}\right)^2 \left(\frac{j}{n}\right) \int_0^\pi \sin\theta \cdot \sin n\theta \cdot d\theta \int_0^\pi \cos j\theta' \, (\cos\theta' - \cos\theta) \cdot$$

---

[*] The relationship between σ_{yo} and [v] for parallel cracks can be determined by superimposeing the stress distribution for a single crack. When [v] is given in Equation (12), σ_{yo} is expressed as follows:

$$\sigma_{yo} = \frac{E}{2\ell} \sum_{n=1}^{\infty} n \, B_n \frac{\sin n\theta}{\sin\theta}$$

$$= \frac{E}{2\ell} \sum_{n=1}^{\infty} n \, A_n \frac{\sin n\theta}{\sin\theta}$$

$$+ \frac{E}{2\ell} \cdot \frac{2}{\pi} \left\{ \sum_{n=1}^{\infty} n \, A_n \left[\sum_{m=1}^{\infty} \int_0^\pi \right. \right.$$

$$\left. \left. \frac{\cos n\theta' \, (\cos\theta' - \cos\theta) \, \{(\cos\theta' - \cos\theta)^2 + 3m^2\lambda^2\}}{\{(\cos\theta' - \cos\theta)^2 + m^2\lambda^2\}} \, d\theta' \right] \right\}$$

Equation (20) is obtained by solving the above equation. (Details of the analysis are given in Appendix of BMI Report 4.)

$$\left[\sum_{m=1}^{\infty} \frac{(\cos \theta' - \cos \theta)^2 + 3m^2\lambda^2}{\{(\cos \theta' - \cos \theta)^2 + m^2\lambda^2\}^2} \right] d\theta' \tag{20-2}$$

$$\lambda = \frac{p}{\ell}$$

$$\delta_{nj} = \begin{cases} 1 & (n = j) \\ 0 & (n \neq j) \end{cases}$$

In order to determine values of A_1, A_2, A_3, $\cdots\cdots$ for given values of B_1, B_2, B_3, $\cdots\cdots$, values of α_{nj} and γ_{nj} must be known. Numerical computations of α_{nj} and γ_{nj} have been done for several combinations of the crack interval-to-crack length ratio, $\lambda = p/\ell$**. Table A-2 in Appendix shows values of α_{nj}, and Table A-3 shows values of γ_{nj}.

The strain energy released by the occurrence of each one of the parallel cracks, W_{e1}, is given by:

$$W_{e1} = \frac{E}{8} \cdot \frac{\pi}{2} \left(\sum_{n=1}^{\infty} \sum_{j=1}^{\infty} n \gamma_{nj} B_n B_j \right) \tag{21}$$

The decrease in total energy caused by the occurrence of each crack, U_1, is given by:

$$U_1 = W_{e1} - 2\rho\ell$$

The energy decrease per unit length in the y-direction, $\overline{U}$, is given by:

$$\overline{U} = \frac{1}{p} U_1 \tag{22}$$

The combination of ℓ and p that gives the maximum value of $\overline{U}$ determines the crack pattern.

Numerical Analysis for Parabolic Stress Distribution. A numerical analysis of parallel cracks was made for the parabolic stress distribution expressed by Equation (16), which simulates the distribution of residual stresses in the vicinity of a simple-butt weld. This was done because most predominant cracks observed in the hydrogen-induced-cracking tests of weldments were short transverse cracks in regions near the weld. Results of the mathematical analysis are summarized in Table 6. $\overline{U}$ is expressed as follows:

** The computations were carried out on an IBM 650 computer by M. S. Edwards and M. Tikson of the Systems Engineering Division of Battelle.
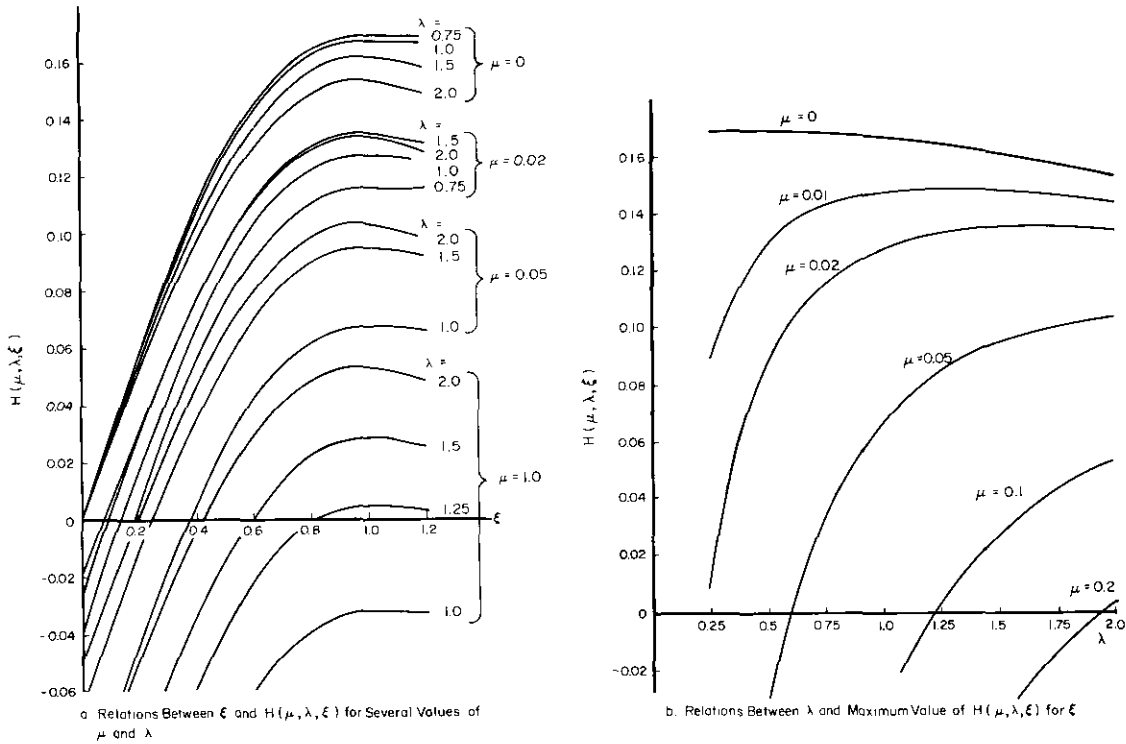
Fig. 40. Curves of H (μ, λ, ξ) for parallel cracks.

$$\overline{U} = \frac{\pi}{2} \left(\frac{\sigma_o}{E} \right) (\sigma_o f) \cdot H(\mu, \lambda, \xi) \tag{23}$$

For a given value of μ, or for a given material property, the most stable crack pattern is determined as the combination of $\lambda = \frac{p}{\ell}$ and $\xi = \frac{\ell}{b}$ that provides the maximum value of $H(\mu, \lambda, \xi)$.

The results of numerical computation of $H(\mu, \lambda, \xi)$ are shown in Figure 40. Figure 40(a) shows the relations between ξ and $H(\mu, \lambda, \xi)$ for several combinations of μ and λ. In almost all cases the maximum value of H occurs at around $\xi = 1.0$. This indicates that the length of the most stable crack is approximately the same as the width of the longitudinal residual stress tension zone.

Relations between λ and the maximum value of $H(\mu, \lambda, \xi)$ for ξ are shown in Figure 40(b) for several values of μ. The combination of ξ and λ which gives the maximum value of H can be obtained for a given value of μ; thus, the most stable crack pattern for a given material and stress distribution is determined.

The maximum value of H occurs at $\lambda = 1.0$ to 1.25 for $\mu = 0.01$; and $\lambda = 1.5$ to 1.75 for $\mu = 0.02$. When μ increases, the value of λ which gives the maximum value of increases; in other words, when the material becomes tougher the interval between cracks increases. The value of H itself also decreases as μ increases, and it becomes negative when μ becomes larger than a certain critical value; in other words, a stable crack will not occur due to residual stress when the material has a higher toughness than some critical value. Since the maximum energy decrease for a given crack, U_1, occurs when there are no other cracks, the limiting value of μ can be obtained for a single crack. According to the analysis presented in the previous section, the limiting μ value is about 0.29 for the modified parabolic stress distribution and is about 0.254 for the parabolic stress distribution.

<div align="center">

Analyses for Circular and Radial Cracks in
Radially Symmetric Stress Fields

</div>

Numerical analyses have been made for a circular crack observed in a circular groove weld (Specimen B32) and radial cracks observed in press-fit specimens. In these specimens residual stresses are radially symmetric.

Analysis for Circular Crack
in a Circular Groove Weld

On the basis of information obtained by Kihara, et al.,[26] the distribution of residual stresses in a circular groove weld is assumed as shown in Figure 41(a), and expressed as follows:

$$\sigma_r = \sigma_\theta = \sigma_o \qquad r \leqq b$$

$$\sigma_r = -\sigma_\theta = \sigma_o \left(\frac{b}{r}\right)^2 \qquad r > b \tag{24}$$

where

σ_r = radial component of residual stress
σ_θ = circumferential component of residual stress
  r = ordinate of a point
  b = radius of the circular groove weld.

To simplify the analysis, it is assumed the circular groove weld is made in an infinite plate. It is believed that the stress distribution shown in Figure 41 represents fairly accurately the distribution of residual stresses in Specimen B32. High tensile stresses in the radial and circumferential directions exist in regions inside the circular groove, $r \leqq b$. In regions outside the groove, $r > b$, σ_r is tensile and σ_θ is compressive both decreasing with an increase in the distance from the weld.
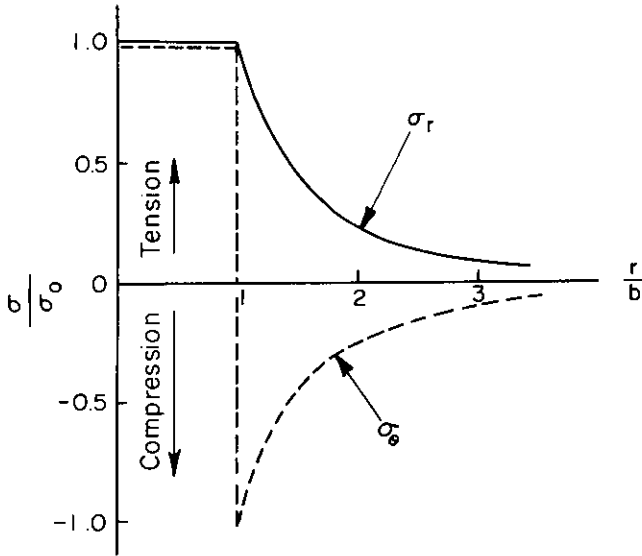
a. *Residual-stress distribution*
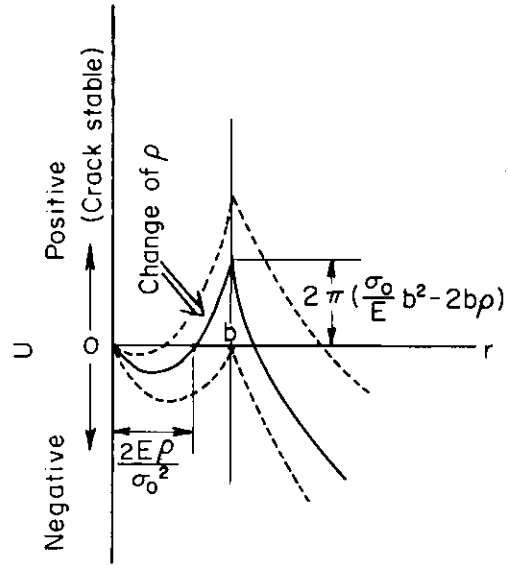
b. *Strain-energy release (Schematic)*

Fig. 41.   *Stability of circular crack in*
           radially symmetric stress field.
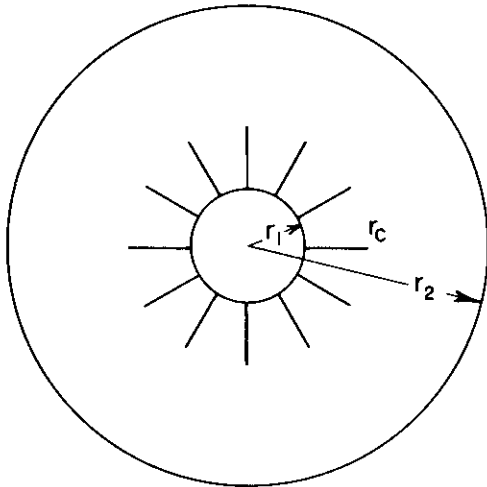
Fig. 42.   *A system of radial cracks.*

Since the tensile stresses exist in the radial direction, a
circular crack is likely to occur. When a circular crack of radius r
occurs, the crack opening, $[\nu_r]$, is given by:

$$[\nu_r] = \frac{2r}{E}\,\sigma_o \qquad r \leqq b$$

$$= \frac{2}{E}\,\frac{b^2}{r}\,\sigma_o \qquad r > b \tag{25}$$

The decrease in total energy caused by the occurrence of a circular crack, U, is:

$$U = \frac{2\pi}{E} r^2 \sigma_o^2 - 4\pi r \rho \qquad r \leqq b$$

$$= \frac{2\pi}{E} \frac{b^4}{r^2} \sigma_o^2 - 4\pi r \rho \qquad r > b \tag{26}$$

The relation between the radius of a circular crack, r, and U is shown in Figure 41(b). The value of U becomes a maximum of $r = b$; in other words, a crack is most likely to occur at the outer edge of the highly stressed area. In Specimen B32, a circular crack occurred just outside the circular groove weld, as shown in Figure 12.* In order that a circular crack occurs, the maximum stress σ_o must be greater than the critical stress σ_{cr} given below:

$$\sigma_o > \sigma_{cr} \equiv \sqrt{\frac{2E\rho}{b}} = \frac{K_c}{\sqrt{b}} \tag{27}$$

Analysis for Radial Cracks
in Press-Fit Specimens

Systems of radial cracks, as shown in Figure 22, were formed during the hydrogen-induced-cracking tests of press-fit specimens. The cracks were caused by the tensile circumferential stress. When stresses increased, cracks became longer and the number of cracks increased. When stresses exceeded a certain value, complete fracture of the specimen took place. An approximate analysis was made of a system of radial cracks.

When a material contains residual stresses of a radially symmetric distribution as given by Equation (1), a system of radial cracks of equal length and located in equal intervals will be produced, as shown in Figure 42. In calculating the decrease of elastic strain energy due to cracking, W_e (per unit plate thickness), it is assumed, as a first approximation, that some percentage of the strain energy stored in the area where cracks occur is released due to the formation of cracks:

$$W_e = \alpha \int_0^{2\pi} \int_{r_1}^{r_c} \left\{ \frac{1}{2E} (\sigma_r + \sigma_\theta)^2 - \frac{\nu}{E} \sigma_r \sigma_\theta \right\} dr \, rd\theta$$

---

* Several short transverse cracks observed on Specimen B32 are believed to be caused by tensile residual stresses in the direction of welding caused by the longitudinal shrinkage of the weld.

$$= \alpha \; \frac{1 + \nu}{E} \; \pi \; r_1^2 \; \sigma_{\theta 1}^2 \left[\frac{1 - \nu}{1 + \nu} \; \frac{\varkappa^4}{(1 + \varkappa^2)^2} \left(\frac{r_c^2}{r_1^2} - 1 \right) + \frac{1}{1 + \varkappa^2} \left(1 - \frac{r_1^2}{r_c^2} \right) \right] \quad (28)$$

where, cracks are formed from $r = r_1$ to $r = r_c$. The value of α increases and approaches 1 when the number of cracks increases.

The rate of strain-energy release due to the extension of cracks, $\dfrac{dW_e}{dr}$, is:

$$\frac{dW_e}{dr} = \alpha \cdot \frac{1 + \nu}{E} \; 2 \; \pi \; r_1 \; \sigma_{\theta 1}^2 \; f \left(\varkappa, \frac{r_c}{r_1} \right) \quad (29)$$

where

$$f \left(\varkappa, \frac{r_c}{r_1} \right) = \frac{1 - \nu}{1 + \nu} \; \frac{\varkappa^4}{(1 + \varkappa^2)^2} \left(\frac{r_c}{r_1} \right)^2 + \frac{1}{(1 + \varkappa^2)^2} \left(\frac{r_1}{r_c} \right)^3 \quad (29\text{-}1)$$

The equilibrium condition for cracking is given by:

$$\frac{dW_e}{dr} = n \cdot 2\rho = n \cdot \frac{K_c^2}{E} \quad (30)$$

Equation (30) can be expressed as follows:

$$K_c = \sqrt{\frac{2\alpha}{n} (1 + \nu) \; f \left(\varkappa, \frac{r_c}{r_1} \right)} \cdot \sqrt{\pi r_1} \cdot \sigma_{\theta 1} \quad (31)$$

Thus the K_c value of the hydrogen-embrittled material can be determined from knowing the crack pattern.

Application of Analytical Investigations to the Interpretation of Experimental Results

Determination of K_c Value of the Hydrogen-Embrittled Materials

Equation (31) indicates that the K_c value of the hydrogen-embrittled material can be determined from the knowledge of the crack

pattern obtained in the press-fit specimen. Average lengths of hydrogen-induced cracks in Specimens K2, K3, and K4 were 2.5, 3.1, and 2.75 inches, respectively, as shown in Figure 22. The specimens had about 6 cracks. K_c values of the heat treated SAE 4340 steel embrittled by hydrogen can be calculated as follows:

	Specimen K2	Specimen K3	Specimen K4
$\sigma_{\theta 1}$, psi	68,000	98,000	81,000
r_c, inches	2.5	3.1	2.75
n	6	6	6
α*	0.3	0.3	0.3
K_c, psi $\sqrt{in.}$	16,300	17,100	16,900

---

* The value of α, given in Equation (28) is approximately equal to square of rate of reduction of strain due to the formation of cracks. Based on the information obtained in the measurement of strain change during the hydrogen-induced-cracking test (Figure 23), the rate of reduction of strain near $r = r_c$ was estimated to about 55 percent. Then, $\alpha = (0.55)^2 = 0.3$.

K_c values determined on the three specimens agree very well; the mean value is 16,800 psi $\sqrt{in.}$

Transverse Cracks in Butt Welds

It has been found in the analytical investigation that the following conditions must be satisfied in order that hydrogen-induced-cracking technique works effectively on a weldment:

(1) The μ value of the weldment before hydrogen charging must be greater than about 0.3 so that no crack is formed during welding

(2) The μ value of the weldment after hydrogen charging must be as low as 0.02 for extensive cracks can be formed.

Many research programs have been carried out for determining K_c values of various high-strength materials. It is believed that the K_c value of SAE 4340 steel oil-quenched and tempered at 500 F is about 175,000 psi $\sqrt{in.}$[19] By analyzing hydrogen-induced crack patterns in press-fit specimens, the K_c value of heat-treated SAE 4340 steel embrittled by hydrogen has been determined to be 16,800 psi $\sqrt{in.}$ Then, the μ values of a weldment with a known residual-stress distribution, or with a given K_w value, under the as-welded and hydrogen-embrittled conditions can be calculated. As shown in Table 5, it has been found that the K_w values of SAE 4340 steel welds 1/2 to 5/8 inch thick are about 100,000 to 200,000 psi $\sqrt{in.}$ Then, the μ values of the weldments will be as follows:

$$\mu = \left(\frac{K_c}{K_w}\right)^2$$

K_w, psi $\sqrt{in.}$	As-Welded (K_c = 175,000 psi $\sqrt{in.}$)	Hydrogen-Embrittled (K_c = 16,800 psi $\sqrt{in.}$)
100,000	3.1	0.028
150,000	1.4	0.013
200,000	0.77	0.007

The μ values are larger than 0.3 in the as-welded condition, and about 0.02 or lower in the hydrogen-embrittled condition. The hydrogen-induced-cracking technique should work effectively on weldments made in SAE 4340 steel oil quenched and tempered at 500 F.

Circular Crack in a
Circular Groove Weld

Equation (27) provides the critical value of residual stress, σ_o, for a circular crack in a circular groove weld. For a 3-inch-diameter circular groove weld (b = 1.5 inches), values of the critical residual stress under the as-welded and the hydrogen-embrittled conditions will be:

	As-Welded (K_c = 175,000 psi $\sqrt{in.}$)	Hydrogen-Embrittled (K_c = 16,800 psi $\sqrt{in.}$)
Critical value of residual stress, σ_o, psi	143,000	13,700

On the basis of information on residual stresses measured on SAE 4340 steel weldments (refer to Table 5), the maximum residual stress in Specimen B32 is believed to be lower than 143,000 psi and definitely higher than 13,700 psi. This indicates that a circular crack will not occur in Specimen B32 under the as-welded condition but a circular crack should occur under the hydrogen-embrittled condition.

SUMMARY AND DISCUSSIONS OF FINDINGS OBTAINED IN THE
EXPERIMENTAL AND ANALYTICAL INVESTIGATIONS

Experimental Investigations

Hydrogen-Induced-Cracking Tests on Weldments

Experimental hydrogen-induced-cracking tests were conducted on 45 weldments including 29 weldments in SAE 4340 steel, 6 in a commercial high-strength structural steel (presently supplied under ASTM A516, Grade F), 4 in HY-80 steel, and 6 in mild steel. In order to produce a variety of residual-stress distributions, the weldments were made in various designs and with various welding procedures. The weldments were electrolytically charged with hydrogen to produce hydrogen-induced cracks. The experimental results are summarized in Table 3.

Effects of Type of Steel, Heat Treatment, and Plate Thickness. The type of steel and heat treatment had significant effects on the tendency for hydrogen-induced cracking.

Extensive and systematic crack patterns were found in weldments made in SAE 4340 steel oil quenched and tempered at 500 and 600 F. (Only one specimen was prepared with steel tempered at 600 F.) Cracks were found after hydrogen charging for less than a few hours. In butt joints made from SAE 4340 steel oil quenched and tempered at 750 or 1000 F, fairly systematic cracks were obtained after hydrogen charging for several hours. No cracks were observed in a weldment made from SAE 4340 steel in the as-rolled condition after hydrogen charging for 14 hours.

Hydrogen-induced-cracking tests were made on five weldments prepared from a commercial high-strength structural steel heat treated to the "hard condition". Cracks were found in three specimens after hydrogen charging for 5 to 24 hours. However, crack patterns were less pronounced than those obtained on heat-treated SAE 4340 steel specimens. Cracks were not produced in a weldment made from a commercial high-strength structural steel heat treated to the "soft condition" after hydrogen charging for 4-1/2 hours.

With regard to HY-80 steel specimens, no cracks were observed in two 1/2-inch-thick weldments after hydrogen charging for 20 and 140-1/2 hours. Small cracks were found in the heat-affected zone in a weldment 1-1/2 inches thick (after 22 hours), and a series of transverse cracks was obtained in a weldment 2 inches thick (after 216 hours).

With regard to mild-steel specimens, no cracks were observed on four weldments 1/2 and 3/4 inch thick after hydrogen charging for up to 126-1/2 hours. Very small cracks were found in the heat-affected zone of a butt joint 2 inches thick after hydrogen charging for 379 hours. Very small cracks also were found in the heat-affected zone in a butt joint 5/8 by 24 by 38 inches after repeated hydrogen charging (total time: 219 hours) followed by cooling to -30 F to embrittle the material.

Simcoe, et al.[7] made an investigation of hydrogen-induced delayed brittle failure of SAE 4340 steel heat treated to different strengths. Relationships were obtained between the applied stress and the time to rupture while the
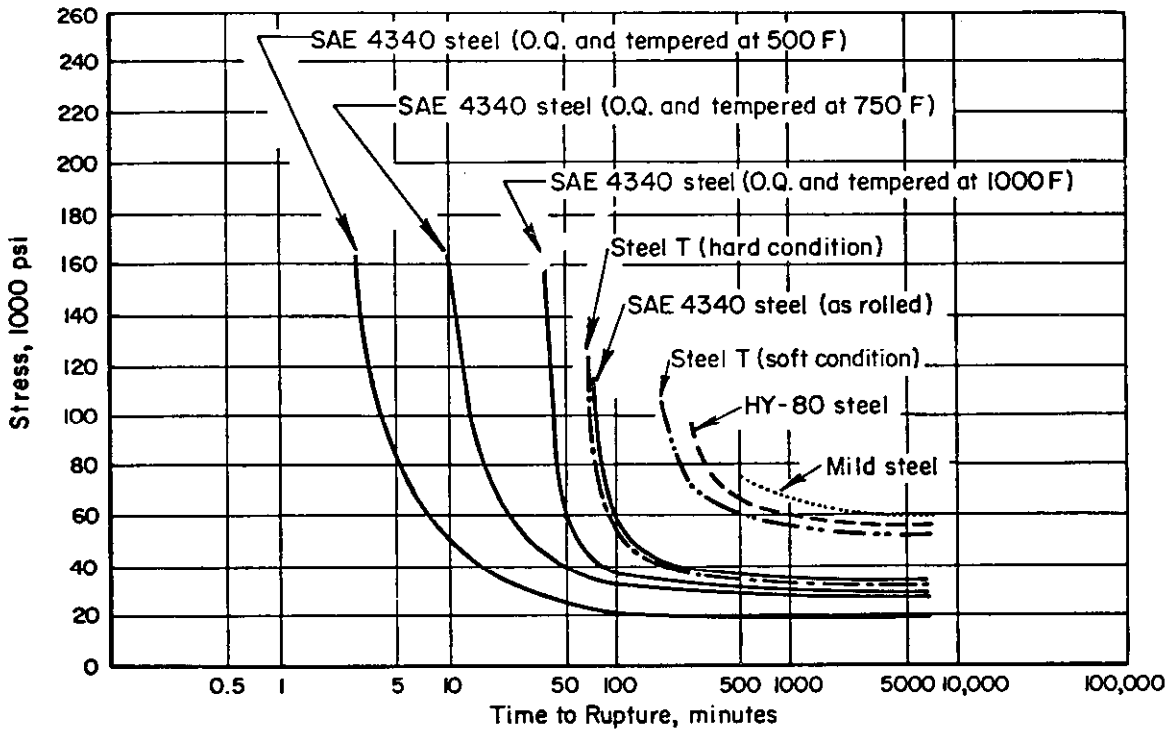
Fig. 43. *Hydrogen-induced delayed-fracture characteristics of various steels used in this research. Curves were estimated from results obtained by Simcoe, et al. (9) The commercial high-strength structural steel is identified as Steel T in the above figure.*

stress was applied during hydrogen charging. As the ultimate strength of the steel increased, the tendency for hydrogen-induced fracture increased; fracture occurred at a lower stress in a shorter period.

An effort was made to investigate the correlation between the results obtained by Simcoe et al. and the results obtained in this research. Stress-rupture characteristics during hydrogen charging of various steels used in this research were estimated as shown in Figure 43, based on the information obtained by Simcoe, et al. For SAE 4340 steel oil quenched and tempered at 500 F, fracture occurs at about 20,000 psi after hydrogen charging for 1 to 2 hours. In this research, hydrogen-induced cracks were obtained in weldments made from heat-treated SAE 4340 steel and a commercial high-strength structural steel heat treated to the "hard condition". Figure 43 shows that the lowest stress for hydrogen-delayed fracture for these steels is less than 40,000 psi. Considering the fact that the maximum tensile residual stresses were about 50,000 psi for mild-steel and SAE 4340 steel butt joints, the results obtained by Simcoe, et al. and the results obtained in this research during the hydrogen-induced-cracking test of weldments agree reasonably well.

A limited study was made of effects of the thickness of a weldment on the tendency for hydrogen-induced cracking. Results obtained in the hydrogen-induced-cracking tests on heavy weldments made in HY-80 steel and mild steel showed that cracks were more pronounced in heavy weldments than in weldments made from thinner plates. The effect of plate thickness, however, was not great.

Characteristics of Crack Patterns in SAE 4340 Weldments. Hydrogen-induced-cracking tests were conducted on several complex weldments made from SAE 4340 steel oil quenched and then tempered at 500 F. Complex butt joints, a circular-groove weld, continuous and intermittent fillet joints, and complex structures were tested. Various crack patterns that could be related to the residual-stress distribution were obtained. Three types of crack pattern can be identified.

The first type is characterized by a series of short transverse cracks adjacent to a weld. This type of crack, which occurs in almost every weld, is a result of the longitudinal tensile residual stresses that are always present in the vicinity of a weld. In a simple butt joint, this type of crack is most predominant. In most cases, the crack pattern on one surface of a specimen is repeated on the other side. This shows that residual stresses of nearly the same magnitude are produced on both surfaces.

The second type of crack pattern is one caused by stress concentration. The concentration of residual stress can be produced by an abrupt interruption of welding as well as by an abrupt change in section. This type of crack generally has a parabolic form and penetrates into the base metal to form a long crack.

The third type of crack pattern contains cracks caused by residual stresses transverse to a weld, and bending stresses associated with angular distortion due to fillet welding.

Results of the hydrogen-induced-cracking test on a weldment made by the Battelle Narrow-Gap welding process indicated that the tension zone of residual stresses produced by the Narrow-Gap process is narrower than that produced by the ordinary shielded-metal-arc process.

Initiation and Propagation of Hydrogen-Induced Cracks. Initiation and propagation of hydrogen-induced cracks were observed on several specimens which were placed in a container which had a transparent wall during hydrogen charging.

On weldments made from SAE 4340 steel oil quenched and tempered at 500 F, cracks were first observed after hydrogen charging for about 45 minutes. Apparently, there is an incubation period before cracks occur. This has been pointed out by Troiano.[6] Most cracks were formed in a short period (usually in a few minutes) after the first crack was observed.

When the hydrogen charging was continued for an extended period some of the cracks--usually one or two--in a specimen grew extensively. Cracks also sometimes grew greatly after hydrogen charging was stopped. The delayed growth of cracks was caused by the hydrogen that remained in specimens after the hydrogen-induced-cracking test.

When a crack grows extensively, residual stresses in a large area surrounding the crack are released, and the tendency to form other cracks in adjacent areas decreases. As a result, a few long cracks, instead of a series of short cracks, are formed even in an area where the distribution of residual stress is uniform. Since the extended cracks are likely to be misinterpreted as an evidence of stress concentration, it is advisable to try to prevent the occurrence of the irregularly extended cracks.

First, it is advisable not to continue hydrogen charging longer than necessary to produce hydrogen-induced cracks. Continuously observing a specimen during testing will permit the determination of the proper time to stop the

hydrogen-induced-cracking test. Second, it is recommended that a specimen be baked after testing to remove the residual hydrogen. Baking in a furnace at 400 F for a few hours appears to be adequate.

Effect of Mechanical Stress Relieving. Hydrogen-induced-cracking tests were made on weldments (bead-on-plate type) that had been mechanically stress relieved. Cracks were found in as-welded specimens and specimens that had been mechanically stress relieved by loading, in a testing machine, up to 60 percent of the yield stress. However, cracks were not found in the specimen that had been loaded to 80 percent of the yield stress. The results indicate that hydrogen-induced cracking is stress sensitive, and not plastic-strain sensitive; in other words, cracks obtained in a welded specimen are caused by residual stresses, not by plastic deformation produced by welding.

Hydrogen-Induced-Cracking Test on Press-Fit Specimens

Radial cracks were found in the press-fit specimens made from SAE 4340 steel oil quenched and then tempered at 500 F and the commercial high-strength heat-treated steel. The test results indicate that hydrogen-induced cracks can be caused by stresses produced by purely elastic deformation.

An attempt also was made to investigate the correlation between the test results obtained on the press-fit specimens and those obtained by Simcoe, et al.[7] Since values of the circumferential stress at the inner circle, $\sigma_{\theta 1}$, were determined, the regions where circumferential stresses, σ_θ, exceeded 20,000 psi (refer to Figure 21) are determined as follows:

$$
\begin{aligned}
&\text{Specimen K1:} \quad r < 3.9 \text{ inches} \\
&\text{Specimen K2:} \quad r < 2.5 \text{ inches} \\
&\text{Specimen K3:} \quad r < 3.1 \text{ inches} \\
&\text{Specimen K4:} \quad r < 2.75 \text{ inches}
\end{aligned}
$$

Complete fracture occurred in Specimen K1 in which circumferential stress exceeded 20,000 psi in most areas. In studying the crack pattern obtained in Specimens K2, K3, and K4, circles of 2.5, 3.1, and 2.75 inches are drawn in Figures 22b, c, and d, respectively. The average crack lengths coincided reasonably well with the circles; although in Specimen K4, one crack extended greatly after the hydrogen-induced-cracking test was completed and the specimen fractured completely. The results indicate that the critical stress required for the propagation of hydrogen-induced cracks is about 20,000 psi for SAE 4340 steel oil quenched and tempered at 500 F.

Stress-Corrosion-Cracking Tests on Weldments

A limited study was made of stress-corrosion cracking of welded specimens. Weldments were made from various steels including mild steel, HY-80 steel, the commercial high-strength structural steel, and SAE 4340 steel. Specimens were immersed in a boiling aqueous solution consisting of 60 percent of $Ca(NO_3)_2$ and 4 percent NH_4NO_3.

In mild-steel specimens, cracks were observed in two of the five specimens tested. In specimens made from steels of higher strength, cracks were

observed in all (five) specimens tested. A system of transverse cracks was obtained in the stress-corrosion-cracking test on a specimen made from the commercial high-strength treated steel. The crack pattern was similar to those obtained in the hydrogen-induced-cracking tests of SAE 4340 steel specimens. A small number of relatively long transverse cracks were obtained in the stress-corrosion-cracking tests on specimens made from mild steel, HY-80 steel, and SAE 4340 steel.

Metallographic Examinations of Cracks

Metallographic examinations were made of sections cut through the ends of cracks. In the commercial high-strength structural steel, hydrogen-induced cracks were transgranular, while stress-corrosion-induced cracks were intergranular. In heat-treated SAE 4340 steel specimens, cracks produced by both types of tests were intergranular.

Measurement of Residual Stresses by Stress-Relaxation Techniques

Measurements of residual stresses by stress-relaxation techniques using strain gages were made on 8 weldments in mild steel and SAE 4340 steel, including 6 butt joints up to 24 by 38 inches in size and 2 complex welded structures. Distortions due to welding of the complex structures also were measured. The experimental results are summarized in Table 5.

The most important finding obtained in this phase of research is that distributions of residual stresses in mild-steel and SAE 4340 steel weldments were quite similar. It was proved in butt joints as well as in complex welded structures. In all welded specimens, high-tensile longitudinal residual stresses were found in regions near the weld and compressive longitudinal stresses in regions away from the weld. Values of the maximum longitudinal residual stress at the weld center, σ_0 , were 45,000 to 75,000 psi. SAE 4340 steel specimens appeared to have higher residual stresses than mild-steel specimens, but the difference was minor. The widths of the tension zone of longitudinal residual stress were 2.5 to 6 inches.

The following experimental evidences also were obtained on the magnitude and distribution of residual stresses in SAE 4340 steel weldments:

(1) Whether or not the weld reinforcement was removed by grinding had little effect on the magnitude and distribution of residual stresses, as shown in Table 5.

(2) The results of measurement of residual stresses along the weld show that residual stresses reached the maximum values in the central portion of the 38-inch-long butt joint (see Figure 32).

These experimental evidences indicate that the residual stresses in heat-treated SAE 4340 steel weldments are considerably lower than the yield strengths of the base metal and the weld metal that were 224,000 psi and about 150,000 psi, respectively.

Investigations of the mechanisms which caused residual stresses in SAE 4340 steel weldments to be low were not carried out in this research. The preheating and interpass temperature at 400 F applied to SAE 4340 steel weldments probably contributed to reduce residual stress to some extent. However, there might be limitations in the magnitude of residual stresses which are primarily

caused by plastic deformation as a result of thermal expansion and contraction during welding. The value of coefficient of linear thermal expansion of steel is 6.5 microinches/inch/F, while modulus of elasticity is about 30×10^6 psi at room temperature. The thermal strain produced by a temperature change of 250 F is equal to the elastic strain which corresponds to the stress of 45,000 psi. This indicates that in a mild-steel weldment contraction of the material during cooling can easily produce residual stresses as high as the yield stress. However, temperature changes of 750 and 1100 F are required to produce thermal strains equal to elastic strains which corresponds to the stresses of 150,000 psi (yield stress of weld metal made from E15016 electrodes) and 224,000 psi (yield stress of SAE 4340 steel oil quenched and tempered at 500 F), respectively. Since SAE 4340 steel softens drastically at temperatures above about 800 F, it may not be possible to produce high residual stresses during the welding thermal cycle. More study of this problem is needed.

Analytical Investigations

General Theory of Crack Pattern Produced by Residual Stresses

An attempt was made to develop a general theory of the crack pattern produced in a solid containing residual stresses by modifying the Griffith-Irwin fracture-mechanics theory. It has been found that, by using the energy concept, the crack pattern that is most likely to occur can be determined theoretically when the residual-stress distribution and properties of the material are known. However, a unique solution of residual-stress distribution cannot be determined from knowledge of the crack pattern because of indeterminate coefficients associated with the integration of the unknown functions. Further mathematical analyses were made of simple crack patterns including (1) transverse cracks in butt-welded specimens, and (2) circular and radial cracks in radially symmetric stress fields.

Analysis for Transverse Cracks in Butt-Welded Specimens

Mathematical analyses were made of a system of transverse cracks which was commonly obtained in butt-welded specimens during the hydrogen-induced-cracking test. Numerical analyses were made of two mathematically expressed stress distributions which simulate the residual-stress distributions in a butt weld. A parabolic stress distribution was used in an analysis of short transverse cracks, and a modified parabolic-stress distribution was used in an analysis of a crack which extended into the region where residual stresses were originally compressive.

A dimensionless parameter, μ, which is called "relative toughness of a weldment (against transverse cracking)" has been introduced to characterize the tendency for hydrogen-induced cracking of a weldment. The parameter is determined by the residual-stress distribution and the properties of the material as follows:

$$\mu = \left(\frac{K_c}{K_w}\right)^2$$

where K_c = critical stress-intensity factor of the material

$K_w = \sigma_0 \sqrt{\frac{\pi}{2}b}$ = effective stress-intensity factor of the residual stresses

σ_0 = maximum longitudinal residual stress at the weld center

b = width of the tension zone of longitudinal residual stresses.

The following results have been obtained:

(1) A series of cracks will be obtained when the μ-value of a weldment is smaller than approximately 0.02.

(2) No crack will be obtained when the μ-value is larger than about 0.3. The critical value of μ is 0.29 for the parabolic stress distribution, and 0.25 for the modified parabolic stress distribution.

(3) The length of stable serial cracks is approximately the same as the width of the tension zone.

(4) When a weldment is very brittle, say μ-value is around 0.01, one or a few cracks of a series of cracks can easily penetrate into the region where residual stresses were originally compressive.

The results indicate that there are limitations on the properties of material to be used in the hydrogen-induced-cracking test. The μ-value of a weldment before hydrogen charging must be larger than about 0.3, otherwise cracking may occur without hydrogen charging. The μ-value of the weldment, however, must decrease to about 0.02 during hydrogen charging in order for systematic cracks to occur. When cracks are formed due to hydrogen, it is recommended not to charge for too long a time, since cracks may grow beyond the most stable crack length.

Analysis for Circular and Radial Cracks in Radially Symmetric Stress Fields

A mathematical analysis was made, in previous research, of a circular crack obtained in a circular-groove weld. It was found that the most stable circular crack occurs just outside the highly stressed area. An analysis also was made of a system of radial cracks obtained in press-fit specimens. An equation has been developed to estimate the critical crack length of the material from the crack pattern.

Applications of Analytical Investigations to the Interpretation of Experimental Results

Attempts have been made to apply the information obtained in the analytical investigations to the interpretation of crack patterns obtained in the experimental hydrogen-induced-cracking tests. Crack patterns obtained in press-fit specimens were analyzed to determine the K_c value of heat-treated SAE 4340 under the presence of hydrogen. The K_c value was 16,800 $psi\sqrt{in}$. According to information obtained by other investigators, the K_c value of heat-treated SAE 4340 steel in air is about 175,000 $psi\sqrt{in}$. indicating that the K_c value is decreased by about 90% by hydrogen charging. According to the results of measurement of residual stresses, the K_c values of SAE 4340 steel weldments were 100,000 to 200,000 $psi\sqrt{in}$. Then, the μ values of SAE 4340 steel weldments are apparently higher than 0.3 in the as-welded condition, but will be as low as or even below 0.02 after hydrogen charging. The results indicate that the hydrogen-induced-cracking technique works effectively on weldments made in heat-treated SAE 4340 steel.

CONCLUSIONS

On the basis of the information obtained in the experimental and analytical investigations conducted in this research it can be concluded that the hydrogen-induced-cracking techniques are useful for studying the distribution of residual stresses in a complex weldment.

It has been found that the hydrogen-induced-cracking technique works very effectively on weldments made in heat-treated SAE 4340 steel. Systematic crack patterns that could be related to the residual-stress distribution were obtained on weldments with various designs and made with various procedures. It also has been found that distribution of residual stresses in weldments made in mild steel and heat-treated SAE 4340 steel are similar. Therefore, it is recommended that experimental hydrogen-induced-cracking tests be made on weldments in heat-treated SAE 4340 steel.

Oil quench from 1550 F followed by tempering at 500 F for 1 hour appears to be an adequate heat-treatment condition for the base plate. Cracks are usually formed after hydrogen charging for an hour or less. Charging should not be continued for longer than necessary to produce the initial crack pattern. Baking the specimen (at about 400 F) after the hydrogen charging to remove remaining hydrogen is recommended. These procedures help to prevent the occurrence of irregular cracks which may cause a misinterpretation of the crack pattern. Crack patterns obtained in various types of weldments can be classified as follows:

(1) A system of short transverse cracks which are caused by the longitudinal tensile stresses in the vicinity of a weld

(2) Cracks caused by a concentration of residual stress as a result of an abrupt interruption of welding or an abrupt structural change in a weldment

(3) Cracks caused by residual stresses transverse to a weld, bending stresses associated with angular distortion, and other secondary stresses.

Hydrogen-induced cracking is stress sensitive rather than plastic-strain sensitive. This has been proved by hydrogen-induced-cracking tests on mechanically stress-relieved specimens and press-fit specimens in which residual stresses were produced by purely elastic deformation.

The hydrogen-induced-cracking technique may be used as a method of demonstrating existence of residual stress in weldments made from steels of lower strength. When steel of lower strength is used, longer charging time is required to produce cracks, and crack patterns are less pronounced. The hydrogen-induced-cracking technique, however, does not seem to work on mild-steel weldments.

Analytical investigations of crack patterns have been made. Mathematical equations have been developed to express relationships among (1) the residual-stress distribution, (2) properties of the material, and (3) the crack pattern. The analytical investigations are useful for evaluating crack patterns obtained experimentally.

FUTURE WORK

Phase 1. Use of the Hydrogen-Induced-Cracking Technique for Studying Practical Fabrication Problems

In the design and fabrication of welded ships, there are a number of practical problems related to the selection of proper design details and welding procedures to avoid excessive concentration of residual stresses and possible cracking during and after welding. It is recommended that research on the use of the hydrogen-induced-cracking technique for studying these practical problems be carried out. It has been found that distributions of residual stresses in mild-steel and SAE 4340 steel weldments are similar. Therefore, structural models made in SAE 4340 steel could be used for studying residual-stress problems in ship structures made in mild steel or high-strength ship steels.

Phase 2. Residual Stresses in Weldments in High-Strength Materials

It has been found in this research that magnitudes and distributions of residual stresses in mild-steel and SAE 4340 steel weldments are similar. However, mechanisms which caused residual stresses in 4340 steel weldments to be lower than the yield stresses of the material have not been established. It also has not been found whether similar phenomena occur in weldments made in high-strength materials other than heat-treated SAE 4340. It is recommended that research be made to study:

(1) Magnitudes and distributions of residual stresses in weldments made in various types of high-strength ferrous and nonferrous materials

(2) Mechanisms of the formation of residual stresses in weldments in high-strength materials.

ACKNOWLEDGMENT

REFERENCES

(1) Masubuchi, K., "Nondestructive Measurement of Residual Stresses in Metals and Metal Structures", RSIC 410, Redstone Scientific Information Center, U.S. Army Missile Command, Redstone Arsenal, Alabama (April, 1965).

(2) Gunnert, R., "Measuring of Residual Stresses and Strains", Document No. X-286-62-OE, Commission X of the International Institute of Welding (1962).

(3) Treuting, R. G., Wishart, H. B., Lynch, J. J., and Richards, D. G., Residual Stress Measurements, American Society for Metals (1952).

(4) Hetényi, M., editor, Handbook of Experimental Stress Analysis, John Wiley and Sons, Inc., New York (1950).

(5) Zandman, F., "Photoelastic-Coating Technique for Determining Stress Distribution in Welded Structures", The Welding Journal, 39 (5), Research Supplement, 191s-198s (1960).

(6) Troiano, A. R., "The Role of Hydrogen and Other Interstitials in the Mechanical Behavior of Metals", Transaction of the American Society for Metals, 52, 54-80 (1960).

(7) Simcoe, C. R., Slaughter, E. R., and Elsea, A. R., "The Hydrogen-Induced Delayed-Brittle Fracture of High-Strength Steel", unpublished manuscript.

(8) McKinsey, C. R., "Effect of Low-Temperature Stress Relieving on Stress-Corrosion Cracking", The Welding Journal, 33 (4), Research Supplement, 161s-166s (1954).

(9) Rädeker, W., "A New Method for Proving the Existence of Internal Stress Caused by Welding", Schweissen und Schneiden, 10 (9), 351-358 (1958). See also abstract by Dr. Claussen, The Welding Journal, 38 (4), 300 (1959).

(10) Standard Specification for High-Yield Strength Quenched and Tempered Alloy Steel Plate, Suitable for Welding, ASTM, A514-64 (1964).

(11) Hucek, H. J., Elsea, A. R., and Hall, A. M., "Evolution of Ultrahigh-Strength, Hardenable Steels for Solid-Propellant Rocket-Motor Cases", DMIC Report 154, Defense Metals Information Center, Battelle Memorial Institute (May, 1961).

(12) Lewis, W. J., Faulkner, G. E., and Martin, D. C., "Development of Methods of Making Narrow Welds in Thick Steel Plates by Automatic Arc-Welding Process", Final Report to Bureau of Ships on Contract No. NObs-86424, Battelle Memorial Institute (March 23, 1964).

(13) Timoshenko, S., Theory of Elasticity, McGraw-Hill Book Co., Inc., New York (1934).

(14) DeGarmo, E. P., Mariam, J. L., and Jonassen, F., "The Effect of Weld Length upon the Residual Stresses of Unrestrained Butt Welds", The Welding Journal, 25 (8), Research Supplement, 485s-487s (1946).

(15) Griffith, A. A., "The Phenomena of Rupture and Flow in Solids", Phil. Trans. Roy. Soc., 221, 163-198 (1921).

(16) Petch, N. J. and Stables, P., "Delayed Fracture of Metals under Static Load", Nature, 169, 842-843 (May 17, 1952).

(17) Fracture, Proceedings of an international conference on the atomic mechanisms of fracture held in Swampscott, Massachusetts, April 12-16, 1959, published jointly by The Technology Press of Massachusetts Institute of Technology and John Wiley & Sons, Inc., New York (1959).

(18) Irwin, G. R., "Fracture", Encyclopedia of Physics, Vol. 6, Elasticity and Plasticity, Springer-Verlag, Berlin, 551-590 (1958).

(19) "Fracture Testing of High Strength Sheet Materials: A Report of a Special ASTM Committee", ASTM Bulletin, No. 243, 29-40 (June, 1960); No. 244, 18-28 (February, 1960); and "Materials Research and Standards", 1 (11), 877-885 (November, 1961).

(20) Fracture Toughness Testing and Its Applications, ASTM Special Technical Publication No. 381 (1965).

(21) Felbeck, D. K., and Orowan, E., "Experiments on Brittle Fracture of Steel Plates", The Welding Journal, 34 (11), Research Supplement, 570s-575s (1955).

(22) Masubuchi, K. and Martin, D. C., "An Analytical Study of Cracks in Weldments", unpublished manuscript.

(23) Masubuchi, K., "Dislocation and Strain Energy Released during Crack Propagation in Residual Stress Field", Proc. 8th Japan National Cong. Appl. Mech., 147-150 (1958).

(24) Masubuchi, K., "Analytical Investigation of Residual Stresses and Distortions due to Welding", The Welding Journal, 39 (12), Research Supplement, 525s-537s (1960).

(25) Barenblatt, G. I., "On Some Basic Ideas of the Theory of Equilibrium Cracks, Forming during Brittle Fracture", Problems of Continuum Mechanics published by the Society for Industrial and Applied Mathematics, 21-38 (1961).

(26) Kihara, H., Masubuchi, K., and Ogura, Y., "Radial Contraction and Residual Stresses in Circular Patch-Weld", Journal Soc. Naval Arch., Japan, 99, 111-122 (1956) and 100, 163-170 (1956).

APPENDIX

TABLE A-1. VALUES OF $b_n = \sum\limits_{m=o}^{\infty} Q_{nm}\, \xi^{2m}$

$$Q_{nm} = (-1)^m \frac{2m+1}{2^m+1} \frac{(2m)!}{m!\left(m+\dfrac{n+1}{2}\right)!\left(m-\dfrac{n-1}{2}\right)!}$$

$\xi \quad b_n$	$n=1$ b_1	3 b_3	5 b_5	7 b_7	9 b_9	11 b_{11}	13 b_{13}
0.2	0.4926	-0.2469×10^{-2}	0.6178×10^{-5}	--	--	--	--
0.4	0.4710	-0.9514×10^{-2}	0.9545×10^{-4}	-0.6374×10^{-6}	--	--	--
0.6	0.4373	-0.2012×10^{-1}	0.4560×10^{-3}	-0.6866×10^{-5}	--	--	--
0.8	0.3946	-0.3283×10^{-1}	0.1330×10^{-2}	-0.3569×10^{-4}	--	--	--
1.0	0.3465	-0.4600×10^{-1}	0.2931×10^{-2}	-0.1233×10^{-3}	0.3874×10^{-5}	--	--
1.2	0.2964	-0.5810×10^{-1}	0.5371×10^{-2}	-0.3265×10^{-3}	0.1481×10^{-4}	--	--
1.4	0.2477	-0.6794×10^{-1}	0.8616×10^{-2}	-0.7156×10^{-3}	0.4426×10^{-4}	--	--
1.6	0.2026	-0.7480×10^{-1}	0.1249×10^{-1}	-0.1360×10^{-2}	0.1101×10^{-3}	-0.7096×10^{-5}	--
1.8	0.1628	-0.7842×10^{-1}	0.1670×10^{-1}	-0.2307×10^{-2}	0.2370×10^{-3}	-0.1937×10^{-4}	--
2.0	0.1289	-0.7898×10^{-1}	0.2090×10^{-1}	-0.3572×10^{-2}	0.4533×10^{-3}	-0.4578×10^{-4}	--
2.2	0.1012	-0.7693×10^{-1}	0.2474×10^{-1}	-0.5134×10^{-2}	0.7886×10^{-3}	-0.9636×10^{-4}	0.9783×10^{-5}
2.4	0.7893×10^{-1}	-0.7301×10^{-1}	0.2800×10^{-1}	-0.6907×10^{-2}	0.1261×10^{-2}	-0.1834×10^{-3}	0.2215×10^{-4}
2.6	0.6153×10^{-1}	-0.6783×10^{-1}	0.3043×10^{-1}	-0.8796×10^{-2}	0.1884×10^{-2}	-0.3213×10^{-3}	0.4550×10^{-4}
2.8	0.4822×10^{-1}	-0.6190×10^{-1}	0.3205×10^{-1}	-0.1071×10^{-1}	0.2650×10^{-2}	-0.5224×10^{-3}	0.8563×10^{-4}
3.0	0.3810×10^{-1}	-0.5573×10^{-1}	0.3283×10^{-1}	-0.1250×10^{-1}	0.3534×10^{-2}	-0.7963×10^{-3}	0.1495×10^{-3}
3.2	0.3044×10^{-1}	-0.4978×10^{-1}	0.3289×10^{-1}	-0.1409×10^{-1}	0.4500×10^{-2}	-0.1149×10^{-2}	0.2445×10^{-3}
3.4	0.2466×10^{-1}	-0.4419×10^{-1}	0.3231×10^{-1}	-0.1541×10^{-1}	0.5511×10^{-2}	-0.1578×10^{-2}	0.3773×10^{-3}
3.6	0.2020×10^{-1}	-0.3910×10^{-1}	0.3125×10^{-1}	-0.1644×10^{-1}	0.6516×10^{-2}	-0.2067×10^{-2}	0.5525×10^{-3}
3.8	0.1679×10^{-1}	-0.3456×10^{-1}	0.2986×10^{-1}	-0.1716×10^{-1}	0.7473×10^{-2}	-0.2626×10^{-2}	0.7724×10^{-3}
4.0	0.1412×10^{-1}	-0.3055×10^{-1}	0.2827×10^{-1}	-0.1758×10^{-1}	0.8345×10^{-2}	-0.3209×10^{-2}	0.1036×10^{-2}
4.2	0.1201×10^{-1}	-0.2706×10^{-1}	0.2656×10^{-1}	-0.1775×10^{-1}	0.9106×10^{-2}	-0.3807×10^{-2}	0.1340×10^{-2}

TABLE A-2.   VALUES OF $\alpha_{nj}^{(a)}$

(1) $\lambda = 0.25$

n\j	1	3	5	7	9	11	13	15
1	12.6078	-2.6395	-0.2815	-0.0264	0.0165	0.0126	0.0039	-0.0000
3	-0.8798	2.5733	-0.9600	-0.0751	0.0135	0.0146	0.0051	0.0003
5	-0.0563	-0.5760	1.1949	-0.5167	-0.0111	0.0179	0.0081	0.0011
7	-0.0038	-0.0322	-0.3690	0.6570	-0.3116	0.0118	0.0134	0.0034
9	0.0018	0.0045	-0.0062	-0.2424	0.3870	-0.1963	0.0183	0.0089
11	0.0011	0.0040	0.0081	0.0075	-0.1606	0.2357	-0.1259	0.0180
13	0.0003	0.0018	0.0031	0.0080	0.0127	-0.1065	0.1459	-0.0812
15	-0.0000	0.0001	0.0004	0.0016	0.0054	0.0132	-0.0703	0.0911

(2) $\lambda = 0.5$

n\j	1	3	5	7
1	5.8441	-1.2166	-0.0489	0.0212
3	-4.055	0.9120	-0.3528	0.0177
5	-0.0098	-0.2117	0.3091	-0.1377
7	0.0030	0.0076	-0.0984	0.1181

(3) $\lambda = 0.75$

n\j	1	3	5	7
1	3.6081	-0.7153	0.0106	0.0119
3	-0.2384	0.4164	-0.1514	0.0179
5	0.0021	-0.0909	0.0974	-0.0394
7	0.0017	0.0077	-0.0281	0.0245

(4) $\lambda = 1.0$

n\j	1	3	5	7
1	2.5044	-0.4572	0.0218	0.0040
3	-0.1524	0.2087	-0.0674	0.0094
5	0.0044	-0.0405	0.0329	-0.0114
7	0.0006	0.0040	-0.0082	0.0054

TABLE A-2.   (Continued).

(5)   λ = 1.25

n\j	1	3	5	7
1	1.8542	-0.3043	0.0192	0.0009
3	-0.1014	0.1103	-0.0308	0.0043
5	0.0038	-0.0185	0.0116	-0.0034
7	0.0001	0.0018	-0.0024	0.0012

(6)   λ = 1.5

n\j	1	3	5	7
1	1.4309	-0.2079	0.0140	-0.0001
3	-0.0693	0.0606	-0.0144	0.0018
5	0.0028	-0.0087	0.0043	-0.0011
7	-0.0000	0.0008	-0.0008	0.0003

(7)   λ = 1.75

n\j	1	3	5	7
1	1.1374	-0.1451	0.0095	-0.0002
3	-0.0484	0.0345	-0.0070	0.0008
5	0.0019	-0.0042	0.0017	-0.0004
7	-0.0000	0.0003	-0.0003	0.0001

(8)   λ = 2.0

n\j	1	3	5	7
1	0.9246	-0.1033	0.0063	-0.0002
3	-0.0344	0.0203	-0.0035	0.0004
5	0.0013	-0.0021	0.0007	0.0001
7	-0.0000	0.0002	-0.0001	0.0000

(a) Values in the tables are rounded to four decimal places.

TABLE A-3.   VALUES OF γ_{nj} [a]

(1) $\lambda = 0.25$ $n = 1, 3, 5, \cdots, 15$

n\j	1	3	5	7	9	11	13	15
1	0.0778	0.0642	0.0410	0.0173	0.0024	-0.0020	-0.0013	-0.000
3	0.0214	0.3211	0.1541	0.0647	0.0118	-0.0053	-0.0042	-0.000
5	0.0082	0.0925	0.5266	0.1747	0.0420	-0.0044	-0.0075	-0.001
7	0.0025	0.0277	0.1248	0.6659	0.1521	0.0148	-0.0101	-0.004
9	0.0003	0.0039	0.0234	0.1183	0.7616	0.1195	-0.0011	-0.008
11	-0.0002	-0.0014	-0.0020	0.0094	0.0978	0.8326	0.0893	-0.007
13	-0.0001	-0.0010	-0.0029	-0.0054	-0.0008	0.0755	0.885	0.064
15	-0.0000	-0.0002	-0.0006	-0.0020	-0.0052	-0.0058	0.056	0.92

(2) $\lambda = 0.25 - 2.0$ $n, j = 1, 3$

λ	γ_{11}	$\gamma_{13} = 3\gamma_{31}$ [b]	γ_{33}
0.25	0.0778	0.0642	0.3211
0.50	0.1521	0.1004	0.5612
0.75	0.2229	0.1134	0.7316
1.0	0.2901	0.1098	0.8430
1.25	0.3538	0.0969	0.9100
1.5	0.4137	0.0811	0.9482
1.75	0.4694	0.0658	0.9697
2.0	0.5205	0.0527	0.9819

(a)   Values in the tables are rounded to four decimal places.

(b) $n\gamma_{nj} = \gamma_{jn}$, for $n \neq j$.

DOCUMENT CONTROL DATA - R&D

(Security classification of title, body of abstract and indexing annotation must be entered when the overall report is classified)

1. ORIGINATING ACTIVITY (Corporate author)	2a. REPORT SECURITY CLASSIFICATION
Ship Structure Committee	None
	2b. GROUP

3. REPORT TITLE

Investigation of Residual Stresses in Steel Weldments

4. DESCRIPTIVE NOTES (Type of report and inclusive dates)

Final Report on Project SR-167

5. AUTHOR(S) (Last name, first name, initial)

Masubuchi, K. and Martin, D. C.

6. REPORT DATE	7a. TOTAL NO. OF PAGES	7b. NO. OF REFS
September 1966	103	26

8a. CONTRACT OR GRANT NO.	9a. ORIGINATOR'S REPORT NUMBER(S)
Bureau of Ships NObs 92521	SSC-174
b. PROJECT NO.	
c.	9b. OTHER REPORT NO(S) (Any other numbers that may be assign this report)
d.	

10. AVAILABILITY/LIMITATION NOTICES

Distribution of this document is unlimited.

11. SUPPLEMENTARY NOTES	12. SPONSORING MILITARY ACTIVITY
	Bureau of Ships, Dept. of the Navy Washington, D. C.

13. ABSTRACT

Experimental hydrogen-induced-cracking tests were made on 45 weldments mild steel, HY-80 steel, a commercial high-strength structural steel, and SAE 43 steel. Extensive cracks were found in weldments made in SAE 4340 steel (oil quenched and tempered at 500 F) after hydrogen charging for relatively short tim Systematic crack patterns that could be related to residual stress distributions were obtained on various complex weldments. When steels of lower strengths were used, longer charging time was required to produce cracks, and crack patterns we less pronounced. The hydrogen-induced-cracking technique does not seem to work mild-steel weldments.

It has been found that hydrogen-induced cracking is stress sensitive rather than plastic-strain sensitive. This has been proved by hydrogen-induced-cracking tests on mechanically stress-relieved specimens and press-fit specimens in which residual stresses were produced by purely elastic deformation. It was found that distributions of residual stresses in mild-steel and SAE 4340 steel weldments were quite similar despite the considerable differences in the yield strengths of the two base plates and the weld metals. This was proved in butt joints up to 38 inches long and complex welded structures.

DD FORM 1473
1 JAN 64

14. KEY WORDS	LINK A		LINK B		LINK C	
	ROLE	WT	ROLE	WT	ROLE	WT
Ship hull structures Weld metal Welding Residual stresses Hydrogen-induced cracking tests Stress corrosion cracking Metallography HY-80 steel SAE 4340 steel						

INSTRUCTIONS

1. ORIGINATING ACTIVITY: Enter the name and address of the contractor, subcontractor, grantee, Department of Defense activity or other organization (corporate author) issuing the report.

2a. REPORT SECURITY CLASSIFICATION: Enter the overall security classification of the report. Indicate whether "Restricted Data" is included. Marking is to be in accordance with appropriate security regulations.

2b. GROUP: Automatic downgrading is specified in DoD Directive 5200.10 and Armed Forces Industrial Manual. Enter the group number. Also, when applicable, show that optional markings have been used for Group 3 and Group 4 as authorized.

3. REPORT TITLE: Enter the complete report title in all capital letters. Titles in all cases should be unclassified. If a meaningful title cannot be selected without classification, show title classification in all capitals in parenthesis immediately following the title.

4. DESCRIPTIVE NOTES: If appropriate, enter the type of report, e.g., interim, progress, summary, annual, or final. Give the inclusive dates when a specific reporting period is covered.

5. AUTHOR(S): Enter the name(s) of author(s) as shown on or in the report. Enter last name, first name, middle initial. If military, show rank and branch of service. The name of the principal author is an absolute minimum requirement.

6. REPORT DATE: Enter the date of the report as day, month, year; or month, year. If more than one date appears on the report, use date of publication.

7a. TOTAL NUMBER OF PAGES: The total page count should follow normal pagination procedures, i.e., enter the number of pages containing information.

7b. NUMBER OF REFERENCES: Enter the total number of references cited in the report.

8a. CONTRACT OR GRANT NUMBER: If appropriate, enter the applicable number of the contract or grant under which the report was written.

8b, 8c, & 8d. PROJECT NUMBER: Enter the appropriate military department identification, such as project number, subproject number, system numbers, task number, etc.

9a. ORIGINATOR'S REPORT NUMBER(S): Enter the official report number by which the document will be identified and controlled by the originating activity. This number must be unique to this report.

9b. OTHER REPORT NUMBER(S): If the report has been assigned any other report numbers (either by the originator or by the sponsor), also enter this number(s).

10. AVAILABILITY/LIMITATION NOTICES: Enter any limitations on further dissemination of the report, other than those imposed by security classification, using standard statements such as:

(1) "Qualified requesters may obtain copies of this report from DDC."

(2) "Foreign announcement and dissemination of this report by DDC is not authorized."

(3) "U. S. Government agencies may obtain copies of this report directly from DDC. Other qualified DDC users shall request through

_____ ."

(4) "U. S. military agencies may obtain copies of this report directly from DDC. Other qualified users shall request through

_____ ."

(5) "All distribution of this report is controlled. Qualified DDC users shall request through

_____ ."

If the report has been furnished to the Office of Technical Services, Department of Commerce, for sale to the public, indicate this fact and enter the price, if known.

11. SUPPLEMENTARY NOTES: Use for additional explanatory notes.

12. SPONSORING MILITARY ACTIVITY: Enter the name of the departmental project office or laboratory sponsoring (paying for) the research and development. Include address.

13. ABSTRACT: Enter an abstract giving a brief and factual summary of the document indicative of the report, even though it may also appear elsewhere in the body of the technical report. If additional space is required, a continuation sheet shall be attached.

It is highly desirable that the abstract of classified reports be unclassified. Each paragraph of the abstract shall end with an indication of the military security classification of the information in the paragraph, represented as (TS), (S), (C), or (U).

There is no limitation on the length of the abstract. However, the suggested length is from 150 to 225 words.

14. KEY WORDS: Key words are technically meaningful terms or short phrases that characterize a report and may be used as index entries for cataloging the report. Key words must be selected so that no security classification is required. Identifiers, such as equipment model designation, trade name, military project code name, geographic location, may be used as key words but will be followed by an indication of technical context. The assignment of links, roles, and weights is optional.

The Ship Hull Research Committee undertakes research service activities in the general fields of materials, design, and fabrication, as relating to improved ship hull structure, when such activities are accepted by the Academy as part of its functions. The Committee recommends research objectives and projects; provides liaison and technical guidance to such studies; reviews project reports; and stimulates productive avenues of research.

SHIP HULL RESEARCH COMMITTEE

Chairman: Mr. T. M. Buermann
Gibbs & Cox, Inc.

Vice-Chairman:

Mr. Maurice L. Sellers
Newport News Shipbuilding
and Dry Dock Company

Vice-Chairman:

Dr. J. M. Frankland
Retired
National Bureau of Standards

Members

Dr. H. Norman Abramson
Director, Dept. of Mechanical
Sciences
Southwest Research Institute

Mr. Harold G. Acker
Shipbuilding Division
Bethlehem Steel Corp.

Mr. Alvin E. Cox
Assistant Naval Architect
Newport News Shipbuilding
and Dry Dock Company

Mr. Robert Dippy, Jr.
Structural Design Engineer
Sun Shipbuilding & Dry
Dock Company

Dr. N. H. Jasper
Technical Director
U. S. Navy Mine Defense
Laboratory

Mr. F. J. Joyce
Manager Marine Design
National Bulk Carriers, Inc.

Mr. William R. Jensen
Structural Methods Engineer
Grumman Aircraft Engineering
Corporation

Mr. J. A. Kies
Head, Ballistics Branch
Mechanics Division
Naval Research Laboratory

Dr. William R. Osgood
School of Engineering and
Architecture
Catholic University of America

Dr. G. M. Sinclair
Research Professor of Theoretical
and Applied Mechanics
University of Illinois

Mr. Merville Willis
Naval Architect
New York Shipbuilding
Corporation

Professor Raymond A. Yagle
Dept. of Naval Architecture
Marine Engineering
University of Michigan

Arthur R. Lytle
Technical Director

E. A. Burke
Executive Secretary

SHIP STRUCTURE COMMITTEE PUBLICATIONS

These documents are distributed by the Clearinghouse, Springfield, Va. 22151. These documents have been announced in the Technical Abstract Bulletin (TAB) of the Defense Documentation Center (DDC), Cameron Station, Alexandria, Va. 22314, under the indicated AD numbers. There is no charge for documents for registered users of the DDC services. Other users must pay the prescribed rate set by the Clearinghouse.

Index of Ship Structure Committee Publications (1946 - April 1965)

SSC-163, *Investigation of Bending Moments within the Midship Half Length of a Mariner Model in Extreme Waves* by N. M. Maniar. June 1964. AD 605345

SSC-164, *Results from Full-Scale Measurements of Midship Bending Stresses on Two C4-S-B5 Dry-Cargo Ships Operating in North Atlantic Service* by D. J. Fritch, F. C. Bailey and N. S. Wise. September 1964. AD 605535

SSC-165, *Local Yielding and Extension of a Crack Under Plane Stress* by G. T. Hahn and A. R. Rosenfield. December 1964. AD 610039

SSC-166, *Reversed-Bend Tests of ABS-C Steel with As-Rolled and Machined Surfaces* by K. Satoh and C. Mylonas. April 1965. AD 460575

SSC-167, *Restoration of Ductility of Hot or Cold Strained ABS-B Steel by Treatment at 700 to 1150 F* by C. Mylonas and R. J. Beaulieu. April 1965. AD 461705

SSC-168, *Rolling History in Relation to the Toughness of Ship Plate* by B. M. Kapadia and W. A. Backofen. May 1965. AD 465025

SSC-169, *Interpretative Report on Weld-Metal Toughness* by K. Masubuchi, R. E. Monroe and D. C. Martin. July 1965. AD 466805

SSC-170, *Studies of Some Brittle Fracture Concepts* by R. N. Wright, W. J. Hall, S. W. Terry, W. J. Nordell and G. R. Erhard. September 1965. AD 476684

SSC-171, *Micro-and Macrocrack Formation* by B. L. Averbach. October 1965. AD 473496

SSC-172, *Crack Extension and Propagation Under Plane Stress* by A. R. Rosenfield, P. K. Dai and G. T. Hahn. March 1966. AD 480619